Master Thesis

Investigation of Plugging and Scaling Behaviour of Selected Sand Screen Materials under Simulated Reservoir Conditions

Written by:
Anitha Andiappan
M1131795

Advisor:
Univ.-Prof. Dipl.-Ing. Dr.mont. Herbert Hofstätter
Dipl. -Phys. Dr. rer. nat Siegfried Müssig
Hon. Prof. Dipl.-Ing. Dr. mont. Markus Oberndorfer

Vienna, 15.10.2013

EIDESSTATTLICHE ERKLÄRUNG

Ich erkläre an Eides statt, dass ich die vorliegende Diplomarbeit selbständig und ohne fremde Hilfe verfasst, andere als die angegebenen Quellen und Hilfsmittel nicht benutzt und die den benutzten Quellen wörtlich und inhaltlich entnommenen Stellen als solche erkenntlich gemacht habe.

15. Oktober 2013 Anitha Andiappan

AFFIDAVIT

I hereby declare that the content of this work is my own composition and has not been submitted previously for any higher degree. All extracts have been distinguished using quoted references and all information sources have been acknowledged.

15th October 2013 Anitha Andiappan

Acknowledgement

I am indebted to Prof. Herbert Hofstätter for making himself available at all times to clarify my doubts not only for the duration of master thesis but also throughout my graduate studies at the Montanuniversität Leoben, Austria.

I express my profound gratitude to my supervisor, Dr. Siegfried Müssig and co-supervisor Hon. Prof. Markus Oberndorfer, both from Rohöl-Aufsuchungs Aktiengesellschaft (RAG) for their continuous guidance throughout my master thesis. Both of them have been assiduous in explaining to me various concepts and making sure that I have a clear understanding of these concepts. My thanks also go to RAG for providing me with the financial means to complete this project.

The thesis would not have been possible without the relentless support of Dr. Peter Barth and Elisabeth Simnacher from ESK Ceramics GmbH & Co. KG during my period of time in Kempten, Germany.

Many thanks go to Denis Rice who proof read my numerous revisions and provided various suggestions and recommendations.

This thesis is dedicated to Lars Bollmann, for enduring each step of the way with me and my parents, who have given me the opportunity of an education from the best institutions.

Kurzfassung

Keramiken zeigen eine höhere Erosions- und Korrosionsbeständigkeit als Edelstahl. Es ist allerdings wenig darüber bekannt, wie sich das Ablagerungs- und Verstopfungsverhalten von Keramikfiltern im Vergleich zu modernen Edelstahlfiltern, welche die Produktion von Sand in Öl- und Gasquellen verhindern sollen, verhält. Das Ziel dieser Arbeit war es, eine detaillierte, vergleichende Analyse zur Verstopfung und Ablagerung zwischen Edelstahl - und Keramikfiltern in einer Laborumgebung zu erarbeiten.

Das Verstopfungsverhalten wurde mithilfe der “standard sand retention test methodology” untersucht. Zur Analyse des Ablagerungsverhaltens wurde eine “scaling behaviour evaluation test methodology” im Labor durchgeführt.

Die Resultate des “sand retention test” zeigen, dass zwischen Keramiken und Edelstahl nur geringe Unterschiede in Druckaufbau, Massenbilanz und Partikelgrößenverteilung ersichtlich sind. Bei genauer Betrachtung der Ergebnisse scheinen die Keramikfilter einen konstanten Differenzdruck entlang des Filters und des Filterkuchens (bzw. gravel pack) zu verursachen. Verstopfungen traten nur bei aufgerauten Edelstahlfiltern auf, die dazu verwendet werden erodierte Filter zu simulieren. Die Resultate zum Ablagerungsverhalten machen deutlich, dass die Keramiken weniger Ablagerungen als Edelstahl zeigen. Diese Eigenschaft kann damit begründet werden, dass Keramiken eine geringere Oberflächenenergie haben.
Zusätzlich konnte gezeigt werden, dass sich bei einem Filter-Design mit vielen Schlitzen die Ablagerungen schwerer auflösen als bei “solid coupon” ohne Spalten – und dies unabhängig vom Filtermaterial.

Die Untersuchungen haben einige Eigenschaften von keramischen Filtern verdeutlicht. Es sind jedoch zusätzliche Untersuchungen nötig, um die folgenden Eigenschaften von Keramikfiltern zu ermitteln:

a. sind differentielle Drücke entlang des “gravel pack” für keramische Filter immer konstant
b. sind die Fluss-Raten entlang des “gravel pack” unabhängig von der Schlitzgröße
c. die Oberflächenenergie von Keramiken und Edelstahl mithilfe von “contact angle measurement”

Abstract

It is clear that ceramic material is highly erosion and corrosion resistant, more so that common stainless steels. However, it is still not fully understood how the plugging and scaling behaviour of ceramic screens compares with the state of the art stainless steel screens most commonly used in oil and gas wells to prevent the production of sand. The aim of this thesis was to analyse in depth, in a laboratory environment, the plugging due to sand and scaling that occurs in stainless steel and ceramic screens.

The plugging behaviour was investigated applying standard sand retention test methodology. The scaling behaviour was analyzed via scaling behaviour evaluation test methodology established in the laboratory.

Results of the sand retention test showed that ceramic and stainless steel have generally the same trend in terms of pressure build-up, mass balance and particle size distribution with relatively small differences. Upon closer examination it appears that ceramic screens have a constant differential pressure across screen and filter-cake (representing a gravel pack). Plugging was only observed on roughened stainless steel screens used to simulate eroded screens. The results of the scaling behaviour revealed that in general less scale deposits on ceramic material than stainless steel material; this is due to the lower surface energy of the ceramic material. Additionally it was found that the screen design, i.e. the slot opening pattern caused scale removal to be more cumbersome as compared to a solid coupon without slots regardless of type of screen material.

The investigation clarified selected characteristics of ceramic screens and material; however further investigations are required to identify the following:

a. Whether or not the differential pressure across a gravel pack is always constant for a ceramic screen
b. Whether or not the flow-rate across a gravel pack is always independent of slot size.
c. The surface energy of ceramic and stainless steel materials, determined via contact angle measurement.

List of Tables

List of Figures

Abbreviations

AISI	American Iron and Steel Institute
API	American Petroleum Institute
ASME	American Society of Mechanical Engineers
$BaSO_4$	Barium sulphate
BG	British Gas
Ca^{2+}	Calcium ions
$CaCO_3$	Calcium carbonate
CAJ	Controlled Acid Jetting
$CaSO_4$	Calcium sulphate
CO_2	Carbon dioxide
CO_3^{2-}	Carbonate ions
Cr_2O_3	Chromium Oxide
CV	Control Valve
E&P	Exploration & Production
EHO	Extra Heavy Oil
EN	European Standards
ESK	ESK Ceramics GmbH & Co. KG
FCV	Flow Control Valve
GP	Gravel Pack
H^+	Hydrogen ions
H_2CO_3	Carbonic acid
H_2O	Water
H_2S	Hydrogen Sulphide
HCO_3^-	Bicarbonate ions
HO	Heavy Oil
HSE	Health, Safety and Environment
LPSA	Laser Particle Size Analyzer
OH	Open Hole
PA	Pressure Accumulators
PEEK	Polyether Ether Ketone
PSD	Particle Size Distribution
PSI	Perforate-Stimulate-Isolate
R&D	Research & Development
RAG	Rohöl-Aufsuchungs Aktiengesellschaft
SCC	Stress Corrosion Cracking
SEM	Scanning Electron Microscopy
$SrSO_4$	Strontium sulphate
SSiC	Sintered Silicon Carbide
STT	Shunt Tube Technology
TSO	Tip Screen Out
US	Ultrasonic
WT	Water Tank

Table of content

Page

1 Introduction

Sand production is a well-known undesired phenomenon in the Exploration & Production (E&P) industry. This is because sand causes many problems that impair hydrocarbon production. Sand causes erosion in downhole equipment such as production string including safety installations (e.g. subsurface safety valves) and also in surface equipment. Sooner or later this may lead to production being shut-in with a consequential lower recovery factor and loss of otherwise producible reserves if a given well has to be prematurely plugged and abandoned [1, p. 1].

An unconsolidated (or poorly consolidated) reservoir is defined as a sand formation where the sand grains are not well cemented to one another [2], [3, p. 2]. Such a reservoir is unequivocally a candidate for sand production when it is exploited for oil and gas. A large number of oil and gas reservoirs in areas such as the Campos Basin offshore Brazil, Gulf of Mexico, North Sea and West Africa are unconsolidated reservoirs [4, p. 98], [5]. Moreover, liquid oil (oil as opposed to oil from tar sands) having an API gravity less than 20°, referred to as Heavy Oil (HO) or Extra Heavy Oil (EHO), accounts for a total of 70% of all types of oil worldwide in unconsolidated reservoirs [6], [7, p. 5], [3, p. 2]. Approximately 15% of worldwide oil has an API gravity between 10° and 20° (HO) and 55% has an API gravity below 10° (EHO) [3, p. 2]. API gravity is a measure of specific gravity but gives a good indication of viscosity; the lower the API gravity the higher the viscosity [8]. The world's largest HO and EHO oil deposits amounting to approximately 60% of the world's known HO and EHO deposits are located in Canada and Venezuela. The majority of these reservoirs are unconsolidated sandstone which being a principal source of today's oil supply are highly vulnerable to sand production [3, pp. 2-8].

Sand production is also a concern in mature fields, causing operational challenges and Health, Safety & Environment (HSE) risks [9], [1]. Although it may not seem particularly important to address the problem of sand production from mature fields considering the fact that individual fields may have marginal oil and gas production it is worth to acknowledge that mature fields as a whole contribute to a remarkable 67% of world's daily oil and gas production [10]. Some of the many mature fields in which sand production is an issue are in Austria in Vienna Basin and internationally in Offshore Brunei, Faja in Venezuela and llanos in Columbia etc. [9, p. 1], [1, p. 2]. For sustainable oil and gas production safeguarding production from these mature fields represents more of a requirement than an option.

The unconsolidated reservoirs and mature fields that are highly prone to sand production and at the same time are the key sources of oil and gas give rise to the necessity to adopt a robust sand management system. Various sand control methods from stand-alone screens (such as wire-wrapped screens, pre-packed screens and woven screens), slotted liners, expandable screens, resin consolidation, gravel packs to Tip Screen Out (TSO) fracture are amongst the many that are available on the market. Each and every sand control technique

has its particular advantages and disadvantages. Therefore the well completion method has to be selected based on weighing numerous criteria such as design complexity, installation feasibility, robustness, risk of sand production, plugging risk, erosion risk, well productivity and economic feasibility [11].

Screen only systems (such as wire-wrapped screens) and gravel-pack completions are amongst the common options used in long horizontal wellbores in unconsolidated reservoirs [12]. However, in the Danish offshore oil and gas fields two types of completions with stimulation have been used to achieve economic production rates, namely, the Perforate-Stimulate-Isolate (PSI) principle as shown in Figure 1a) where each section is separately fracced [13] and the Controlled Acid Jetting (CAJ) as shown in Figure 1b) which is a liner principle [14]. Figure 1c) depicts how the PSI system and CAJ system appear in combination downhole. These completions have been effective for horizontal wells in low permeability reservoirs.

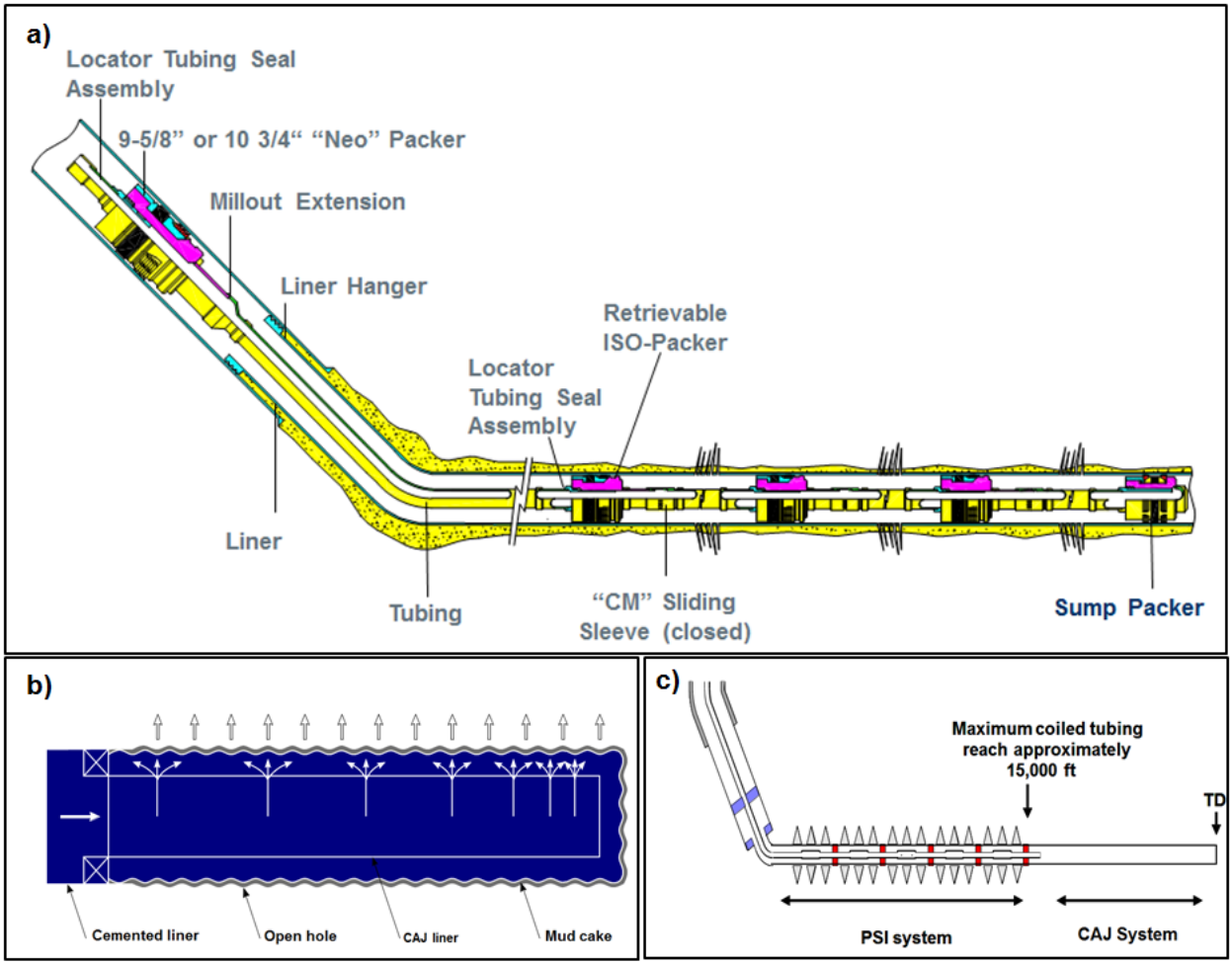

Figure 1: Completion Systems in the Danish Offshore Area. a) PSI System; b) CAJ System; c) Overview of PSI System and CAJ System together [15]

Implementation of such completion methods in the low permeability and porosity region of the Danish Offshore Sector required that the pressure loss across the productive zone to be kept at a bare minimum. Therefore the Sliding Side Door (SSD) which allows for selective production was placed directly opposite the perforation. However the proppant backflow during clean-up as well as bean-up procedures not only gave rise to erosion on downhole and surface equipment but it has also led to HSE issues such as possible tubular leaks through erosion. In addition the selectivity of the production zones is lost right from the beginning. Furthermore, the excessive clean up time required to remove the sand present in equipment such as pipelines and surface facilities e.g. separators has resulted in economic losses. All conventional sand control methods were unsatisfactory at some point in time. Maersk Oil, an E&P company, together with a ceramic manufacturing company ESK designed and developed a new sand screen with Sintered Silicon Carbide (SSiC) as the material instead of the most commonly used stainless steel. It represents an attractive alternative since a ceramic sand screen is not only able to filter the sand in the production but is also highly resistant to erosion. The ceramic sand screen has proved to be highly effective in the Danish offshore operations because it was able to solve the two major problems, namely it prevents proppant backflow in artificially fractured reservoirs and functions as a regular sand screen to prevent sand production in unconsolidated sandstone formations [SPE 146721].

Lime-scale is a renowned term, be it in the household or the oil field. Lime-scale precipitates from hard water, while releasing carbon dioxide, it most commonly forms as calcium carbonate ($CaCO_3$). Naturally radioactive scales such as barium sulphate ($BaSO_4$) and strontium sulphate ($SrSO_4$) may also form. Any sort of scale hinders the production of hydrocarbons. A prerequisite for scale to form is the presence of water. In the oil and gas industry, scaling is a major problem since the production of hydrocarbons is always accompanied by a certain amount of water depending on the maturity of the field. The percentage of water of the total volume of production (referred to as water cut) increases with the age of a field, hence scaling becomes more significant as the field ages. There are many factors that have an influence on scale precipitation such factors are changes in temperature, changes in pressure and changes in concentration due to evaporation.

Plugging and scaling are major issues in the oil and gas industry. Plugging is a common term used in the oil and gas sector, described as the blocking of the near-wellbore formation region, reducing productivity caused by any particles mobilized due to stimulation, completion, workover or enhanced recovery [9]. Sand screens are used as a major sand control technique but can become plugged. Sand screen sizing is a function of the particle size distribution of sand mobilized from the formation. There are many screen sizing selection criteria such as those of Saucier, Coberly, Schwartz and others [16, p. 1]. Analysis of plugged screens shows that the plugging material mainly consists of corrosion products and clay [17, pp. 4-7]. Various sand screens have various thresholds to plugging behaviour. Wire-wrapped screens are generally considered to be the most difficult to plug [18, p. 23]. Scaling can also cause plugging of perforations (production and injection) as well as the near wellbore zone. Scaling is known to cause various problems such as reduced tubing inside

diameter causing higher pressure losses. This not only causes decline in production rate but also results in greater energy consumption required to overcome higher friction losses in production tubing and flow lines. Scale can also deposit on artificial lift components causing the artificial lift system to fail. Radioactive scales such as $BaSO_4$ and $SrSO_4$ may also start to deposit on the wellbore giving rise to HSE concerns and additional costs for disposing. From the surface engineering point of view, plugging of surface facilities and pipelines represents a significant problem. Additionally, plugging materials which can also consist of corrosion products can choke the perforations and downhole equipment [17, pp. 4-7].

At present, it is clear that ceramic material is highly erosion and corrosion resistant. However, it is still not fully understood how the plugging and scaling behaviour of ceramic screens compares with the state of the art (metal) screens.

In this thesis an in-depth comparison is made of selected sand screen types and materials by conducting sand retention and scaling behaviour tests to analyse plugging and scaling behaviour. The investigations of the sand screen materials are conducted under simulated reservoir conditions and downhole conditions.

2 Problem Definition

The E&P companies encounter huge economic losses due to sand production, scaling and plugging. On one hand equipment replacement and well workovers due to scaling and plugging result in high cost, and on the other hand economically recoverable reserves that are left unproduced due to premature abandonment instigated by sand production and scaling is another contributor to economic losses for an E&P company [1, p. 1] [19, p. 777].

2.1 Causes of Sand Production and Sand Control Problems

Besides the two main sources for sand production (unconsolidated reservoir and mature fields) mentioned in Section 1, there are several other causes. Many wells such as in the Niger-Delta, showed onset of sand production already at the initial production phase. This is due to the fact that the stress situation in the formation has been altered due to fluid losses during drilling, completions and work-overs. Workovers such as re-perforation and/or stimulation changes the characteristics of the formation, specifically altering the cohesive bond between the sandstone grains [19, p. 779]. Additionally, fluctuations in pressure and stress downhole i.e. fatigue effects are other causes for sand production.

When a well suddenly produces sand, the flowing bottom-hole pressure decreases meanwhile the effective stress increases, hence the reservoir rock collapses which in turn causes subsidence [20]. This is a common result of downhole stress changes.

One of the main criterion looked at before selecting a sand control technique is the Particle Size Distribution (PSD) curve. The PSD is defined as the weight or net volume of solid particles that fall into respective size ranges, represented in terms of percentage of the total solids of all sizes in the sample of interest [21]. Information such as nature of the sand grains, percentage of fines and etc. can be deciphered from the PSD results. The PSD analysis together with various sizing criteria [16], enables the suitable selection of slot opening for a selected sand screen. However, the difficulty lies in obtaining a representative sand sample from the reservoir. It would be ideal to obtain a PSD measurement from a reservoir core. Coring is very costly and often not done in well-known areas. Moreover the gain is rather limited as loses of core can occur during coring operations. However, it is rarely possible due to the fact that the reservoir is unconsolidated, hence obtaining a core is not possible. The other frequent occurrence is that cores are attained at the beginning of the field life e.g. during wildcat drilling for petro-physical data. Therefore when the field is mature, there may be hardly any cores left for PSD analyses. To obtain a fresh core sample would be very expensive and this is almost always not done. Therefore in most instances, produced sand is collected and PSD is determined. This is somewhat rather inaccurate, because the heavier components of the produced sand sink downhole due to their weight and the sand produced to surface is mainly the lighter particles. Furthermore, during the movement of the produced sand from downhole to surface, where it is collected, the sand grains maybe subject to wear and become smaller. Hence the PSD of the produced sand is not a valid representation of

the actual sand components. Despite the flaws in the method of attaining PSD of a reservoir sand, it is still the conventional method used till date.

2.2 Causes of Scaling

Scale is an inorganic and solid material that precipitates in the reservoir, near the wellbore or in subsurface and surface equipment during oil and gas production or related operations e.g. water injection.

The build-up of scales as seen in Figure 2 may partially or completely block production from wells causing millions of dollars in damage annually [22]. Cost is incurred not only for required workovers, but also for the significant production losses.

Figure 2: Scaling in Production Tubing [22, p. 1]

The formation of scale can be explained by looking at **eq.1** [23] and **eq.2** [23]**.** When carbon dioxide (CO_2) is in contact with water (H_2O), carbonic acid (H_2CO_3) is formed which further dissociates to form hydrogen ions (H^+) and bicarbonate ions (HCO_3^-) as shown in **eq.1** [23] . The bicarbonate ions could further ionize to form carbonate ions (CO_3^{2-}).

$$CO_2 + H_2O \leftrightarrow H_2CO_3 \leftrightarrow H^+ + HCO_3^- \leftrightarrow 2H^+ + CO_3^{2-} \qquad (1)$$

The bicarbonate ion from **eq.1** [23] reacts with calcium ions (Ca^{2+}) present in the surrounding causing $CaCO_3$ precipitation, expressed as follows in **eq.2** [23]

$$Ca^{2+} + 2HCO_3^- \leftrightarrow Ca(HCO3)_2 \leftrightarrow H_2O + CO_2 + CaCO_3 \qquad (2)$$

The three key causes of scale production are:

i. Pressure decline
ii. Temperature increase
iii. pH change

A decline in pressure caused by the release of CO_2, triggers the equilibrium to shift to the right resulting in the precipitation of calcium carbonate. It is perhaps important to mention that a pressure reduction from formation pressure to near wellbore region pressure is required in order produce oil and gas.

Furthermore scale deposition occurs in near wellbore regions where reduction in flow area due to constrains in production exist. These constrains could be due to tubing restrictions, nipples, safety valves and gas-lift mandrels [22, p. 32] . This follows Bernoulli's principle, where an increase in fluid velocity is accompanied by a decrease in pressure [24, p. 21]. An example of such scale depositions is displayed in Figure 3. In the same way, installation of sand screens downhole also causes a sudden change in cross sectional area produced media to flow through posing a constrain and therefore a reduction in pressure in keeping with Bernoulli's principle. Therefore precipitation of scale is also possible on sand screens due to change in cross sectional area. This may be compared to day to day situations like scale precipitation on shower heads and tap filters.

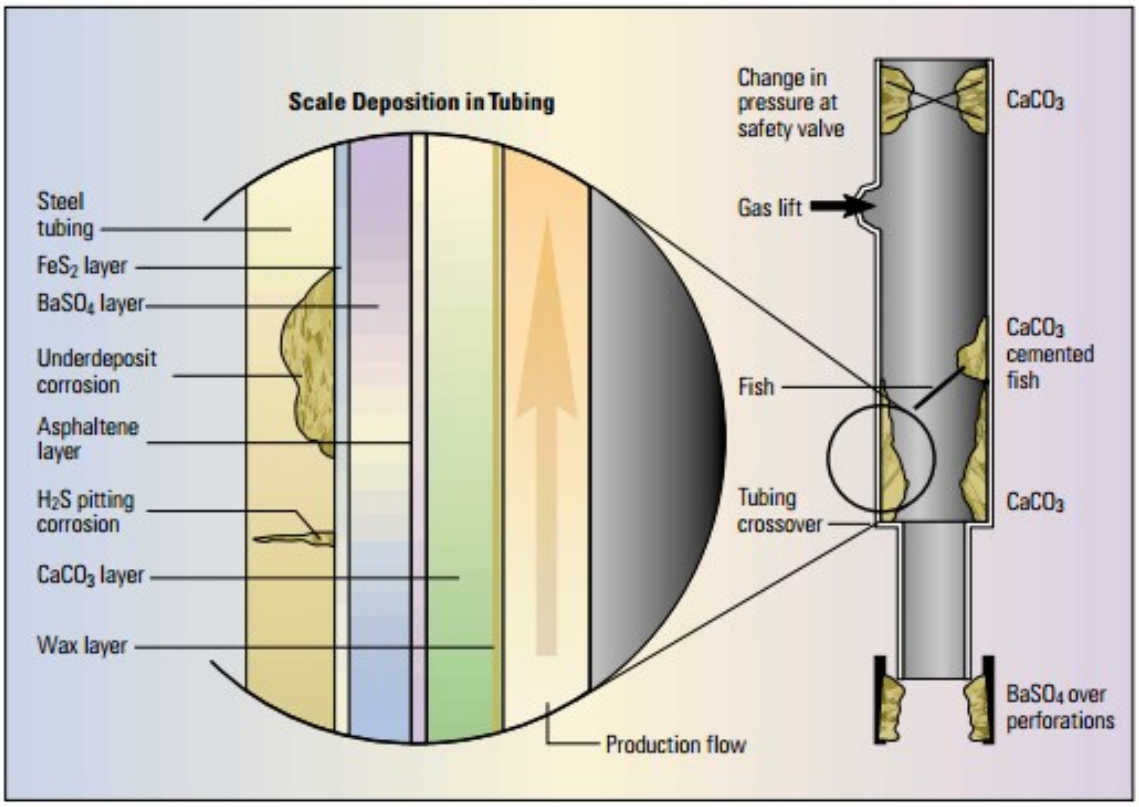

Figure 3: Scale Deposition due to Reduction in Cross Sectional Area [22, p. 32]

Gasses such as CO_2 are less soluble in warm solution than in cold solution. Thus, an increase in solution temperature causes a reduction in the amount of gas in the liquid. This is turn causes the equilibrium of **eq.1** [23] to shift to the right, to replace the dissipated gas and at the same give rise to the formation of more $CaCO_3$.

The pH is a measure of acidity based on the amount of free hydrogen ions present. (The pH is the negative log to the base 10 of the hydrogen ion concentration). The more free hydrogen ions present, the lower is the pH value, i.e. the more acidic is the medium. In general, with CO_2 in solution, free hydrogen ions are present, as can be seen in **eq.1** [23]**,** hence acidic [23]. Therefore referring to **eq.2** [23] , when pH increases, the solution becomes more basic and induces CO_2 to move from aqueous phase (carbonic acid) to gaseous phase, i.e. the equilibrium of the system moves to the right. This causes precipitation of $CaCO_3$. It is of relevance to note that usually in the process of drilling or bringing a well to production, the desired pH value is in the range of 8-9 [25, p. 10], i.e alkaline which of course instigates scale deposition. The reason behind the preference for a higher pH downhole is mainly to neutralize the sour components (such as hydrogen sulfide, H_2S and/or CO_2) that are present or possibly present.

In summary, calcium carbonate precipitation may occur when there is any occurrence or combination of the following: a decline in pressure, an increase in temperature, an increase in pH value, all of which possible scenarios in oil and gas production.

2.3 Sand Production, Scaling and Plugging in Combination

Sand production, scaling and plugging behaviour occurs often at the same time. Hence it is essential to look at these problems as a combination and not in isolation in order to understand the big picture. An anecdote of a common sequence of events in an oil and gas field may help to describe the problem in detail. A metal sand screen regardless of any type (slotted liner or wire-wrapped screen) is installed downhole to prevent sand production. These screens are rarely built on a stand-alone basis instead nearly always combined with a gravel pack (GP) as shown in (Figure 4).

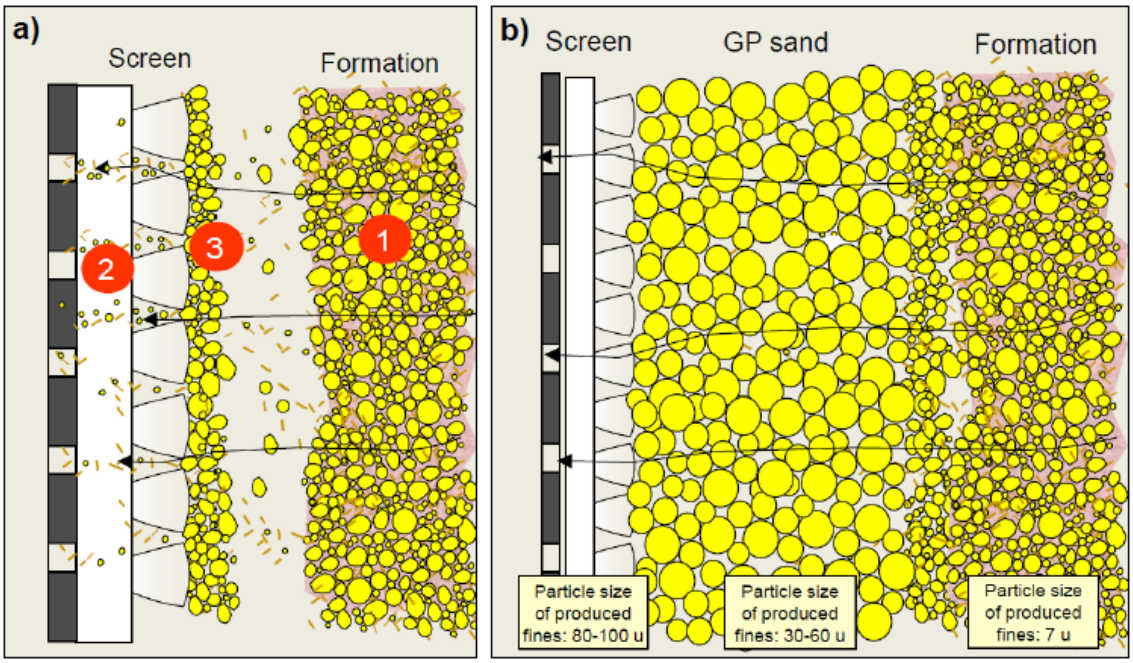

Figure 4: Sand Control in OH. a) Stand-alone Screen; b) Screen and GP [18, pp. 22,72]

An existing challenge in the oil industry is to have an ideally formed GP. An ideally formed GP should look similar to Figure 4b) which has no voids. Failing to have an properly formed GP, leads to the presence of voids which cause channelling, this then leads to sand migration and eventually hotspots are formed. Hot spots are locations where the velocity of produced medium and formation solids are higher than in comparison to other sections of the screen, resulting in erosion [26]. Open Hole (OH) gravel-packing [always accompanied with a screen as shown in Figure 4b)] are common especially in offshore environments due to its assumed reliability and increased production rate [27]. However, horizontal wells with OH gravel-packing exhibit a high rate of premature screen out [27]. Despite various technologies e.g. Shunt Tube Technology (STT) [28], forming an ideal GP, i.e. without voids is still a challenge.

Assuming the GP is ideally formed, with increasing life time of the well, water cut increases. Scale starts precipitating on the surface of the metal screen forming a well-adhered scale layer around the screen resisting production fluid to flow through equally on all areas of the screen; this is termed as plugging. Production fluid is then forced to flow through the remaining unplugged sections of the screen that are free of scale causing productivity decline due to a reduced inflow area. Additionally, the plugging caused by scaling causes a creation of localised high velocity areas referred to as hot spots in non-plugged sections of the screen [29]. This causes erosion which in turn gives rise to significant amount of formation sand and GP particles to being produced. In the case of a stand-alone screen, only formation sand would be produced. Figure 5 is an example where erosion (in zoom) is evident due to plugging caused by scaling in a wire wrapped screen obtained from a borehole.

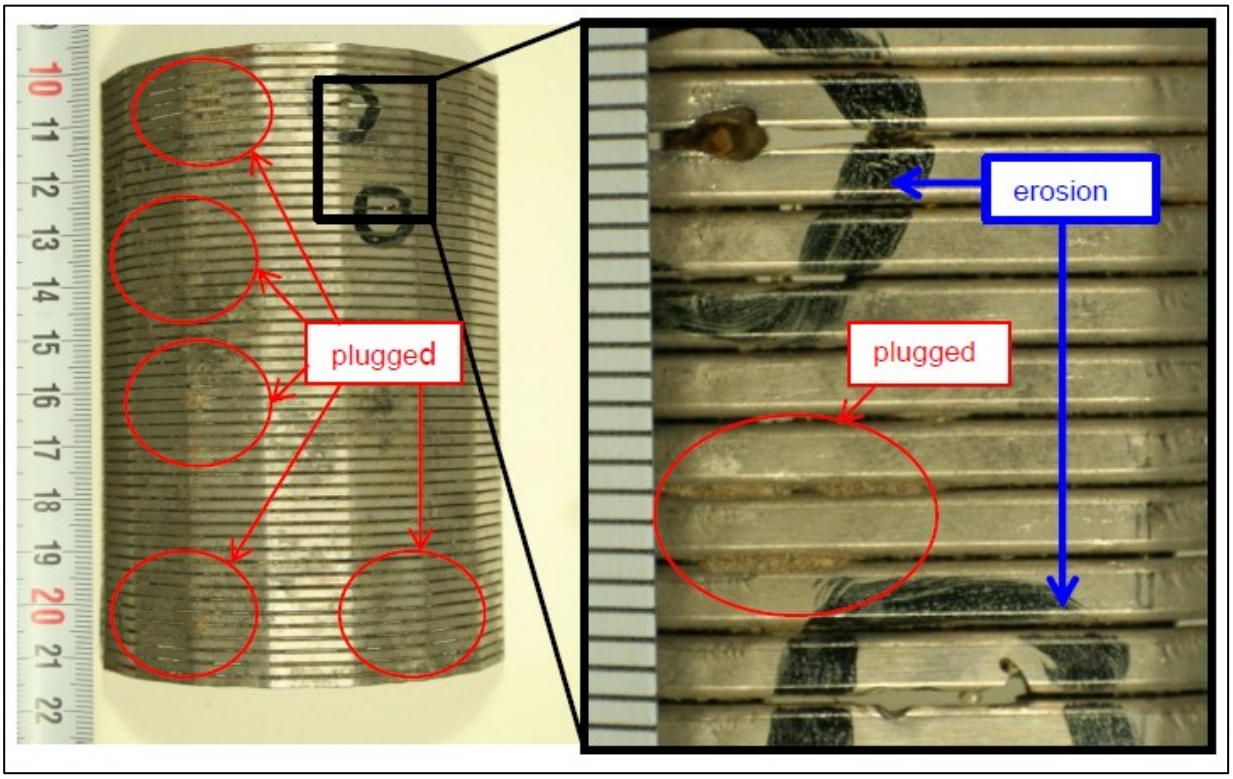

Figure 5: Hotspots due to plugging induced by scaling [30]

Therefore there is still a need for improvement in sand control techniques. It is also worth mentioning, that stainless steel EN 1.4404 (AISI 316L) is a commonly used stainless steel to combat existing problems because it is considered to be robust in any situation. Additionally it is easily available and easily welded. However it must be realized that 316L is not robust all the time. Its resistance to pitting and Stress Corrosion Cracking (SCC) is lower than other stainless steels such as EN 1.4547 (ASME S31254) and EN 1.4462 (ASME 318LN) depending particularly on increasing temperature and chloride content.

The idea of using a silicon carbide (SiC), i.e. ceramic screen is attractive because of its higher hardness and consequently better erosion resistance in comparison to stainless steel (regardless of which stainless steel) as can be seen in Table 1 [31, p. 1]

Table 1: Comparison of typical material properties [31, p. 1]

Material Properties	Stainless Steel	Hard Metal	Silicon Nitride	Silicon Carbide
Knoop Hardness, HK 0.1 GPa	<0.5 (Rc 30–40)	16	14.5	21–25
Compressive Strenght, MPa	2200	5000	>2500	2200–2500
Thermal Conductivity, W/(mK)	35–45	95	25–40	75–125
Density, g/m³	7.8	14.9	3.2	3.1–3.2
Flexural Strenght (4 Point Bending), MPa	N/A	1550	700–800	400–650
Young's Modulus, GPa	200	520–620	310	410
Fracture Toughness K_{ic}, MPa $m^{0.5}$	N/A	10–20	6	4–6

Additionally, the resistance to corrosion of ceramic screen built from SiC is indisputably higher than a stainless steel material from which a typical sand screen is manufactured. For example, Figure 6 shows the corrosion resistance against H_2SO_4 of stainless steel and ceramic. However there are other oil field chemicals in principle showing similar behaviours.

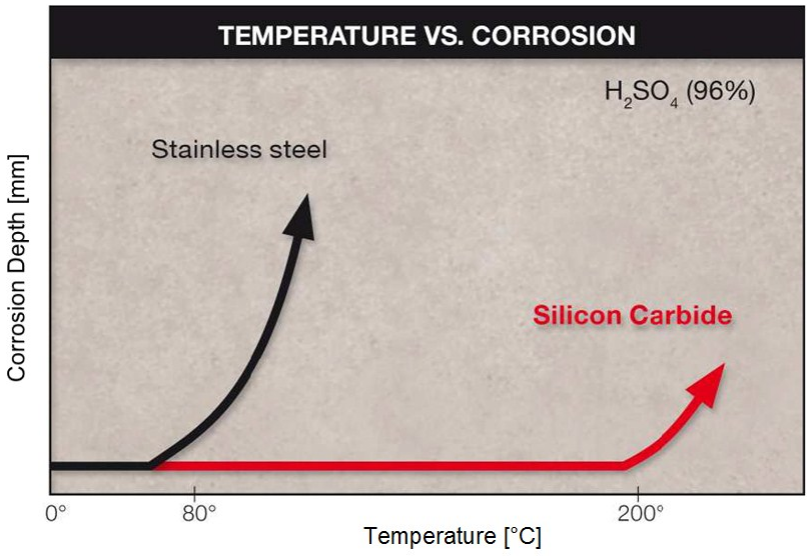

Figure 6: Corrosion Resistance of Stainless Steel and Silicon Carbide [32, p. 3]

However at present less is known about the behaviour of ceramic sand screen other than its being erosion resistant, its predominant characteristic. Thus the aim of this thesis lies is investigating the behaviour of ceramic sand screens in comparison to the standard metallic screens available in the market in terms of sand production, scaling and plugging behaviour.

3 Comparison Tests on Selected Sand Screen Materials

Numerous laboratory investigations of plugging behaviour due to scaling and sand production on various sand screen materials are carried out under simulated reservoir conditions whenever possible. The test conditions are suited to fit the reservoir conditions where possible. The analysis of plugging behaviour due to sand production is conducted via Sand Retention Test. Before going through the experimental methods it is important to have an overview of the sand retention test as described in Section 3.1 and its test variables as described in Section 3.1.4.

The study of scaling behaviour is examined via scaling behaviour test. The overview of scaling behaviour and the scaling behaviour test variables is described in Sections 3.2 and 3.2.1, respectively.

3.1 Description of Sand Retention Test

Laboratory sand retention test is a standard test procedure often conducted for the optimal sand screen selection. This is because sand retention test gives a better understanding of retention and plugging performance [33, p. 1], [34, p. 1], [35, p. 1].

The Sand Retention Test Rig at ESK is a sand retention flow loop consisting of two sections, namely the main loop and the sand slurry loop. The working principle of the Sand Retention Test conducted in this thesis is identical to that described by Weatherford [33, pp. 3-4] and Hydro Oil & Energy [35, p. 8] and therefore corresponds to the ‘state of the art’. The sand retention flow loop diagram is shown in Figure 7. A photo of the Sand Retention Test Rig is attached in Appendix A.

3.1.1 Sand Slurry Loop

The sand slurry loop (highlighted in blue in Figure 7) injects sand slurry into the main loop simulating the sand production that happens in an unconsolidated reservoir. The sand slurry is prepared in the mixing tank using sand and water in appropriate volumes (Refer Section 3.1.4.1b)). The water is obtained via water Tank, WT-10. The slurry is made up using a stirrer, after which this mixture is injected into the main loop via Peristaltic Pump VF-10. This causes the sand slurry to mix with the medium of the main loop at Injection Point A, upstream of the measuring cell.

3.1.2 Main Loop

The main loop (highlighted in yellow in Figure 7) pumps the medium continuously. The medium after Injection Point A is a mixture of water and sand slurry which simulates the fluids produced in the field. As can be seen in Figure 7, medium from the WT-15 is circulated in the main loop via Peristaltic Pump VF-15. This mixture flows through the measuring cell which contains the test screens. Most of the sand is retained forming a filter cake at the test

screen. The resulting filtrate can either be routed through the particle counter back to the water tank or circulated directly to the water tank. If the medium is routed through the Particle Counter, samples can be collected downstream of the Particle Counter at Control Valve, CV-4.

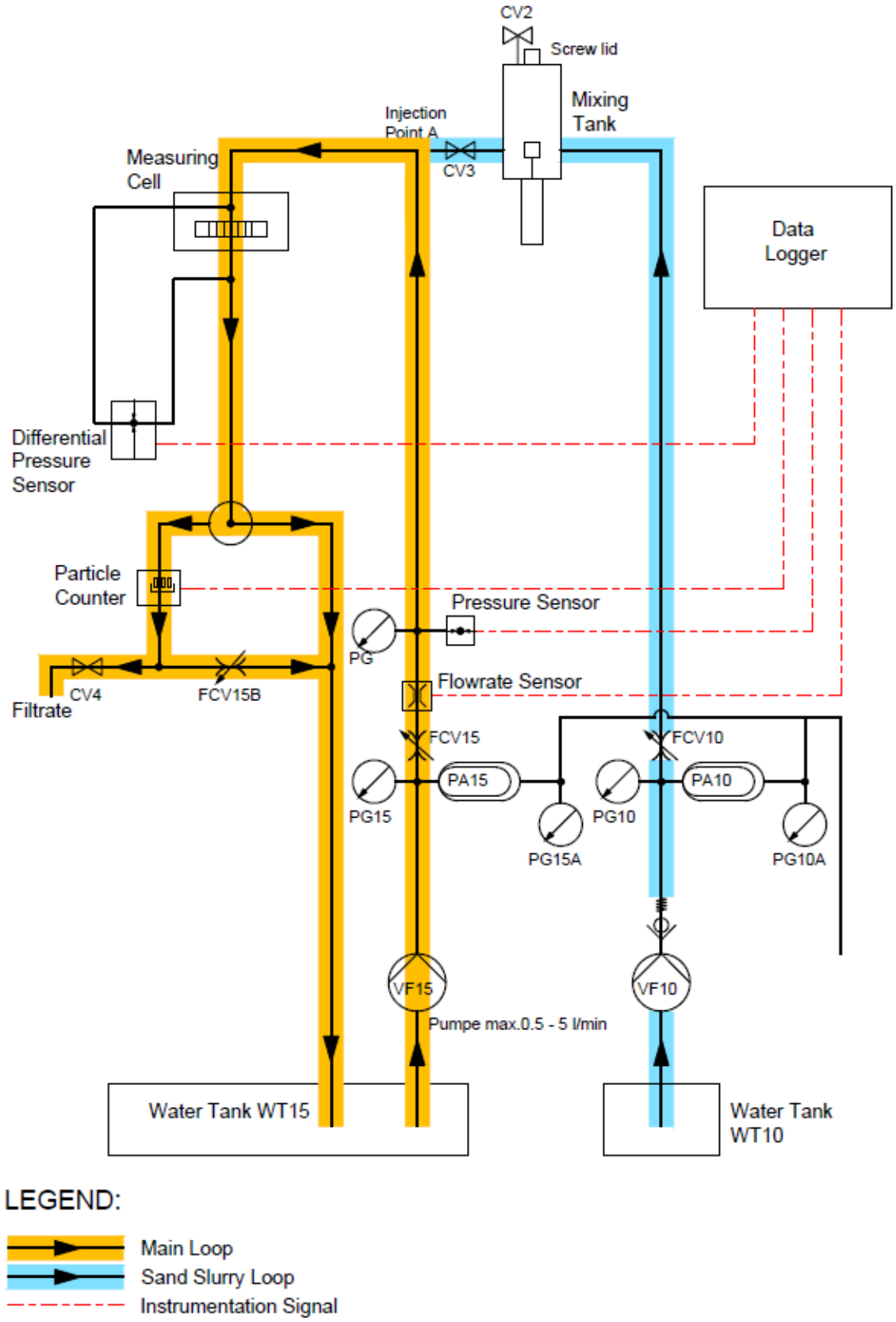

Figure 7: Sand Retention Test Flow Loop

3.1.3 Details of Other Components

Due to the fact that pumps VF-10 and VF-15 are peristaltic pumps with 2 lobes, the outflow pulsates. Hence pressure accumulators, PA-10 and PA-15 are installed for pumps VF-10 and VF-15, respectively to ensure that the outflow pressure from the pumps is smoothened. The outflow from VF-10 and VF-15 is controlled by Flow Control Valves, FCV-10A and FCV-15A, respectively.

The output data namely, system pressure, differential pressure across the measuring cell and flowrate of the main loop is acquired throughout the experiment via the Picolog Data Acquisition Software, referred to as data logger.

3.1.4 Sand Retention Test Variables

Before conducting the experiment, the controlled variables and independent variables are identified. The controlled variables are parameters kept constant throughout the experiment. The controlled variables are chosen in such a way that it is suitable to test all independent variables in the sand retention procedure. The independent variables are the parameters changed such as types of sandscreen, slot openings and etc.

3.1.4.1 Controlled Variables

a) Reservoir Sand Sample

The reservoir sand used throughout for the sand retention test is obtained from the cyclone of the well RAG-022 in Zistersdorf belonging to the Vienna Basin operated by RAG. The Sarmat horizon belongs to a highly permeable and poorly consolidated reservoir, therefore sand production is evident [3]. The sand sample obtained from the cyclone is indeed finer compared to that of the horizon. A sand sample from the core of the producing horizon would be a better representation of the producing horizon; however the cyclone sand sample used is believed to be sufficient to simulate a sand producing reservoir in laboratory size to investigate and compare the influence of various sand screen materials on plugging behaviour.

The sand obtained is mixed with production fluids. Therefore the sand is cleansed via low temperature thermal desorption which is a thermal treatment where the sand sample is heated up in a furnace to temperatures between 700 °C and 800 ° C. This is a technique to remove organic materials efficiently [36]. However due to laboratory limitations the sand sample is heated up in two temperature ramps instead of a single ramp. The temperature ramp used is as depicted in Figure 8 below.

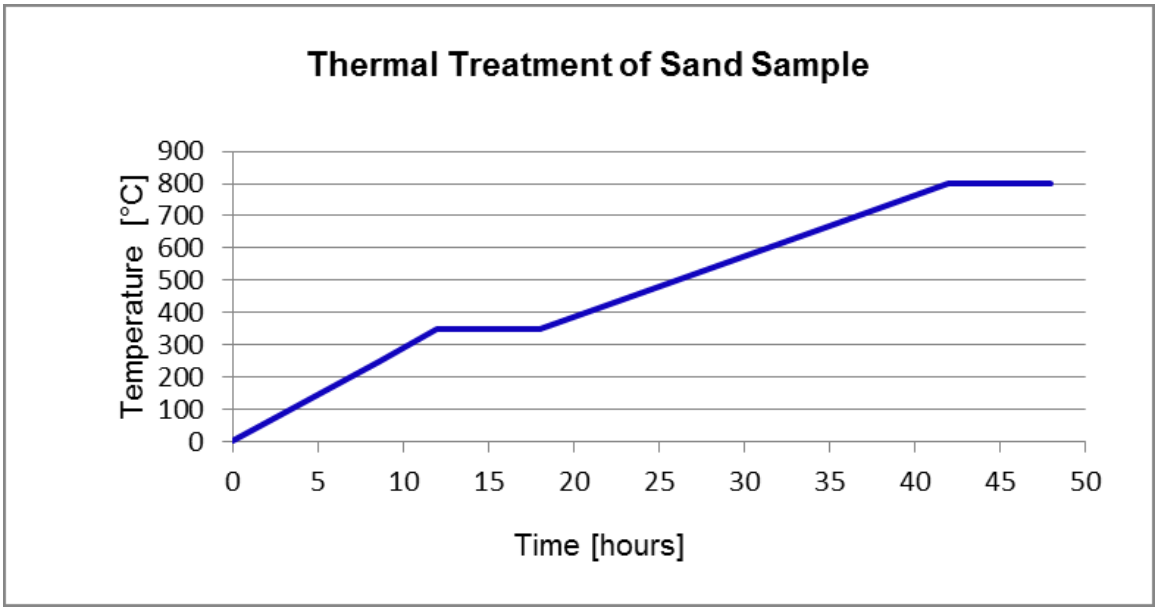

Figure 8: Thermal Treatment of Sand Sample

The PSD of the sand is as shown below in Figure 9. This indicates that the sand size distribution is centred around 100 µm.

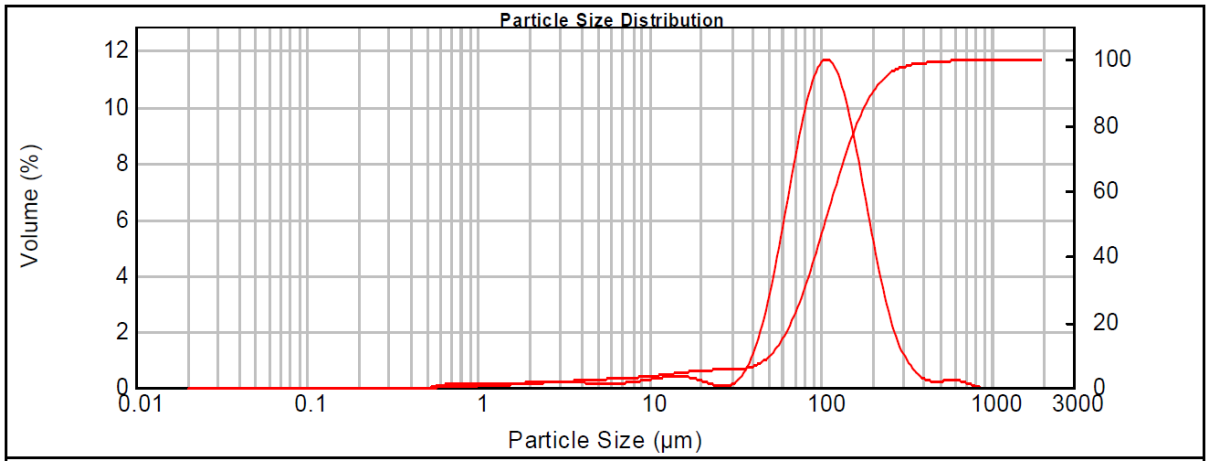

Figure 9: PSD of reservoir sand sample

b) Percentage of sand in the sand slurry

The percentage of sand particles in the sand slurry is set to be 5% w/w. Firstly, with 5% w/w sand concentration the experimental setup is able to produce a filter cake thickness of about 25 mm which is about one-third the length of the measuring cell. This amount is sufficient to obtain a pressure build up in the system. Secondly, it is a sufficient amount to

enable other tests to be conducted, such as PSD tests on the filtrate and residue. Additionally, a producing well which produces up to 1% of sand is commonly accepted. However if the sand production increases above 10%, this is not acceptable and definitely requires a sand control technique [37]. Therefore once again 5% is then considered to be a good average value.

c) Medium for sand slurry

The slurry is made of sand with volumes specified in the section above along with water.

d) Slurry Injection Rate

First the sand slurry injection pump, VF-15 is calibrated. See Figure 10. The quadratic equation obtained through the method of least squares with an accuracy of R^2=0.9989 as shown in Figure 10 is fed into the Picolog Data Acquisition Software. This then allows setting the position of VF-10 pump regulator in order to achieve a required flow rate. After calibration, the slurry injection rate has been optimized such that sand flows continuously between the slurry tank and injection point. A slow and reproducible buildup of the filter cake is also ensured. It is established that 150ml/min is an optimal flow rate. The slurry injection rate ranges between 130ml/min and 160ml/min due to back pressure and how much FCV-10 is opened.

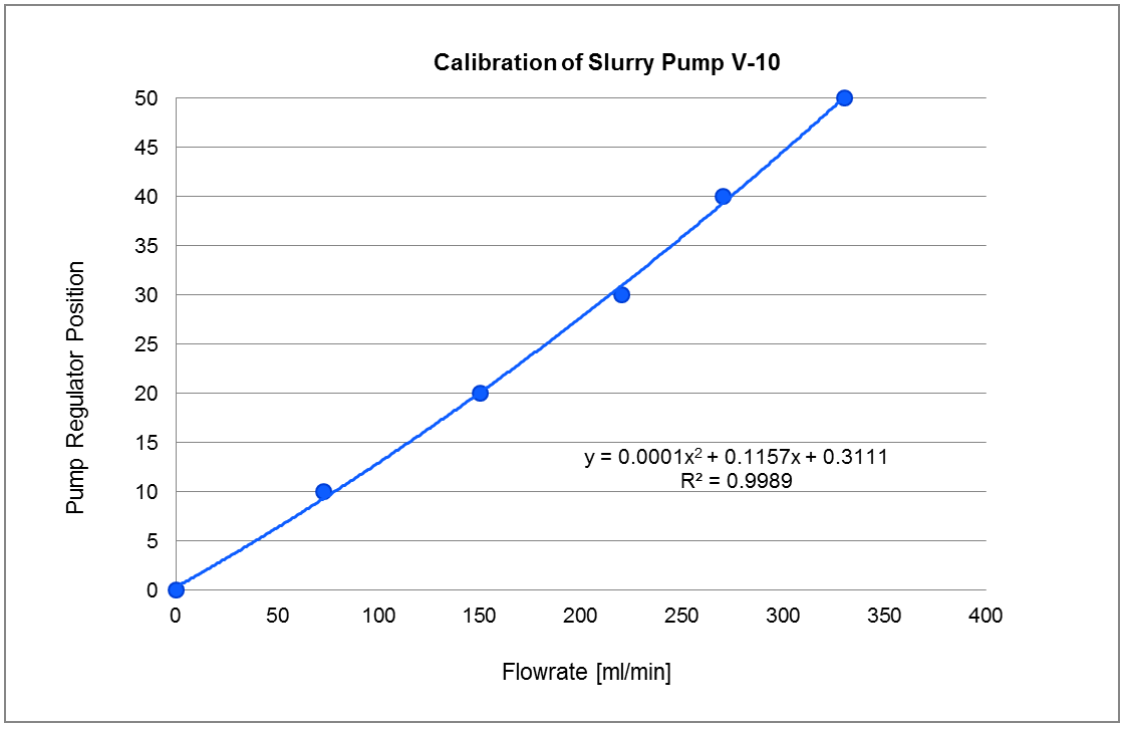

Figure 10: Calibration of Slurry Pump VF-10

e) Flowrate in the main loop

The main loop pump VF-15 is calibrated as depicted in Figure 11. The best fit equation is determined to be a quadratic equation obtained through the method of least squares with an accuracy of R^2=0.9979 which is inserted into the Data Acquisition Software. This then allows setting the position of VF-15 pump regulator in order to achieve a certain flow rate.

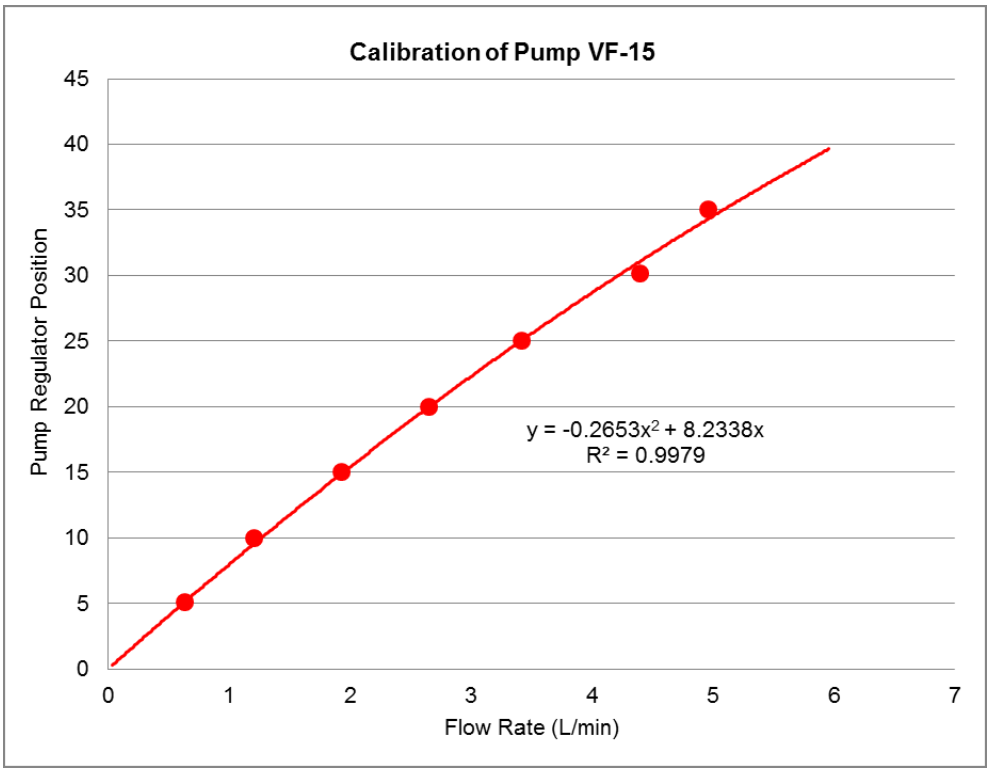

Figure 11: Calibration of Pump VF-15

The flowrate in the main loop is maintained at a low and constant value of 0.25L/min regardless of which slot opening is used. The value of 0.25 L/min is chosen because this flowrate gives rise to a reproducible build-up of the filtercake. A comparison of parameters adopted by Weatherford for their sand retention test rig [34, p. 5], field conditions [34, p. 5] and used in this thesis is shown in Table 2.

Table 2: Comparison of test and field parameters

Parameter	Standard Test as per SPE 151768	Field	Test Carried Out for this Thesis
Aperture Area [cm2]	5.06	depends on well parameters	0.26-0.60
Flowrate [mL/min]	500	10^4-10^6	250
Sand concentration Xanthan [g/l]	100	n/a	n/a
Sand Rate[ml/min]	0.50	unknown	130-160
Sand Concentration in test cell [g/l]	0.01	unknown	50.0
Velocity [cm/s]	1.7	0.01-0.10	10.6-24.4
Reference	[33, p. 5]	[33, p. 5]	n/a

The higher velocity used in the tests carried out for this thesis, as compared to Weatherford for their laboratory tests, as seen in Table 2, is selected to achieve results in a reasonable time frame. The higher velocity has no influence on the results. In fact, with higher velocity, perhaps the effect of erosion on the selected material could be seen.

f) Thickness of filter cake

The slurry test is conducted until the thickness of the filter cake in the measuring cell is about 25 mm which is marked with red line for a possible visual observation. It is of utmost importance to maintain a constant height of filter cake because it influences directly the pressure drop across the filter and thus the measured differential pressure.

3.1.4.2 Independent Variables

a) Types of Screens

There are 5 types of screens used to understand the behavior of sand retention influenced by the type of the sand screen, the material of the sand screen and the effect of erosion. The 5 types of sand screens are 316L stainless steel wire-wrapped screen,

ceramic screen with keystone design, 316L stainless steel screen with keystone design, roughened 316L wire-wrapped screen and roughened 316L stainless steel screen with keystone design.

The 316L wire-wrapped sand screen as shown in Figure 12a) usually together with GP is the standard stainless steel wire-wrapped sand screen available on the market used to prevent sand production in unconsolidated reservoirs. The ceramic sand screens with keystone design manufactured by ESK, Figure 12b) is constructed to the design invented for the use in the Danish Offshore Sector to protect the SSD [4].

Figure 12: Sand Screen. a) Wire-wrapped [38]; b) Ceramic with Keystone Design [39]

The difference in design between the standard 316L stainless steel wire-wrapped sand screen and ceramic sand screen with keystone design is depicted in Figure 13a) and Figure 13b), respectively.

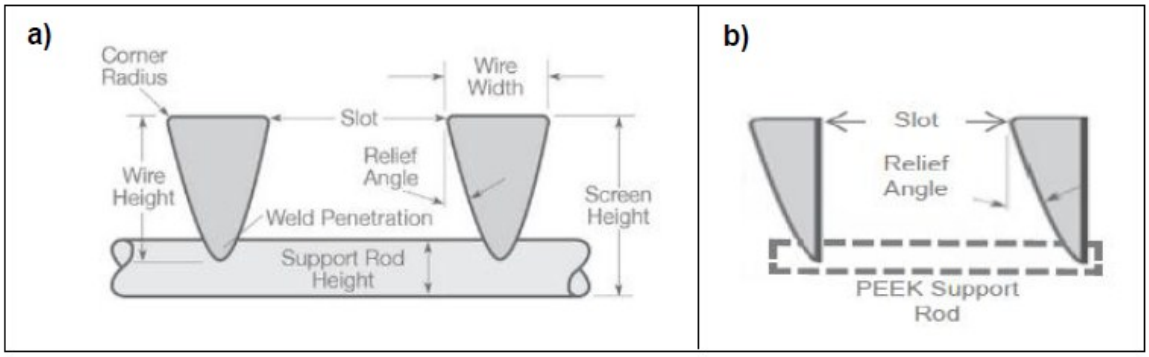

Figure 13: Sand Screen Cross Section. a) Wire-wrapped Screen [40]; b) Ceramic Screen with Keystone Design

The wire-wrapped sand screen has a support rod welded to the screen. The keystone design was selected for the manufacture of the ceramic sand screen for convenience in manufacturing. Since it has proved to serve the purpose, it has been successfully applied in the Danish Offshore Sector by MAERSK, in Gaiselberg field Austria by RAG and in Bolivia by British Gas (BG). This design was maintained. The ceramic sand screen with keystone design has a Polyether Ether Ketone (PEEK) support rod attached to it to ensure that the ceramic rings do not rotate, i.e. keeping the slot openings constant. Both, wire-wrapped sand screen and ceramic screen with keystone design have narrower slot opening on the outside than the inside to allow high laminar flowrate and prevent plugging of the slots. This is because any particle that succeeds in flowing through the narrow slot on the outside surface will continue to flow into the production tubing without clogging the slot [31]. The 316L Stainless Steel sand screen with keystone design was manufactured to have the exact same design as the ceramic sand screen with keystone design. This allowed for the accurate comparison of material without the influence of the design.

Additionally, Sand Retention Tests are conducted with roughened stainless steel screens, wire-wrapped and keystone design, with slot openings of 150 µm. This is done to simulate an eroded surface, hence to be able to understand the influence of erosion. The screens are roughened by blasting with boron carbide (B_4C).

For the purpose of laboratory tests, the screens were fabricated as shown in Figure 14. This is to ensure that each type of screen (Item No. 3 in Appendix B) fits in the measuring cell of the Sand Retention Test Rig. Appendix B gives a clear picture of the measuring cell assembly.

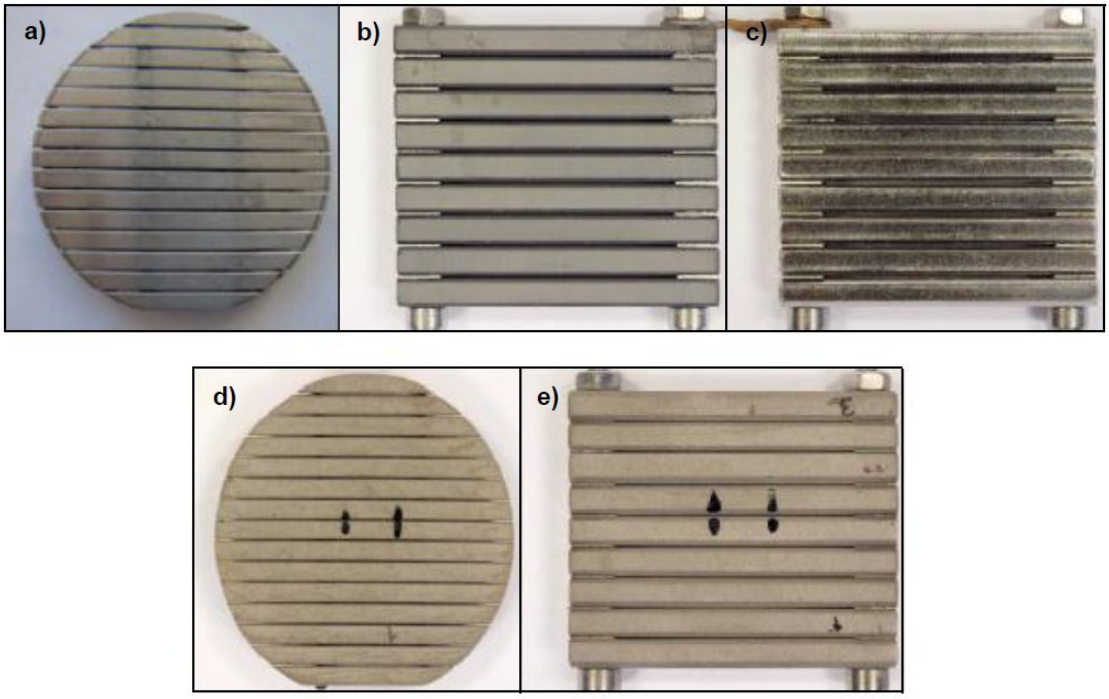

Figure 14: Sand Screens for Laboratory Use[1, 2]. a) Stainless Steel Wire-wrapped Screen; b) Ceramic Screen with Keystone Design; c) Stainless Steel Screen with Keystone Design; d) Sand Blasted Stainless Steel Wire-wrapped Screen; e) Sand Blasted Stainless Steel Screen with Keystone Design

b) Slot Opening of Sand Screen

The slot openings chosen are 150 µm, 200 µm and 250 µm, although the PSD for the sand sample shows that the sand size distribution is predominantly around 100 µm. This is sufficient to investigate the influence of slot size on sand retention test behaviour.

The wire-wrapped screens as shown in Figure 14a) with slot openings from 150 µm to 250 µm slot openings were obtained from Baker Hughes Inc.. Slot opening of the ceramic and 316L stainless steel sand screen with keystone design is varied using a spacer. They are formed by stacking 9 individual rectangular rods alternating with two stainless steel spacers of various thicknesses (150 µm, 200 µm and 250 µm) at both ends of each rectangular rod surface. This then gives the ceramic and 316L stainless steel sand screen with keystone design of the desired slot opening as shown in Figure 14b) and Figure 14c), respectively. The slot openings for the sand blasted with keystone design screens Figure 14d) and Figure 14e) are varied in the same way as the screens with keystone design using spacers.

[1] screens a) and d) are screens obtained from Baker Hughes.inc

[2] screens b) , c) and e) are manufactured in-house by ESK

The slot openings of the assembled screens with keystone design (ceramic and stainless steel) and wire-wrapped screens are checked using an optical microscope. Only one measurement series are conducted for the screen with keystone design, since the spacers were all measured individually using vernier calipers and were accurate to ± 1 µm. It can be seen in Table 3 that the stainless steel screen with keystone design and stainless steel wire-wrapped screen have significant variations from the nominal slot opening size; thus making it difficult to draw a resilient conclusion for the stainless steel wire-wrapped screen.

Table 3: Slot Opening Variations

Type of Screen	Ceramic Screen with Keystone Design	Stainless Steel Screen with Keystone Design	Stainless Steel Wire-wrapped Screen	Stainlees Steel Wire-wrapped Screen	Stainless Steel Wire-wrapped Screen
Nominal Slot Opening [µm]	200	200	150	200	250
No. Of measurements	6	18	99	82	81
Actual Slot Opening (Mean) [µm]	194.25	222.56	146.02	177.07	265.89
Standard Deviation	6.05	12.26	27.45	23.61	35.54
Minimum Value	188.14	200.00	98.79	128.16	194.91
Maximum Value	201.26	244.96	224.28	237.63	365.79

It can be deduced that ceramic screens were manufactured to satisfaction. The error in stainless steel screen with keystone design lies in the manufacture of the rectangular rods and not the spacers since they were measured and deemed to be ±1 µm accurate. In order to achieve the desired nominal slot opening size for the stainless steel screen with keystone design, the screen is always assembled with spacers of thickness of 20 µm less than the desired slot opening size. For instance, to obtain a 200 µm slot opening, spacers with thickness of 180 µm (200 µm less 20 µm) are used to assemble the screen. This results in a standard deviation of 11.90 µm instead of 12.26 µm. In terms of the wire-wrapped screen, nothing much could be done to account for the variations. Therefore the experiments are carried out using the wire-wrapped screens with variations which anyway is the scenario downhole.

c) Test Medium

The medium used for the experiment is distilled water. Water tanks, WT 10 and WT 15 as can be seen in Figure 7 are always filled with distilled water.

3.2 Description of Scaling Behaviour Evaluation Test

The analysis of the scaling behaviour is rather straightforward. The idea is to deposit $CaCO_3$ on various types of screens and coupons hereafter referred to as probes collectively. Once $CaCO_3$ is deposited on the surface of the screens or coupons, this is taken to represent scaling. The amount of scale then formed is measured. This is the first part of the scaling behavior test which is the formation of scale.

The second part of the scaling behavior test, the scale removal is conducted to analyze the formed scale in terms of how strongly it adheres to probes of different materials. This is performed by successive treatment of the probe in an Ultrasonic (US) bath.

3.2.1 Scaling Behaviour Evaluation Test Variables

Before conducting the experiment, the controlled variables and independent variables are identified in a similar manner to the sand retention test. The controlled variables are chosen in such a way that independent variables in the scaling behaviour test procedure could be evaluated. The independent variables are the parameters changed such as types of sand screens.

3.2.1.1 Controlled Variables

a) Water for scale deposition

The water used for the experiments is tap water. The water hardness in the region of Kempten/St. Mang in Germany is reasonably high in the range of 8.4 to 14.0° dH (1.3 to 2.5 mmol/l) being sufficient to obtain scale deposition. The $CaCO_3$ content of the tap water in the laboratory is measured to be 1.63 mmol/l which is within the range of moderately hard classification [41].

b) Amount of distilled water in Ultrasonic (US) bath

For the scale removal part of the scaling behaviour experiment, the US cleaner used is a Bandelin SONOREX type made in Germany as depicted in Figure 15. The US cleaner is a cleaning device that emits ultrasound through a water bath, hence the name US bath. The US bath is made up with distilled water. The amount of distilled water in the US bath is kept constant at 1 liter.

Figure 15: Bandelin SONOREX Ultrasonic Treatment Device

c) Volume of distilled water in the 1 liter 89 mm OD glass beaker placed in the US bath

US treatment can be done with distilled water alone or with a solvent to enhance cleaning effectiveness. In this thesis, the US treatment is conducted with distilled water. The volume of distilled water filled in the 1 L glass beaker of OD 89 mm in which the probes are hung during US treatment is illustrated in Figure 16 is 600 mL. The level of distilled water should be always constant for a reproducible ultrasonic energy transmission. At the same time the whole body of the probe should be submerged. For this series of experiments, an amount of 600ml is sufficient to obtain a constant level of water.

Figure 16: Experimental Setup for Part 2 of Scaling Behaviour Test- Scale Removal

d) Distance of probe from the bottom of the glass beaker

The distance of the probe from the bottom surface of the glass beaker should be same for all probes as depicted in Figure 16. This is because the energy of the ultrasonic waves is strongest at the bottom of the ultrasonic bath and becomes weaker with increasing distance from the bottom surface. Hence it is important that the probes are hung at the same height to ensure that the ultrasonic wave strength distribution is constant.

e) The number of probes per glass beaker in US bath

The number of probes per glass beaker is set to 2 per glass beaker.

3.2.1.2 Independent Variables

a) Types of Probes

There are 8 types of probes used to understand the behavior of scaling influenced by the material and type of the probe. Two of the 8 probes are identical to the probes used in the sand retention test, i.e. the ceramic sand screen with keystone design, Figure 14b) and 316L stainless steel sand screen with keystone design, Figure 14c). The other probes used; namely ceramic coupon, 316L stainless steel coupon, sand blasted ceramic coupon, sand blasted 316L stainless steel coupon, 316L stainless steel wire wrapped screen #1 and 316L stainless steel wire wrapped screen #1 ; are as shown in Figure 17.

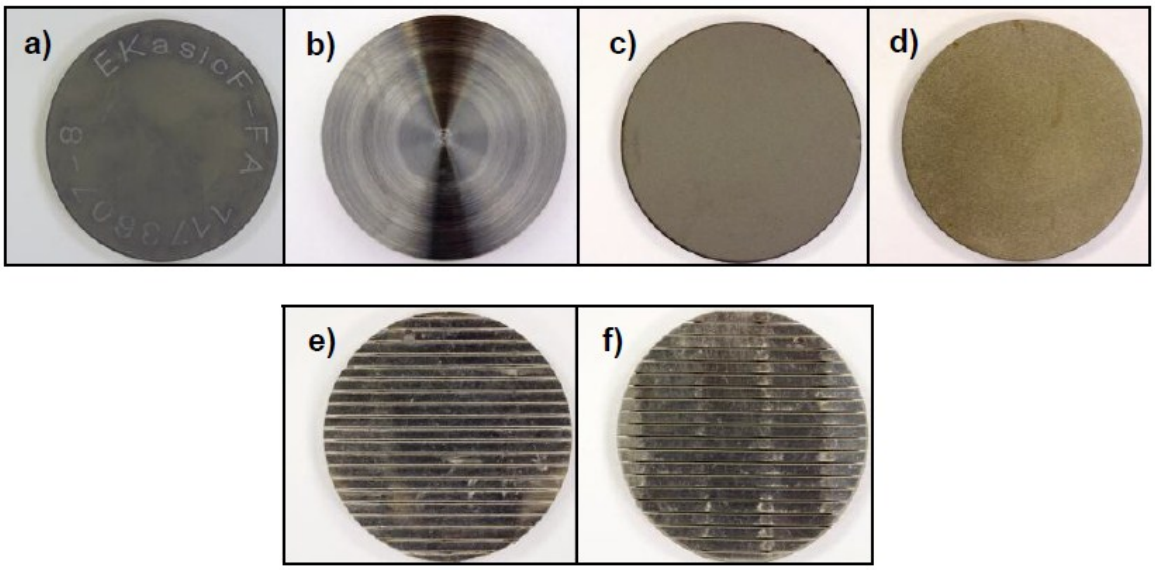

Figure 17: Probes[3,4]. a) Ceramic Coupon; b) 316L Stainless Steel Coupon; c) Roughened Ceramic Coupon; d) Roughened 316L Stainless Steel Coupon; e) 316L Wire-wrapped Screen #1; f) 316L Wire-wrapped Screen #2

The ceramic and stainless steel coupons are analyzed for comparing the effect of different material on scaling behavior. The coupons are solid materials having no slots as can be seen in Figure 17a) to d). Additionally, the ceramic sand screens with keystone design built following the design is compared with the 316L Stainless Steel sand screen with keystone design to get an idea of how the design along with the material impacts the scaling behavior. Note that the ceramic screen with keystone design and 316L stainless steel screen with keystone design are identical to those used for the sand retention test.

The surface roughened coupons are to simulate the effect of erosion on scaling behavior. The stainless steel and ceramic coupons are roughened in the same manner as mentioned in Section 3.1.4.2a), i.e. by blasting with B_4C.

Additionally, two wire wrapped screen test pieces used were pieces cut from standard stainless steel wire wrapped screen available on the market. Such screens are commonly used downhole to prevent sand production in unconsolidated reservoirs. Two wire wrapped screen pieces were used; since these were taken from used screens, they are not identical.

[3] Probes e) and f) are obtained from Baker Hughes Inc.

[4] Probes a) , b), c) and d) are manufactured in-house in ESK

For all 8 probes, screens as well as solid coupons, the surface roughness is measured, since the surface roughness is believed to play an important role influencing how scale adheres on the surface of the probes. This is to ensure that the analysis of scaling behavior considers the possible impact surface roughness might have on scale deposition.

4 Experimental Methods

In this section, the methodologies of the sand retention tests and scaling behaviour tests are explained in detail.

4.1 Experimental Method for Sand Retention Test

There are two types of sand retention test, namely the slurry test and sand-pack test. A slurry sand retention test simulates the situation where the screen system is inside the casing or there is an annulus in an openhole completion; whereas a sand-pack test models the situation where the reservoir sand is in close contact with the screen [42, p. 4]. For this thesis a slurry sand retention test is selected. This is because more sand flows through the screen in a slurry test as compared to a sand-pack test when reservoir sand is used [43, p. 5], hence having a higher possibility to cause erosion. Additionally, a slurry test is representative for a new well.

The slurry sand retention test carried out for this thesis consists of two phases. The first phase is the slurry injection. The slurry injection is carried out according to the ESK Test Rig Manual [44]. The test rig is deaerated before each slurry injection. The first section of the sand retention test provides information on the formation of the filter cake such as how fast it formed and how is the rate of increase in the differential pressure. The concept of how to perform the slurry test is similar to as described in SPE 151768, SPE 98308 and SPE 82244 as mentioned earlier.

In the first section of the slurry sand retention test, the sand retrieved from the filter (residue) and the sand passed through the filter (filtrate) are collected. Dry weight of the filtrate and residue are noted for a mass balance (Details in Section 4.1.1) and PSD analyses (For details see Section 4.1.2) are conducted to provide more insight into the properties of the filter cake.

In the second phase of the sand retention test, the flow resistance of the filter cake is investigated. This is done by flowing liquid (distilled water) through the filter cake formed during the first phase of the slurry sand retention test at increasing flow rates up to the maximum allowed differential pressure of the test rig. The differential pressure vs. flowrate behavior is obtainable through this.

Upon consideration, the second phase of the slurry sand retention test, the filter cake flow resistance test appears similar to a sand-pack test. However, it is necessary to distinguish between the filter cake flow resistance test and a sand-pack test. This is because in a sand pack test, the sand is compacted by means of compressive force [43] and a filter cake is formed. Whereas in the filter cake flow resistance test, the test is performed on an already formed filter cake, i.e. the filter cake is allowed to form by itself without any additional compressive forces. Hence the filter cake in a filter cake flow resistance test is different to

that in a sand-pack test is different. Therefore it is important to differentiate the second phase of the slurry sand retention test which is carried out in this thesis and the routine sand-pack test. The filter cake flow resistance test is believed to better represent a well that has sand production than a sand pack test since the filter cake downhole forms by itself without any additional compressive forces.

Scanning Electron Microscopy (SEM) is conducted on the screens before and after slurry sand retention test is conducted. This is further described in Section 4.1.3.

4.1.1 Mass Balance

The collected filtrate for each experiment is filtered using a cellulose nitrate membrane filter with a poresize of 0.45 µm. The sand retained from the filtrate and residue for each experiment is oven dried at 80°C for 45 minutes. The dried mass of filtrate and residue are measured and retained for PSD analysis. This is to give an idea of the percentage of sand retained in relation to the percentage of sand in the filtrate.

4.1.2 Particle Size Distribution (PSD) Analyses

The PSD analyses can be conducted by Laser Particle Size Analysis (LPSA) method or dry sieving method. The retained filtrate and residue are chosen to be characterized via the LPSA method using the Malvern Mastersizer 2000 unit. LPSA method is chosen instead of dry sieving since the filtrate amount from the test was small. Additionally, LPSA allows for measurement of fine particles while dry sieving does not. Water is used as the dispersion medium with surfactant added. The agitation speed used is 1750 rpm. During pre-treatment, the sample is agitated for 90 seconds. The sample is agitated internally while using a 20% power-level of the US wave generator during pre-treatment and measurement. The PSD is used to analyse the sand retained and sand in the filtrate.

4.1.3 Scanning Electron Microscope (SEM)

All 3 types of screens for all slot openings are analyzed using a SEM before and after the slurry sand retention test. This is to see if erosion had occurred. SEM examinations are carried out at magnification of 100 times, 200 times and 500 times. For the stainless steel wire-wrapped screen, the middle section of the screen is examined under the SEM. However for the stainless steel and ceramic screen with keystone design, the rectangular rod that was placed in the middle is analyzed at two sections, namely the chamfer and slot opening surface, as shown in Figure 18, before and after the test.

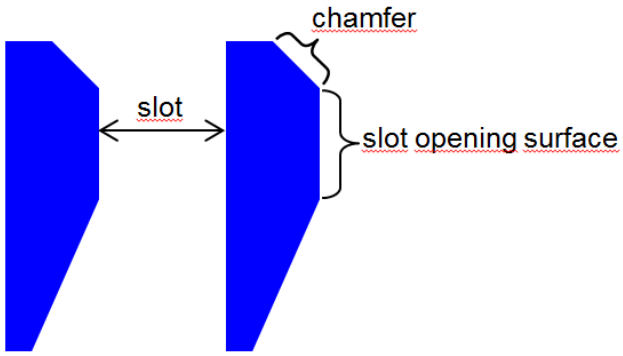

Figure 18: Side-View of the Screen with Keystone Design

Chamfer and slot opening surface region are selected since if any erosion were to happen, the first spot to be effected would be the chamfer and slot opening surface as the sand water mixture flows through the slot.

4.2 Experimental Method for the Evaluation of Scaling Behaviour

The scaling behaviour test procedure consists of two parts. The first section is the scale formation as explained in Section 4.2.1 and the second section is the scale removal described in Section 4.2.2.

4.2.1 Scale Formation

The initial mass, m_o of all 8 probes, namely ceramic coupon, stainless steel coupon, ceramic sand screen with keystone design, 316L stainless steel sand screen with keystone design, and 316 stainless steel wire wrapped screen-1 and 316L stainless steel wire wrapped screen-2 is measured.

A 2 liter glass beaker is filled with 1.5 liter of tap water. All 6 probes are allowed to hang in the water with the help of a support in the presence of a thermometer and a stirrer as shown in Figure 19. The water is heated up to 90°C ± 2°C with the stirrer in operation. The probes are held constantly at this temperature for 10 minutes. After that, the probes are removed from the water and allowed to cool for 30 minutes until they have reached room temperature. This procedure is repeated 9 times with fresh tap water every time. After that, a layer of well adhered scale is observed on all probes as depicted in Figure 41 in Section 5.2.1. It is extremely important to allow the probes to cool down to room temperature, since ceramics are sensitive to thermal shocks.

Figure 19: Experimental Setup for Part 1 of Scaling Behaviour Test – Scale Formation

The probes are dried in an oven at 80°C for 45 minutes, after which the mass of the 100% scale deposited, $m_{100\%}$ is measured.

4.2.2 Scale Removal

The ease of scale removal is examined using an US bath. The US treatment equipment used is a Bandelin SONOREX type made in Germany. The electrical energy and frequency of the US treatment equipment is 240 W and 35 kHz; respectively. The scale deposited probes are allowed to hang in a beaker containing 600 mL of distilled water as shown in Figure 16. The beaker with distilled water containing the probe is treated in an US bath for 30 seconds. After which the probe is rinsed with distilled water to remove loose particles. The probes are then dried at 80°C for 45 minutes. The mass of the dried probes after 30 seconds in ultrasonic bath, $m_{0.5}$ is determined. This scale removal procedure is repeated with increasing time steps in the US bath from 0.5 minutes, 1 minute, 2 minutes, 3 minutes, 4 minutes until a total cumulative time of 45 minutes is achieved.

5 Results

The results of the sand retention test conducted on the sand retention test rig are explained in Section 5.1 and scaling behaviour test results are explained in Section 5.2.

5.1 Sand Retention Test Results

During the 1st part of the slurry sand retention test, the key parameter, the differential pressure across the screen is measured with increasing time. The differential pressure with respect to time is plotted for slot openings 150 µm [Figure 20a)], 200 µm [Figure 21a)] and 250 µm [Figure 22a)] for various types of screens. The types of screens used are namely ceramic screen with keystone design (in blue), stainless steel screen with Keystone Design (in red) and stainless steel wire-wrapped screen (in green). After the filter cake has been developed reaching a height of about 25 mm as described in Section 3.1.4.1f), the pressure is allowed to drop to zero mbar. After which the flowrate in the main loop is increased by the control of FCV-15 while monitoring the pressure build-up. The more the valve is opened, the higher the flowrate. Additionally, the flowrate is controlled by regulating Pump VF-15 Regulator. The differential pressure across the already formed filter cake increases with increasing flowrate. The differential pressure against flowrate behaviour for slot openings 150 µm, 200 µm, and 250 µm is depicted in Figure 20b), Figure 21b) and Figure 22b); respectively for the three types of screens aforementioned with the same colour coding.

The pressure build-up for all slot openings has a similar trend of logarithmic pressure build-up. At a closer look, it can be observed, that there is a slight difference in the way the pressure build-up occurs. For the 150 µm slot opening, for all 3 types of screens, the pressure build-up peaks rapidly as soon as the slurry sand retention test is started. Whereas the 200 µm slot opening has a more gradual pressure build-up than the 150 µm slot opening but a steeper pressure build-up than the 250 µm slot opening. The 250 µm has the most gradual pressure build-up. At time 100s, the differential pressures for the 250 µm, 200 µm and 150µm are in the range of 100 mbar, 250 mbar and 600 mbar. This evidently indicates that 150 µm slot opening reached the highest differential pressure at time 100 s. Therefore it can be summarized that with increasing slot opening size, the pressure build-up is more gradual regardless of screen type. The plots also show that all pressure build-up levels off at about 1000 mbar to achieve the 25 mm filter cake.

The differential pressure against flowrate also has similar trends for all slot openings i.e. with increasing flowrate, the differential pressure is higher. Based on Figure 20b) it can be seen that for 150 µm slot opening, stainless steel screen with keystone design has the steepest slope. In contrast, looking at the differential pressure vs. flowrate plots for 200 µm and 250 µm slot opening; namely Figure 21b) Figure 22b), the ceramic screen with keystone design has the steepest slope. Additionally, the disparity between the trendlines of ceramic screen with keystone design and stainless steel screen with keystone design is rather small for the 150 µm slot opening as compared to the 200 µm and 250 µm slot opening. However, it is

clear that stainless steel wire wrapped screen has the lowest slope for all slot openings, i.e. highest flow for the same amount of differential pressure.

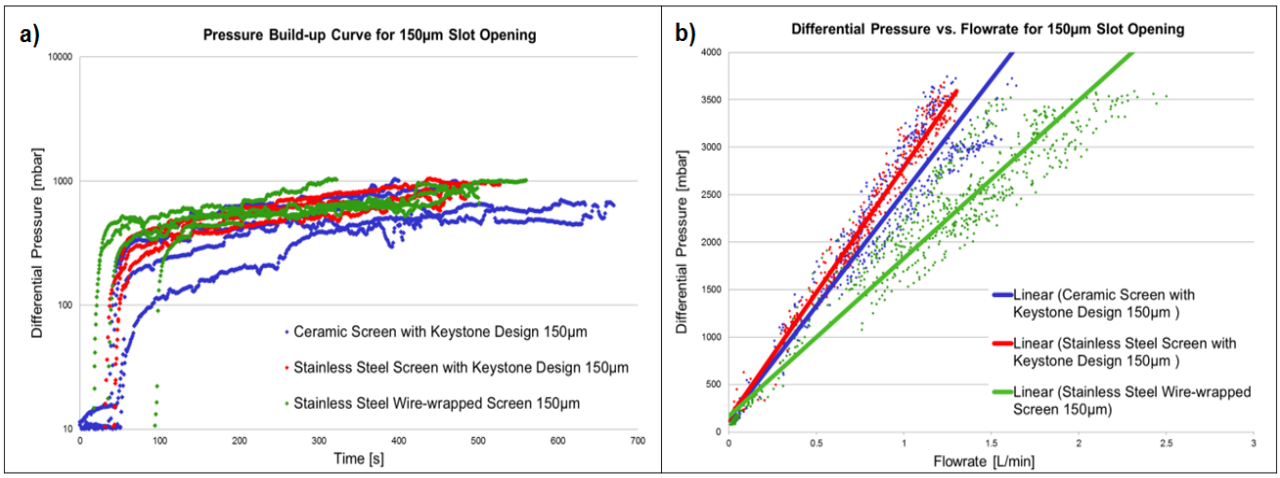

Figure 20: Sand Retention Results for 150 µm. a) Pressure Build-up Curve; b) Differential Pressure vs. Flowrate

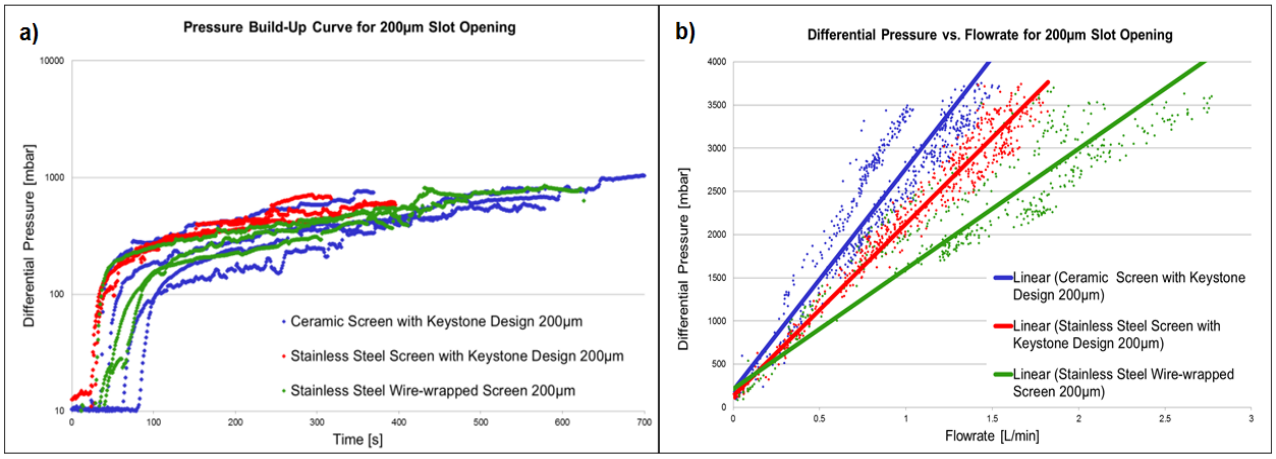

Figure 21: Sand Retention Results for 200 µm. a) Pressure Build-up Curve; b) Differential Pressure vs. Flowrate

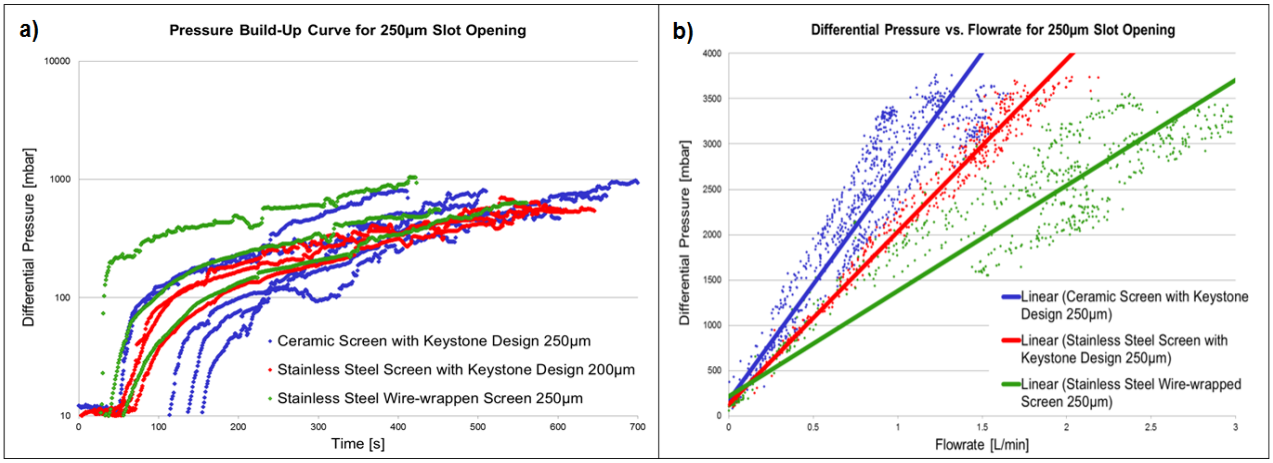

Figure 22: Sand Retention Results for 250 µm. a) Pressure Build-up Curve; b) Differential Pressure vs. Flowrate

As mentioned earlier [in Section 3.1.4.2a)], the 150 µm slot opening for the stainless steel screen with keystone design and stainless steel wire-wrapped screen were roughened to model an eroded surface. The differential pressure with respect to time for roughenened and non-roughened stainless steel screens for slot opening of 150 µm is as depicted below in Figure 23a). The differential pressure vs. flowrate for the same screens is shown in Figure 23b). Non-roughened screens refer to the stainless steel screen with keystone design and stainless steel wire-wrapped screens that were not roughened. It was noticed that the flowrate through the already formed filter cake for the roughened screens for both; stainless steel with keystone design and wire-wrapped screen was lower as compared to the non-roughened screens.

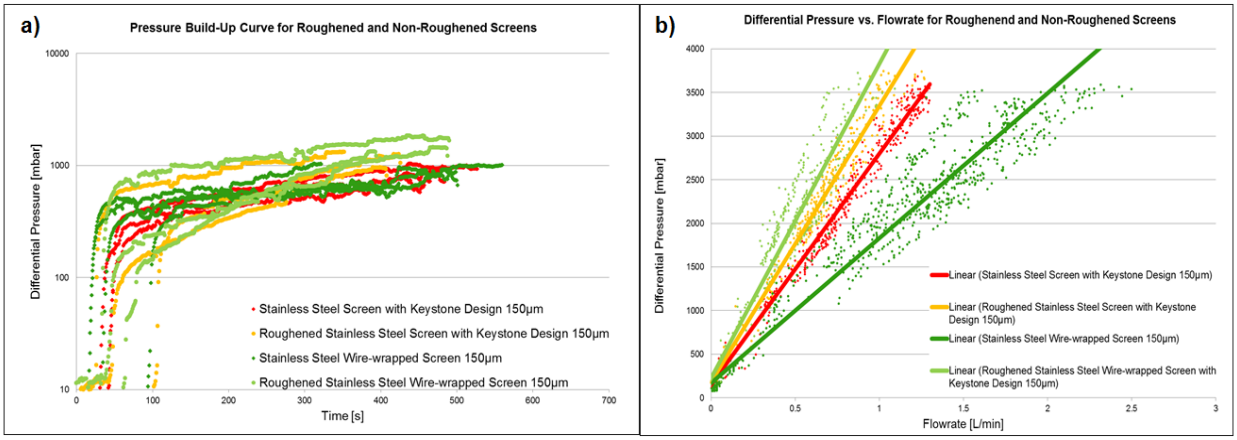

Figure 23: Sand Retention Results for Roughened and Non-Roughened Screens. a) Pressure Build-up Curve; b) Differential Pressure vs. Flowrate

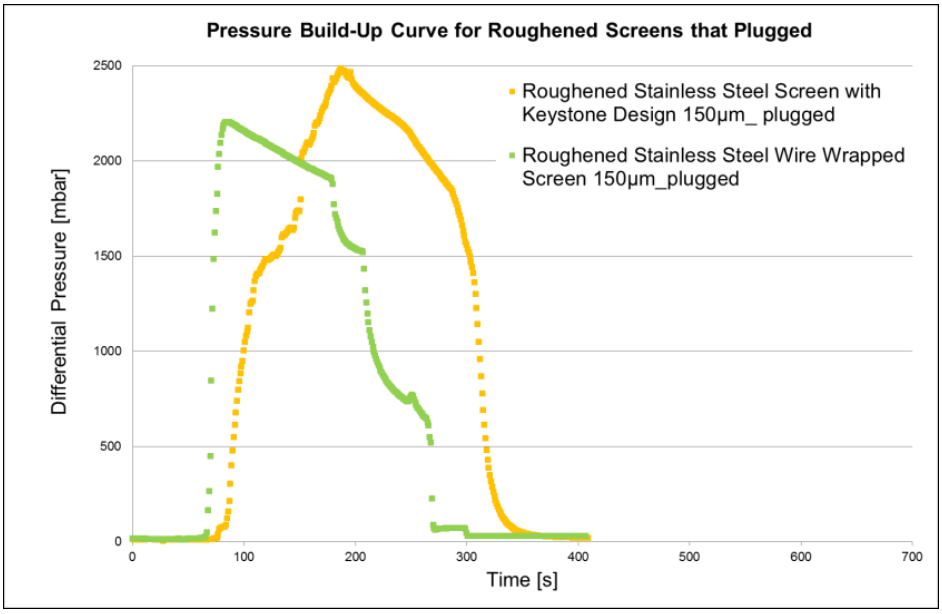

Figure 24: Pressure Build-up Curve for Roughened Screen that Plugged

In fact in some cases, for the roughened stainless steel screens, the pressure build-up peaked immediately at the start of the slurry sand retention test as shown in Figure 24. This is a clear indication of plugging behavior. The retrieved screen after the sand retention experiment where the screen was plugged is shown in Figure 25.

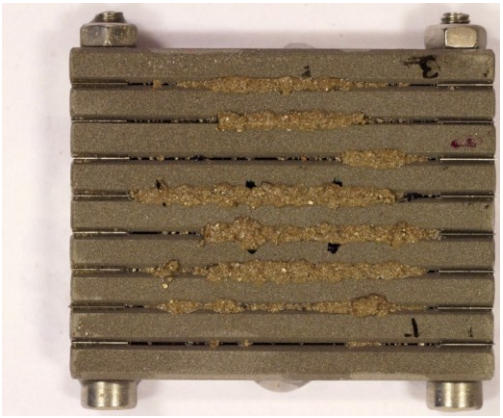

Figure 25: Plugging of Roughened Screen after Sand Retention Experiment

Selected experiment results are chosen to be displayed due to their interesting behavior, referred to as special cases. These were the experiment results for stainless steel wire wrapped screens of slot opening 200 µm, namely W6, W8 and W14 as shown in Figure 26. It can be seen that for W6, the pressure build up picked up slightly later that the others (W8 and W14) as can be seen in Figure 26a).

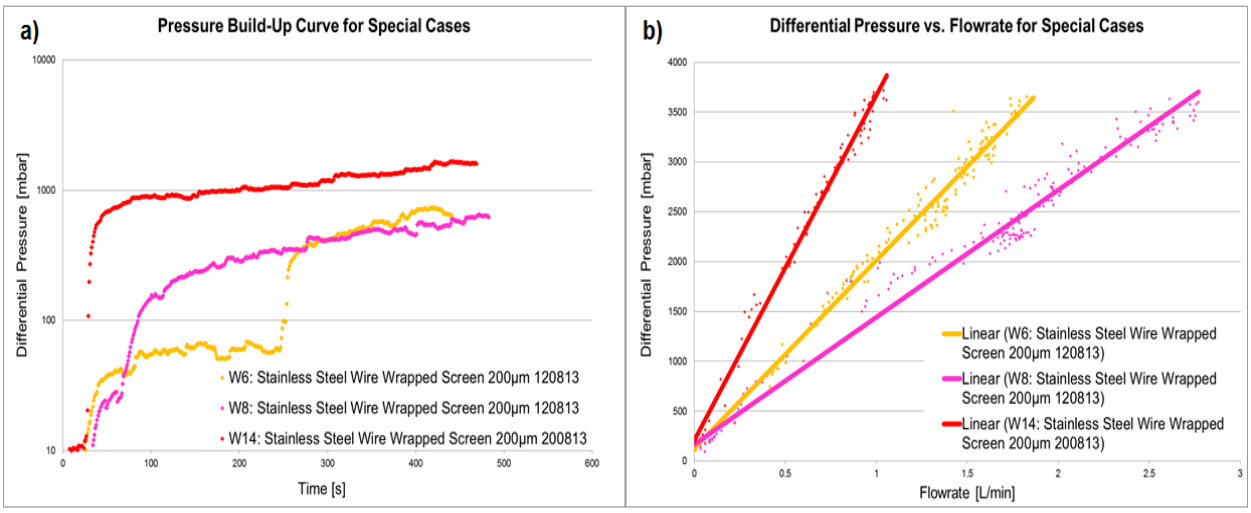

Figure 26: Sand Retention Test Results for Special Cases. a) Pressure Build-Up Curve; b) Differential Pressure vs. Flowrate

This is due to the fact that channeling has occurred. Thus the filter cake was not properly formed and fluid managed to flow through the channel, indicated by the low pressure build-up till about 250 seconds after the start of the experiment. After that, the filter cake is properly formed and the pressure build-up peaks to the region matching to that of W8 and W14. In terms of differential pressure vs. flowrate as seen in Figure 26b) nothing spectacular or different was noticed. As can be seen W14 has a higher pressure build-up than W8 [Figure 26a)] and therefore a higher flow resistance as seen in Figure 26b).

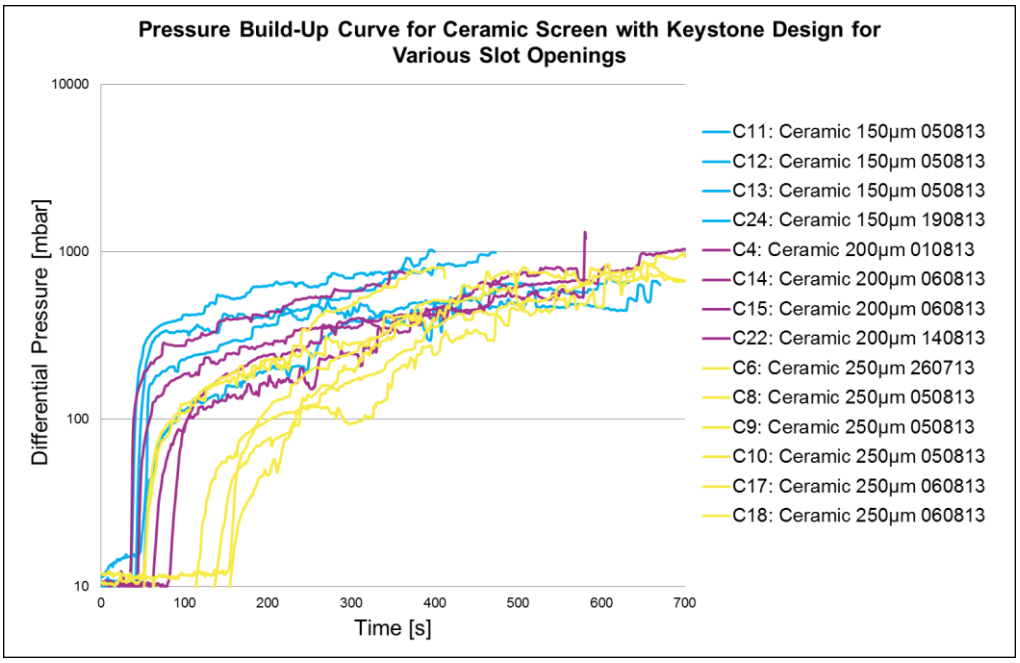

Figure 27: Pressure Build-Up Curve for Ceramic Screen with Keystone Design for Various Slot Openings

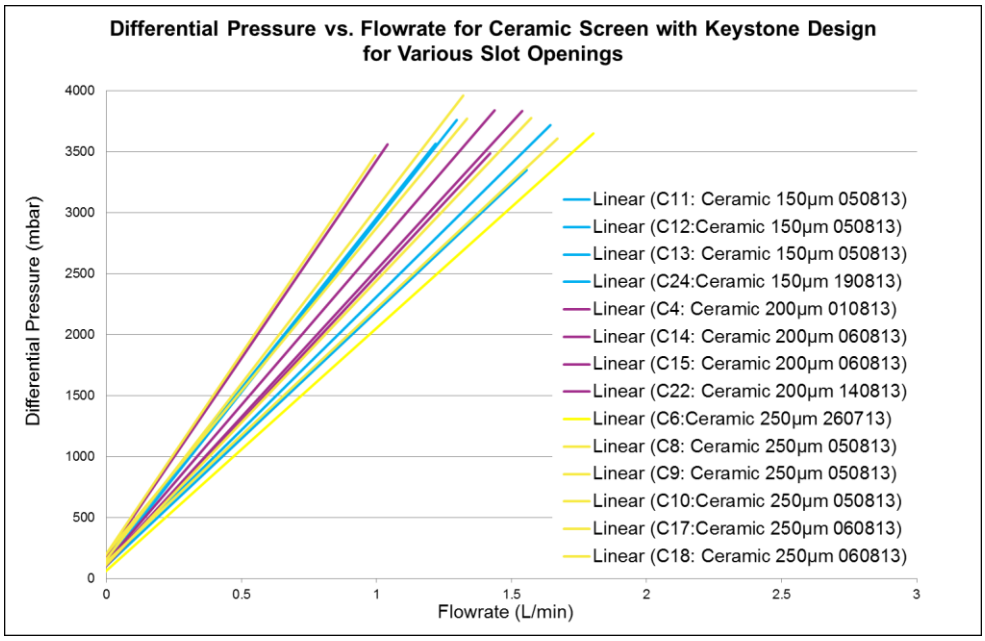

Figure 28: Differential Pressure vs. Flowrate for Ceramic Screen with Keystone Design for Various Slot Openings

Additionally, for ceramic screen with keystone design for various slot openings, the pressure build-up curve is shown in Figure 27 and differential pressure vs. flowrate is shown in Figure 28; respectively. From the pressure build-up curve it is evident that the 250 µm slot opening (in yellow) has the lowest pressure build-up. However in terms of flowrate across of the filter cake, trends in differential pressure are not recognized with changes in slot opening sizes.

5.1.1 Mass Balance

The mass balance results for ceramic screen with keystone design for various slot openings, stainless steel screen with keystone design for various slot openings, and stainless steel wire-wrapped screen for various slot openings are shown in Table 11, Table 12 and Table 13; respectively in Appendix C. The naming convention used for the Sand Retention Test is explained in Figure 29.

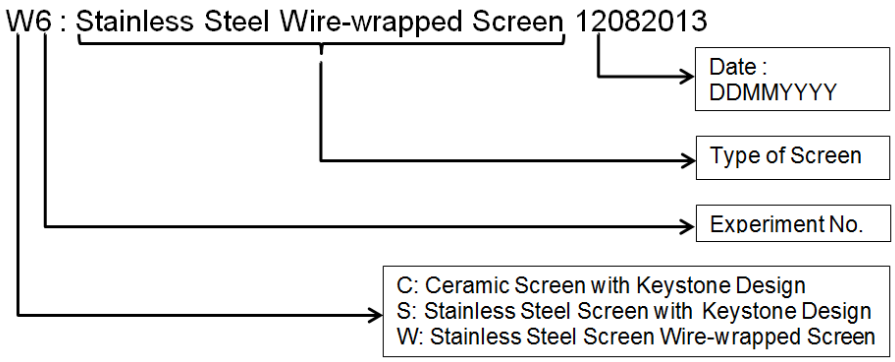

Figure 29: Naming Convention for Sand Retention Experiments

It is obvious, that with increasing slot opening size, more sand is retained in the filtrate for the experiments conducted with ceramic and stainless steel screens, with keystone design. For the experiment with ceramic screen with keystone design, the percentage of sand retained in the filtrate for slot opening 150 µm, 200 µm and 250 µm was at an average of 0.51%, 0.75% and 1.53%; respectively as shown in Table 4. For the experiment using stainless steel screen with keystone design, the percentage of sand retained in the filtrate for slot opening 150 µm, 200 µm and 250 µm was at an average of 0.97%, 1.46% and 1.51%; respectively as shown in Table 4. There is a clear trend of slight increase in the amount of sand retained in the filtrate with increasing slot opening. However, for stainless steel wire-wrapped screen design, the slot opening size did not play a role in the amount of sand retained in the filtrate. There was no trend recognized. Regardless of which slot opening size, the amount of sand retained in the filtrate was constant about 0.63% as can be computed from Table 4.

Table 4: Average Sand Retained in Filtrate for Various Screens Types and Slot Opening

Screen Type	Ceramic Screen with Keystone Design	Stainless Steel Screen with Keystone Design	Stainless Steel Wire-wrapped Screen
Slot Opening [µm]	Average Sand Retained in Filtrate [%]	Average Sand Retained in Filtrate [%]	Average Sand Retained in Filtrate [%]
150	0.51	0.97	0.65
200	0.75	1.46	0.73
250	1.53	1.51	0.51

Table 5: Mass Balance for Special Cases Conducted on Stainless Steel Wire-wrapped Screen of Slot Opening of 150 µm

Slot Opening [µm]	Tests	Mass of:		Percentage of:	
		Residue [g]	Retained in Filtrate [g]	Residue [%]	Retained in Filtrate [%]
150	W6: Stainless Steel Wire-wrapped Screen 120813 (CHANELLING)	21.1735	5.4248	79.60	20.40
	W8: Stainless Steel Wire-wrapped Screen120813	22.1792	0.1409	99.37	0.63
	W14: Stainlesss Steel Wire-wrapped Screen 200813	23.5269	0.1393	99.41	0.59

The mass balance for the special cases, scenarios where the results were found to be interesting is displayed in Table 5. Where channeling occurred, test W6 there was a 20% amount of sand retained in the filtrate. The test which has higher resistance to flow across filter cake [Refer to Figure 26b)], W14 had slightly less percentage of sand retained in the filtrate as compared to W8 as can be seen in in Table 5 where the resistance to flow across filter cake was significantly lower [Refer to Figure 26b)].

Besides that, the filtrate from the sand retention test is collected batch wise in various time intervals to understand the amount of the sand collected in the filtrate with respect to time.

The amount of sand retained in a batch wise filtration is depicted in Figure 30. It is clear that most of the sand is obtained in the first 30 s of the sand retention experiment.

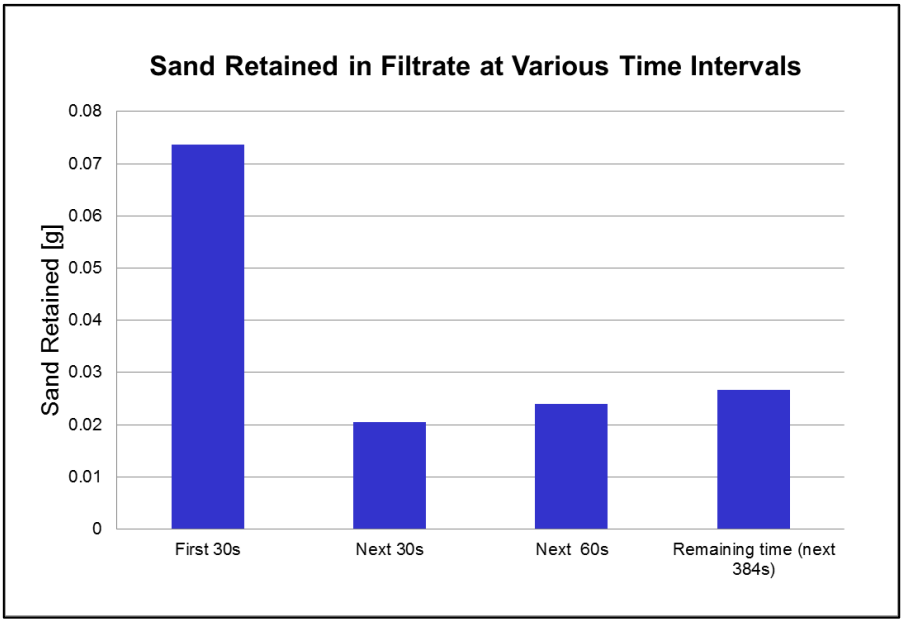

Figure 30: Sand Retained in Filtrate at Various Time Intervals

5.1.2 Particle Size Distribution (PSD) Analyses

For the PSD analyses two experiments of the sand retention test results were chosen as representative for each screen type for a respective slot opening. The cumulative PSD for Various Screens Types with 150 µm, 200 µm and 250 µm Slot Opening are shown in Figure 31, Figure 32 and Figure 33; respectively.

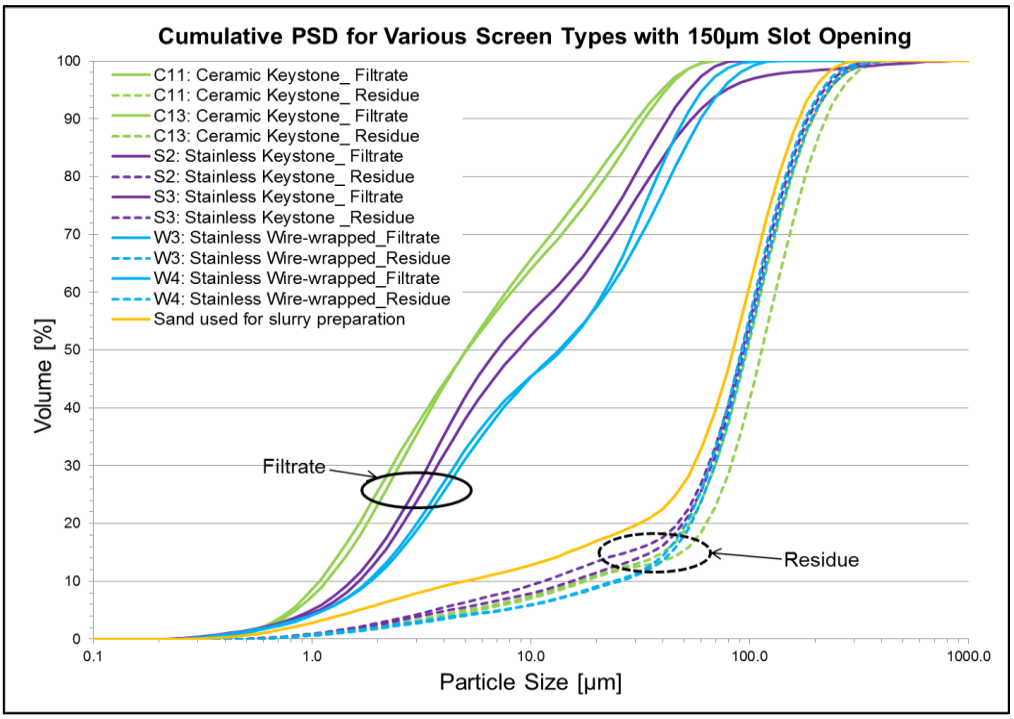

Figure 31: PSD for Various Screen Types with 150 µm Slot Opening

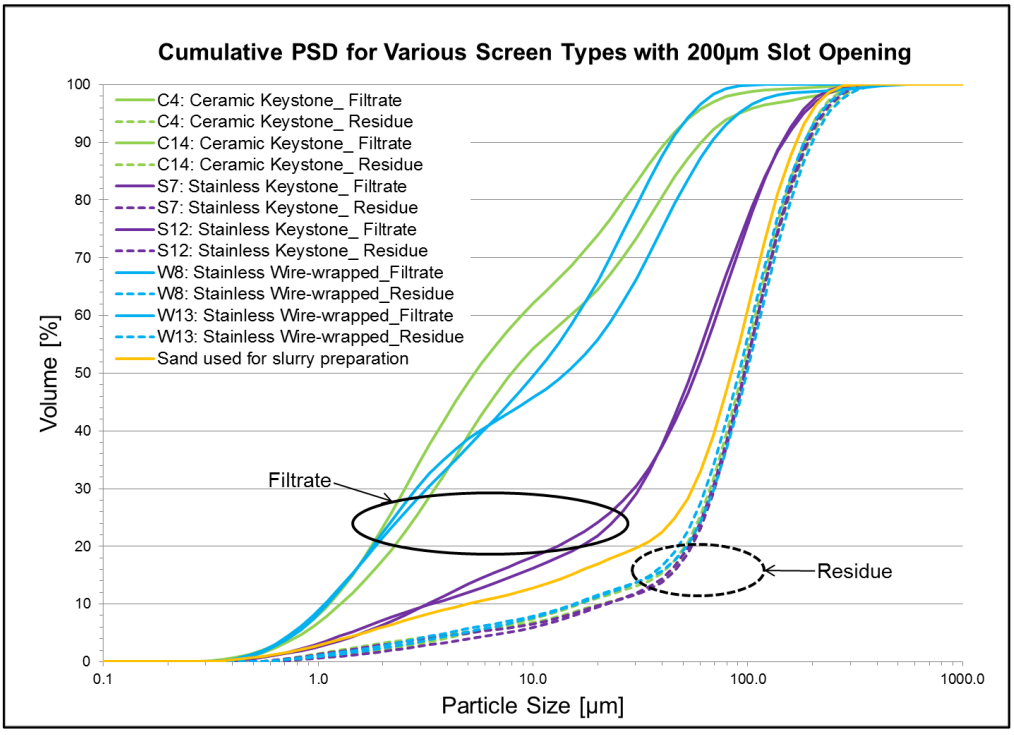

Figure 32: PSD for Various Screen Types with 200 µm Slot Opening

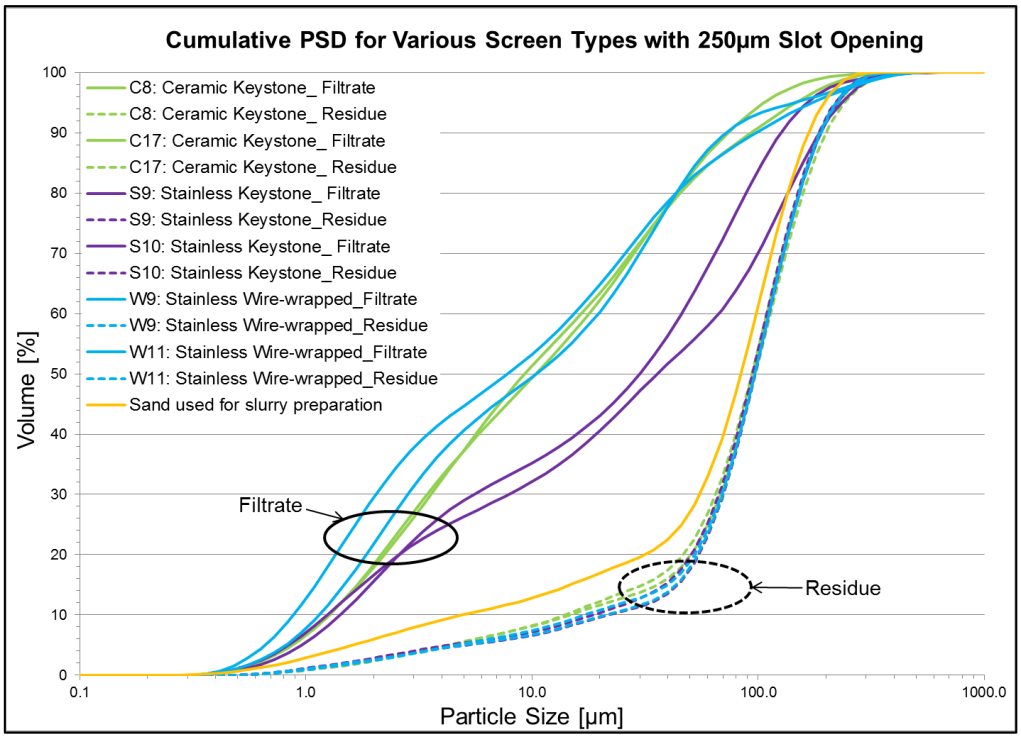

Figure 33: PSD for Various Screen Types with 250 µm Slot Opening

In Figure 31, Figure 32 and Figure 33; the solid line ellipse groups the cumulative PSD of the filtrate and the dotted line ellipse groups the cumulative PSD of the residue. It can be seen that for 150 µm slot opening, the ceramic screen with keystone design has the finest particles in the filtrate followed by stainless steel screen with keystone design and stainless steel screen with wire-wrapped design.

Based on Figure 32, it can be seen that the ceramic screen with keystone design has the finest particles in the filtrate closely behind or similar behaviour is the stainless steel wire-wrapped screen. The stainless steel with keystone design has considerably coarser particles in the filtrate.

Figure 33 identifies that the wire-wrapped screen has slightly more fines in average as compared to the ceramic screen with keystone design. Once again, the stainless steel with keystone design has significantly coarser particles in the filtrate as compared to the ceramic screen with keystone design and stainless steel wire-wrapped screen.

In terms of the distribution of particle size in the residue for all types of screen and slot opening as can be seen in Figure 31, Figure 32 and Figure 33; they are close to the sample sand PSD (in yellow) with which the experiment was conducted. Besides that, no significant differences between the screen types or slot openings were noticed.

Additionally, the PSD for filtrate and residue for all sand retention tests looked similar. For example, PSD of a pair of filtrate and residue for a sand retention experiment is shown in

Figure 34 and Figure 35; respectively. Note that the scale of the y-axis for Figure 34 and Figure 35 are not directly comparable. The filtrate has a marked bimodal distribution. However when closely analyzed the sample sand used [Figure 9] and residue sand [Figure 35] also has two peaks but the first peak occurring between 10 µm and 20 µm is extremely weak. When a PSD analysis is conducted on the filtrate which only consists of finer particles this merely shows the characteristic of the original sand sample. Therefore the bimodal distribution noticed on all filtrates is a characteristic of the sample sand used. The filtrate residue pairs of other sand retention tests conducted can be found in Appendix D.

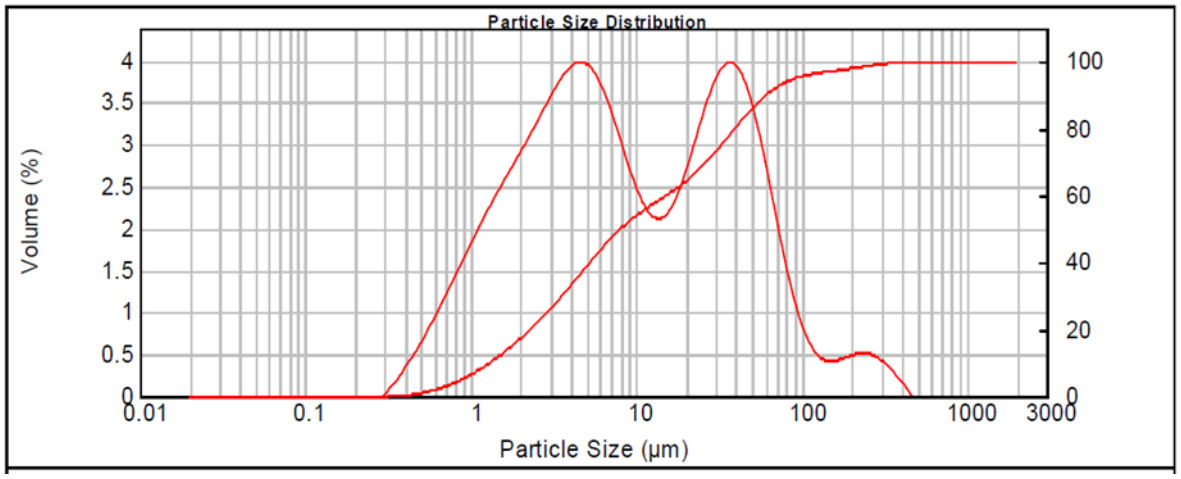

Figure 34: PSD for filtrate of C4: Ceramic Screen with Keystone Design with 200 µm Slot Opening

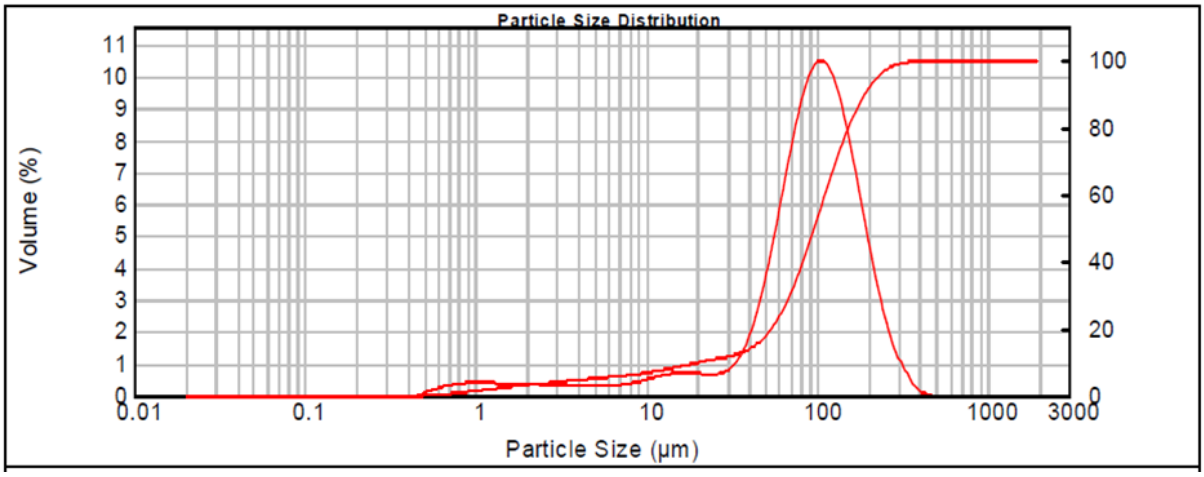

Figure 35: PSD for residue of C4: Ceramic Screen with Keystone Design with 200 µm Slot Opening

5.1.3 Scanning Electron Microscopy (SEM)

The SEM examination results for all magnifications for all screen types did not show any difference before and after the sand retention tests. The SEM result for ceramic screen with keystone design, stainless steel screen with keystone design and stainless steel wire-wrapped screen with keystone design; for 200 µm slot opening at 200 times magnification

are shown below in Figure 36, Figure 37 and Figure 38; respectively. The SEM results for roughened stainless steel wire-wrapped screen and roughened stainless steel screen with keystone design are also shown in Figure 39 and Figure 40, respectively.

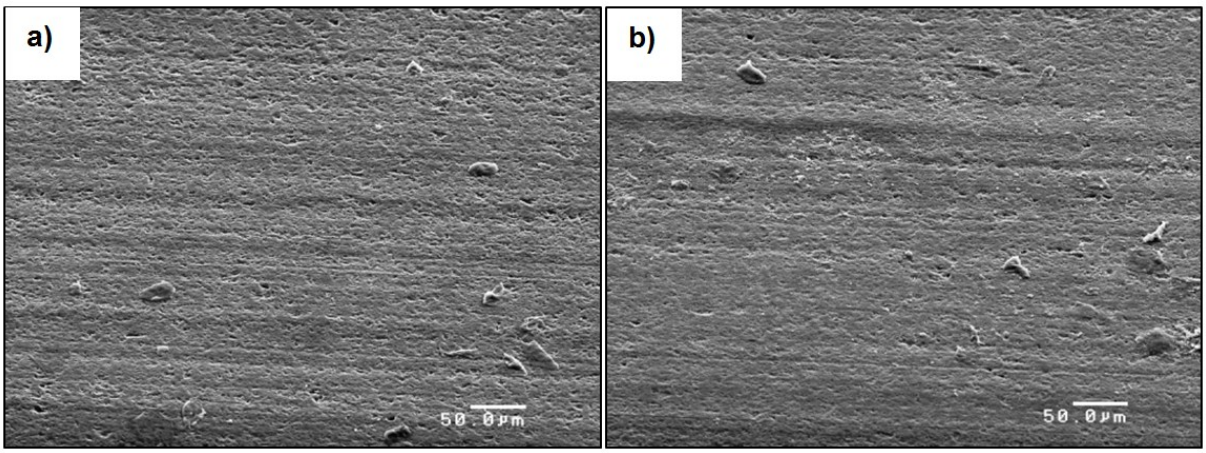

Figure 36: SEM Examination of Ceramic Screen with Keystone Design for 200 µm Slot Opening a) Before Sand Retention Test; b) After Sand Retention Test

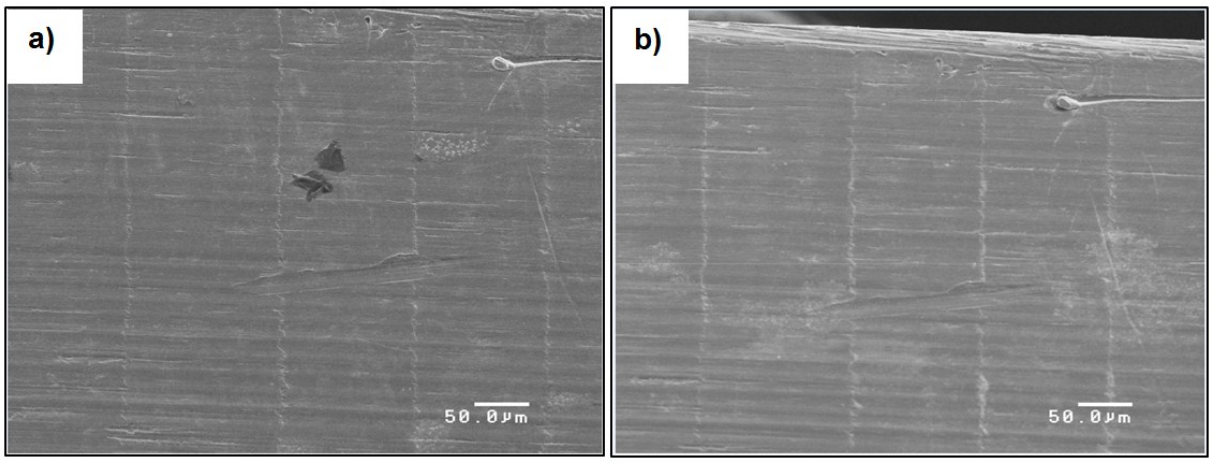

Figure 37: SEM Examination of Stainless Steel Screen with Keystone Design for 200 µm Slot Opening. a) Before Sand Retention Test; b) After Sand Retention Test

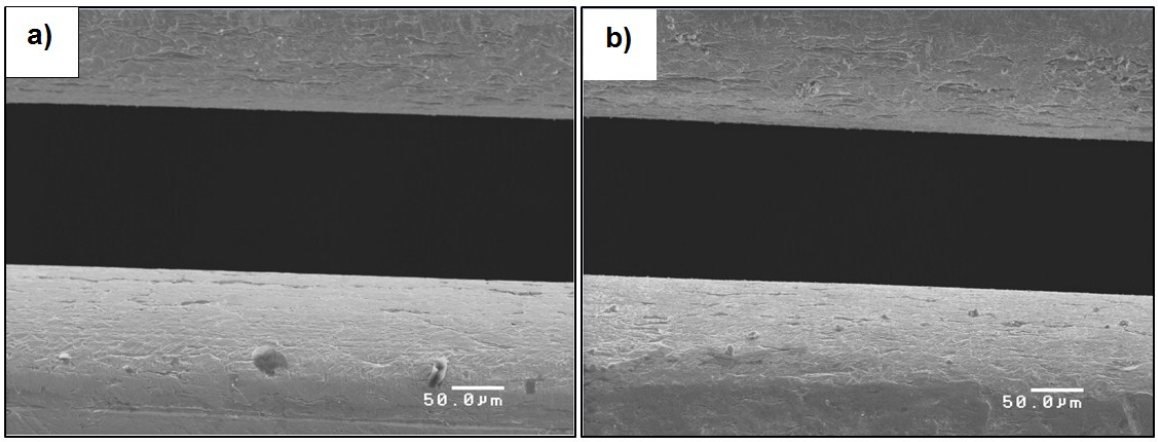

Figure 38: SEM Examination of Stainless Steel Wire-wrapped Screen for 200 µm Slot Opening. a) Before Sand Retention Test; b) After Sand Retention Test

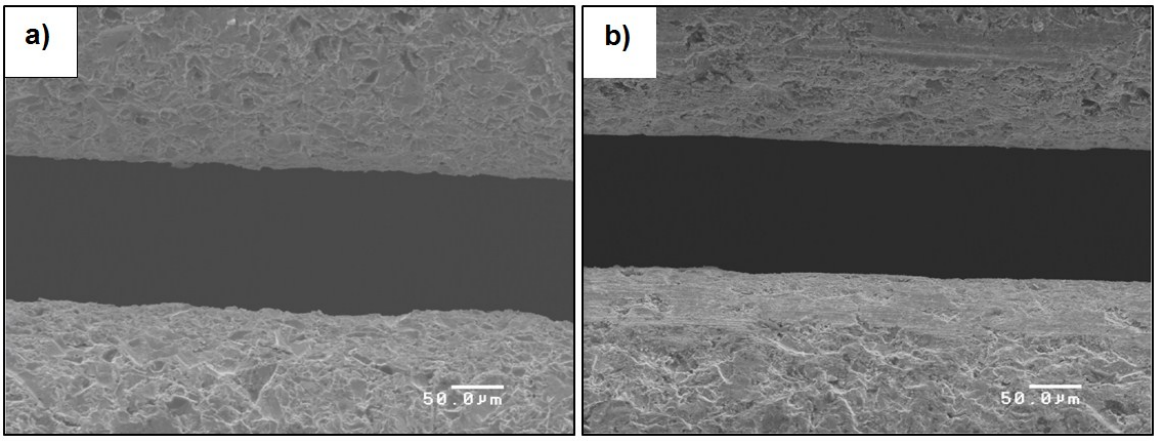

Figure 39: SEM Examination of Roughened Stainless Steel Wire-wrapped Screen for 150 µm Slot Opening. a) Before Sand Retention Test; b) After Sand Retention Test

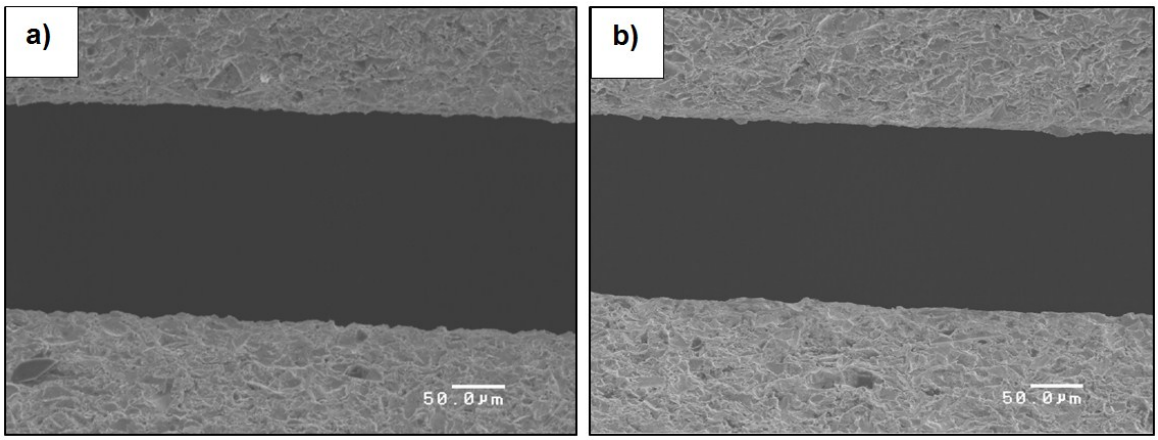

Figure 40: SEM Examination of Roughened Stainless Steel Screen with Keystone Design for 150 µm Slot Opening. a) Before Sand Retention Test; b) After Sand Retention Test

5.2 Scaling Behaviour Evaluation Results

The scaling behaviour test was conducted in two parts as explained in Section 4.2, namely the scale formation part and scale removal part. Section 5.2.1 below depicts the results of the scale formation and the following section, Section 5.2.2 describes the results achieved on scale removal.

5.2.1 Scale Formation

At the end of the scale formation series of experiments, a well adhered scale layer on all probes is observed as seen below in Figure 41. As can be seen in Table 6, the amount of scale deposited on stainless steel materials is significantly higher than that on ceramic materials. It is interesting to note that the wire wrapped screen of the same material and exact same design have quite a different amount of scale deposited. To analyse this discrepancy, the roughness of all probes were measured. Scale deposition appears to be a function of roughness. However, material appears to have a stronger influence of scale deposition. This is because although ceramic coupon is rougher than stainless steel coupon, the amount of scale deposited on ceramic coupon is less than that formed on stainless steel coupon.

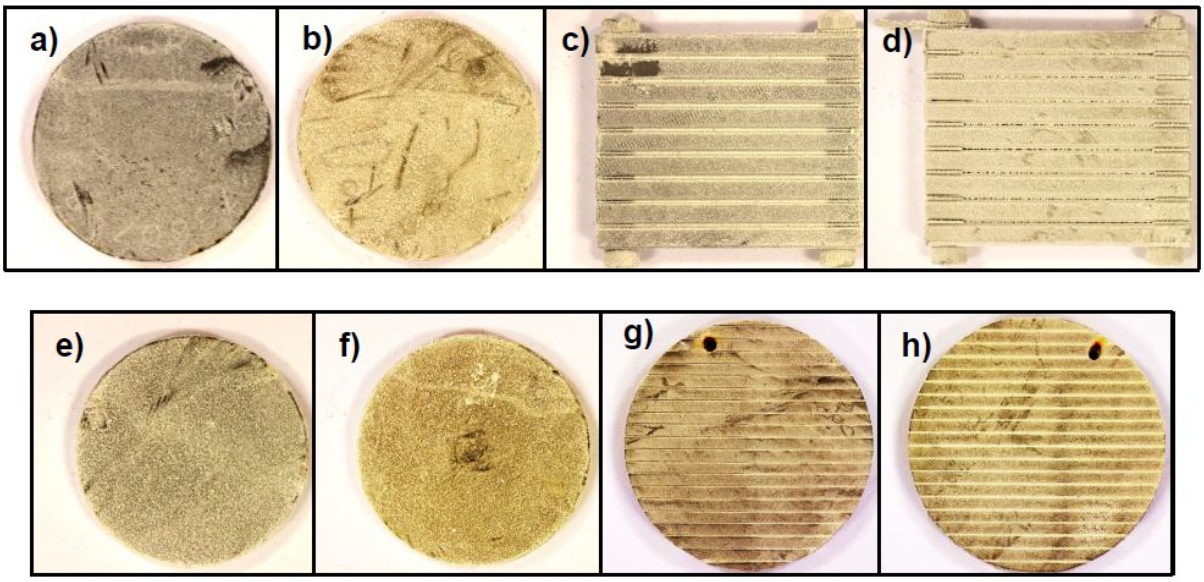

Figure 41: Scale Layer Formed on: a) Ceramic Coupon; b) Stainless Steel Coupon; c) Ceramic Screen with Keystone Design; d) Stainless Steel Screen with Keystone Design; e) Roughened Ceramic Coupon; f) Roughened Stainless Steel Coupon; g) Stainless Steel Wire-wrapped Screen #1; h) Stainless Steel Wire-wrapped Screen #2

Table 6: Scale Formation on Various Types of Probes

Types of Probes	Total exposed area [cm^2]	Initial mass, m_o [g]	Mass after scale deposition, $m_{100\%}$ [g]	Scale deposition [mg/cm^2]	Roughness, R_a [µm]
Ceramic Coupon	23.70	12.27	12.32	1.81	0.77
Stainless Steel Coupon	23.70	30.70	30.77	2.66	0.48
Ceramic screen with keystone design	71.05	29.22	29.35	1.84	0.33
Stainless steel screen with keystone design	71.05	63.03	63.18	2.14	0.45
Stainless Steel Wire-wrapped screen #1	87.06	39.44	39.63	2.19	0.16
Stainless Steel Wire-wrapped screen #2	86.72	41.86	42.03	1.91	0.32
Roughened Ceramic Coupon	23.70	11.83	11.88	1.97	1.54
Roughened Stainless Steel Coupon	23.70	30.70	30.77	2.90	1.61

The relative percentage of scale deposited on stainless steel material compared to ceramic material for each pair of probes compared is shown in Figure 42, i.e. stainless steel coupon relative to ceramic coupon. The intersection of x-axis at y=0% is the ceramic baseline.

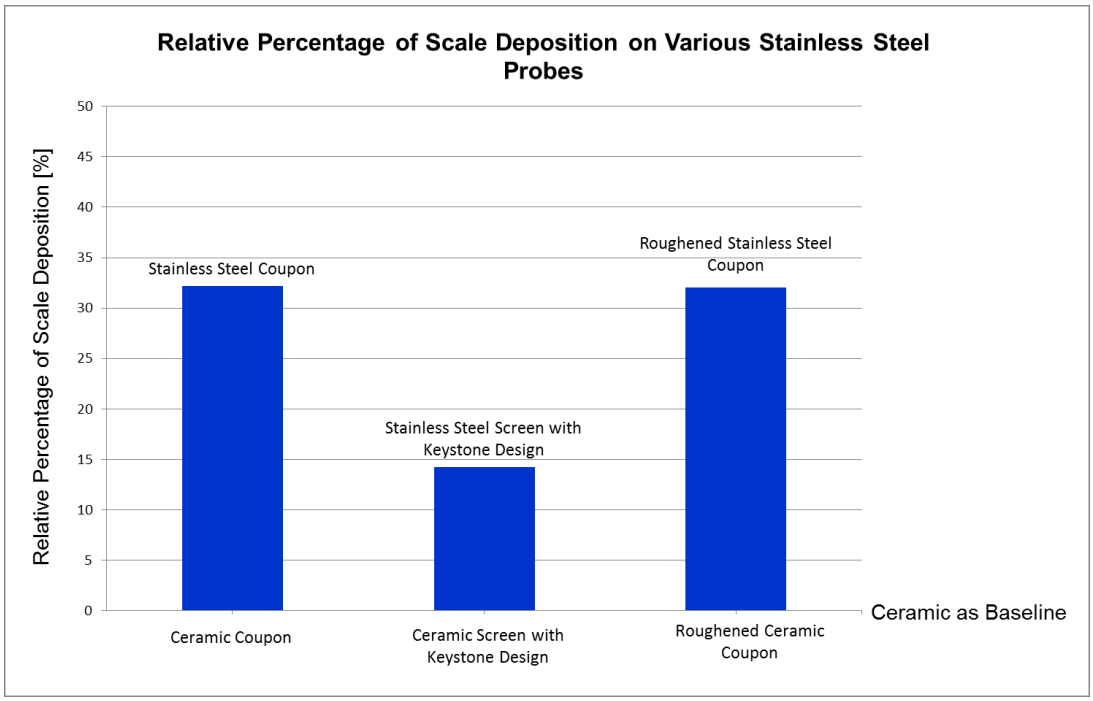

Figure 42: Relative Percentage of Scale Deposition on Various Stainless Steel Probes

Stainless steel coupon and roughened stainless steel coupon have 32% more scale deposited as compared to ceramic coupon and roughened ceramic coupon, respectively. Stainless steel screen with keystone design has 14% more scale deposited compared to the ceramic screen with keystone design. Although having not as much scale deposited as the coupon, there is still a significant difference between stainless steel screen with keystone design and ceramic screen with keystone design.

5.2.2 Scale Removal

The total amount of scale deposited in Table 6 is taken to be of 100% scale formed. The scale formed is removed with increasing time in US bath.

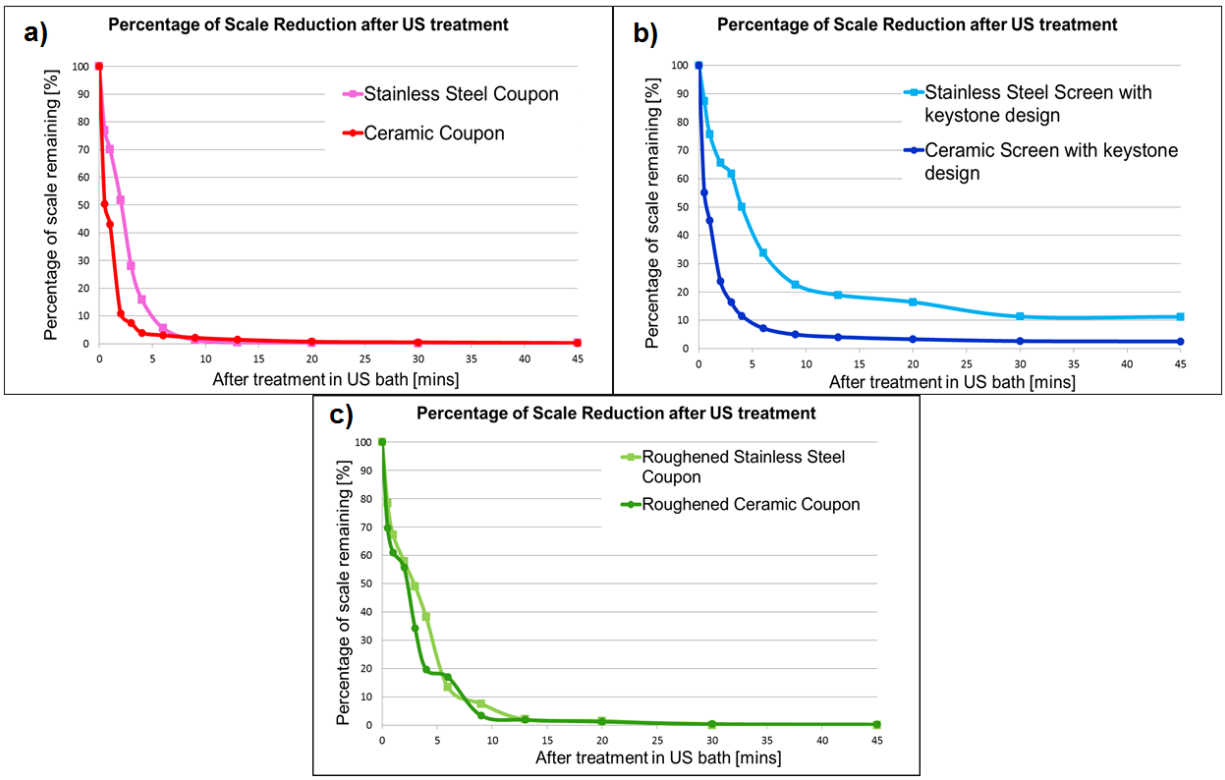

Figure 43: Comparison of Scale Removal based on Material for: a) Coupon; b) Screen with Keystone Design; c) Roughened Coupon

The results of percentage of scale removal for coupon, screen with keystone design and roughened coupon with respect to time are shown in Figure 43a), Figure 43b) and Figure 43c); respectively. For the all designs, it is clear that the scale removal is more easily conducted on the ceramic than the stainless steel material. The percentage of scale remaining after 6 minutes of treatment in US bath for the roughened ceramic coupon (marked in dark green) in Figure 43c) is strongly believed to be an outlier. It also can be noticed that after treatment in US bath for 45 minutes, there was still about 10 % of scale on the stainless steel screen with keystone design as compared to 2% scale on the ceramic screen with keystone design [Refer to Figure 43b)]. This considerable difference between stainless steel and ceramic was not evident in the coupon and roughened coupon designs after 45 minutes [Refer Figure 43a) & c)]. Although the stainless steel coupon and roughened coupon design had 30% of scale and stainless steel screen with keystone design had 14% of scale more than the ceramic types, as seen in Figure 42; the scale removal process from the coupon and roughened coupon design was easier than the screen with keystone design presented in Figure 43.

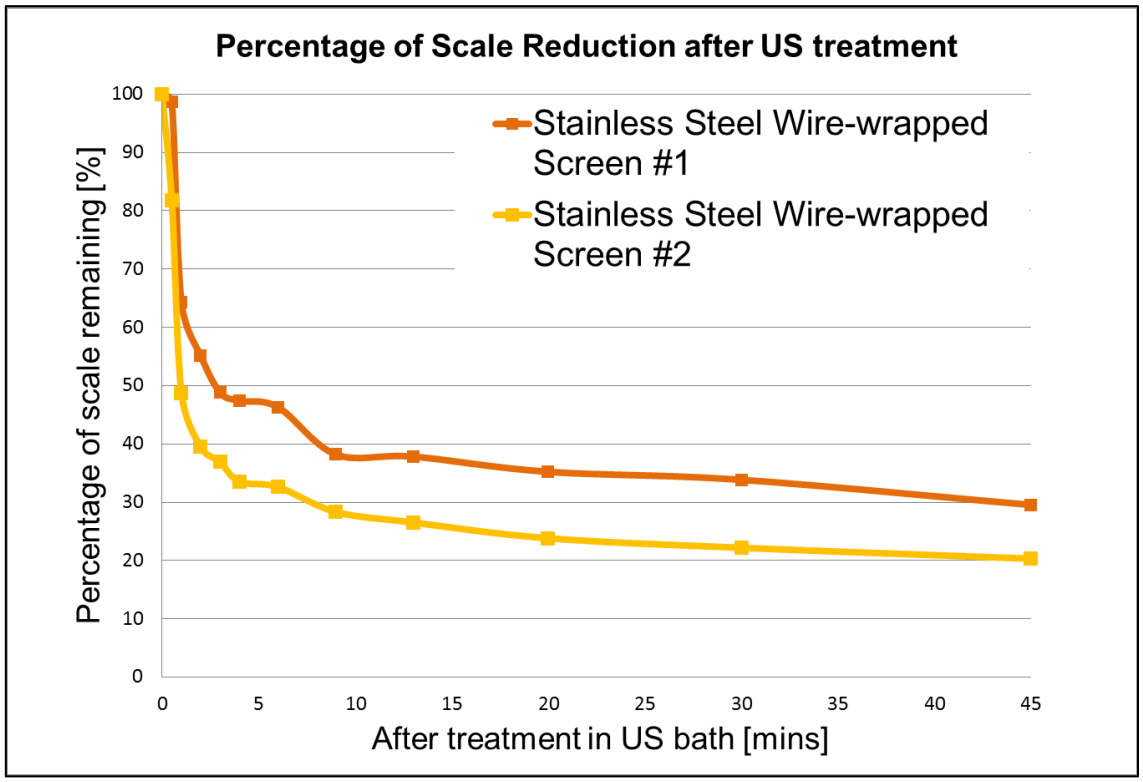

Figure 44: Scale Removal for Stainless Steel Wire-Wrapped Screen #1 and Stainless Steel Wire-wrapped Screen #2

The scale removal for two apparently identical stainless steel wire-wrapped screen namely, 1 and 2 is depicted in Figure 44. Although having the exact same design, the scale deposition [Refer to Table 6] and scale removal behaviour were [Figure 44a)] not comparable. The only difference was the roughness between the two stainless steel wire-wrapped screens. Stainless steel wire-wrapped screen #1 having a Ra value of 0.16 µm is smoother than stainless steel wire wrapped screen #2 having a Ra value twice as much as stainless steel wire-wrapped screen #1. It appears that scale was better adhered on the smoother wire-wrapped screen #1 than the wire-wrapped screen #2, hence being harder to remove. It is interesting to note that the percentage of scale left after the scale removal process is above 10% [Refer to Figure 43& Figure 44] for stainless steel screen with keystone design, stainless steel wire-wrapped screen #1 and stainless steel wire-wrapped screen #2 being 11%, 20% and 30%, respectively. This indicates that scale is extremely well adhered on a stainless steel material having slots as opposed to solid coupons.

To purely compare the effect of design, Figure 45a) for various designs of ceramic materials and Figure 45b) for various designs of stainless steel materials, were plotted. For ceramic material [Figure 45a)], the roughened coupon has the most well adhered scale layer, therefore requiring more time to remove the scale. This was followed by the screen with keystone design and finally ceramic coupon. Stainless steel material [Figure 45b)] does not show the exact same behaviour as the ceramic material. The most well adhered scale layer is formed on the stainless steel screen with keystone design, followed by stainless steel

roughened coupon design and then the stainless steel coupon design (smoother stainless steel coupon design).

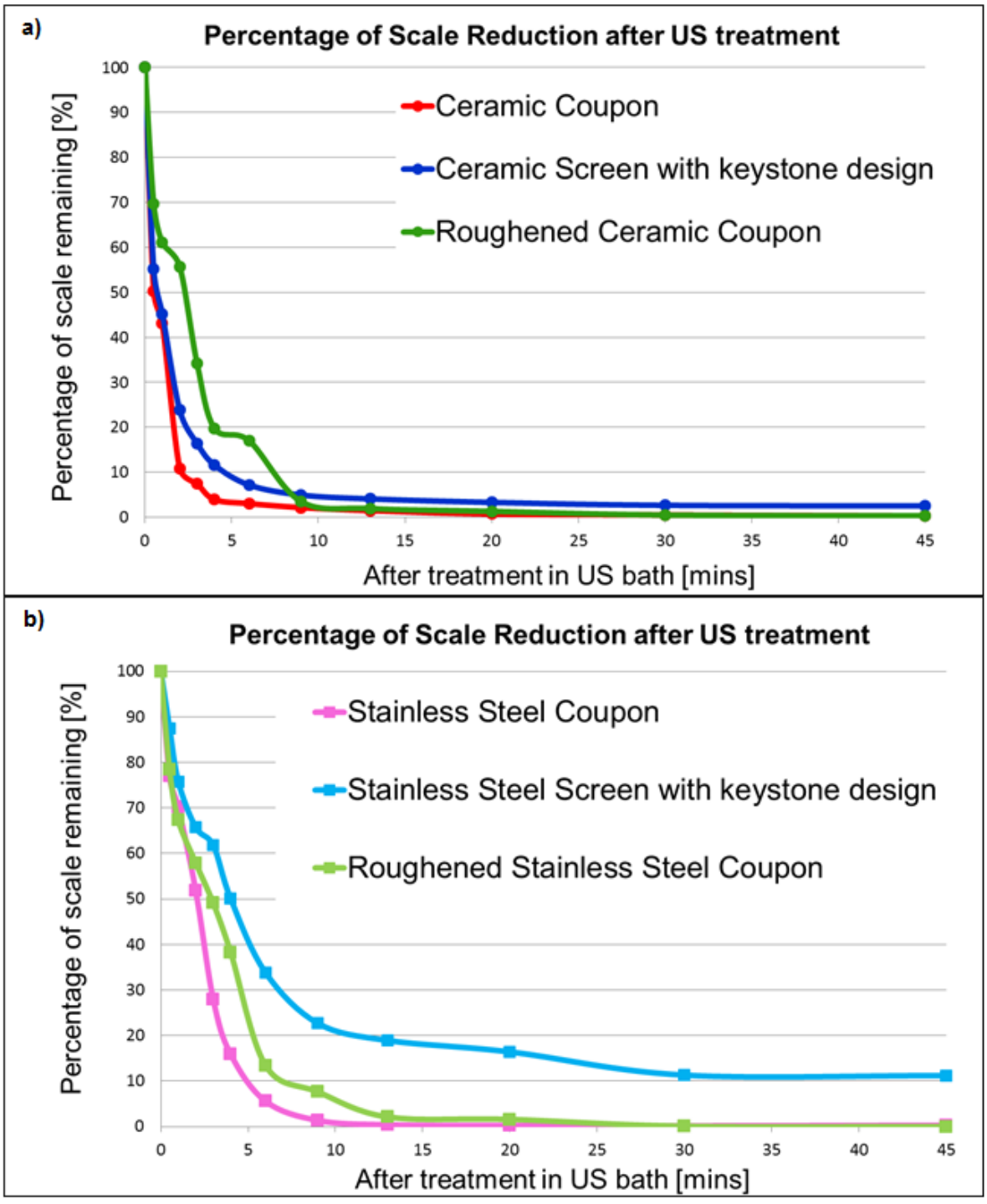

Figure 45: Comparison of Scale Removal based on design for: a) ceramic; b) stainless steel

After 45 minutes treatment in US bath, the probes were oven dried for 45 minutes and then photo of the probes were taken from the front side (Figure 46) and rear side (Figure 47).

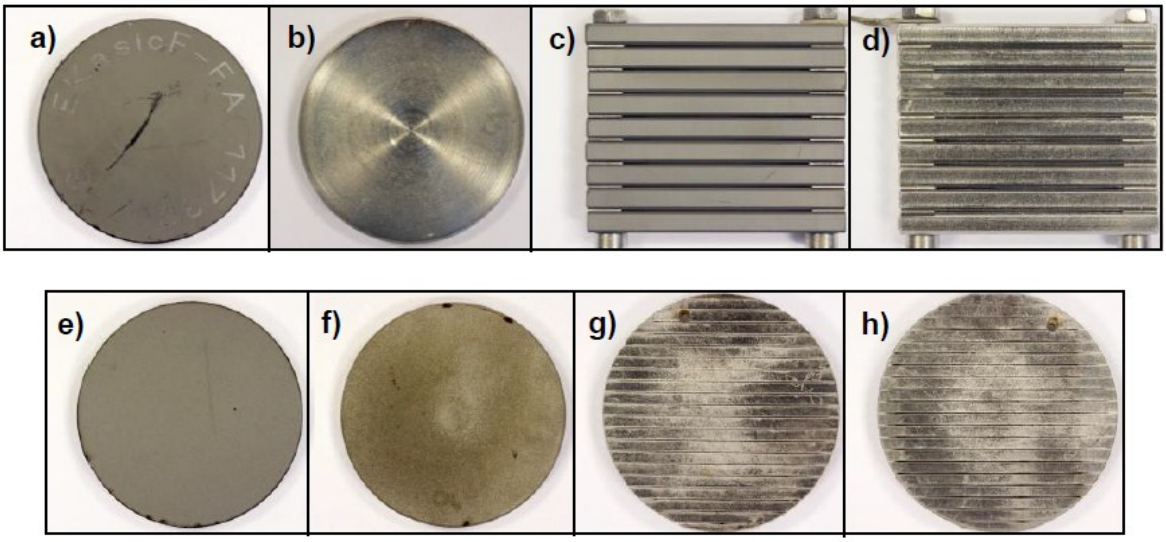

Figure 46: Front Side after 45 minutes treatment in US bath. a) Ceramic Coupon; b) Stainless Steel Coupon; c) Ceramic Screen with Keystone Design; d) Stainless Steel with Keystone Design; e) Roughened Ceramic Coupon; f) Roughened Stainless Steel Coupon; g) Stainless Steel Wire-wrapped Screen #1; h) Stainless Steel Wire-wrapped Screen #2

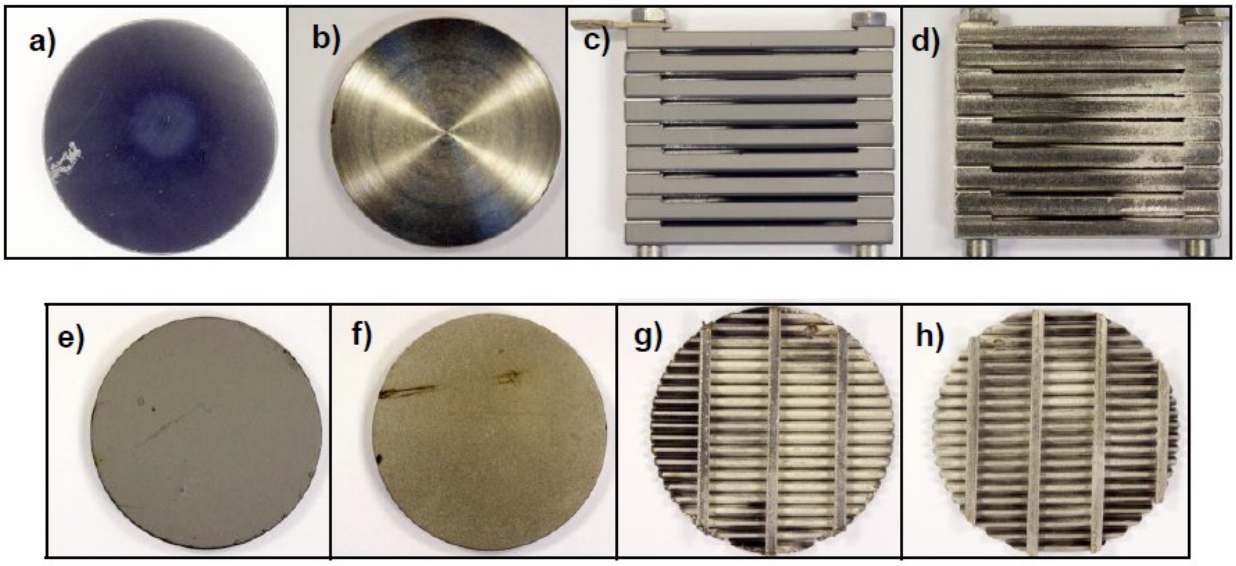

Figure 47: Rear Side after 45 minutes treatment in US bath. a) Ceramic Coupon; b) Stainless Steel Coupon; c) Ceramic Screen with Keystone Design; d) Stainless Steel with Keystone Design; e) Roughened Ceramic Coupon; f) Roughened Stainless Steel Coupon; g) Stainless Steel Wire-wrapped Screen #1; h) Stainless Steel Wire-wrapped Screen #2

On the front side of the probes, only a substantial amount of scale was noticeable on the stainless steel wire-wrapped screens #1 and #2 [Figure 46g) and h)]. Other than these probes, the other probes appear free of scale when viewed with bare eyes.

From the rear side of the probes, it can be seen that probes with screen design have evident scale remaining as compared to the solid coupons especially around the slot opening [Figure 47c), d), g) and h)]. Figure 47a) is a coupon design and has remains of scale but this is due to the interference between the clip that holds the coupon during US bath treatment and the coupon.

6 Discussion

This section discusses the optimizations carried out to achieve reproducible results for sand retention tests and scaling behaviour evaluation tests described in Section 6.1 and Section 6.3; respectively. This is followed by discussions of the results for the sand retention test and scaling behaviour evaluation tests as interpreted in detail in Section 6.2 and 6.4; respectively. Section 6.5 compares the materials based on the results obtained.

6.1 Optimization of Sand Retention Test

The criteria of selection of variables before the sand retention test is conducted are important since sand retention testing is known for being extremely dependent on its experimental conditions [33, p. 1]. The subsection of 6.1, goes in depth to explain the reasons behind the selection of certain variables. This then helps to avoid experimental anomalies which otherwise could be easily produced in a sand retention test.

6.1.1 Sand Retention Test Variables

This section explains the considerations given to the selection of certain variables in the experiments conducted.

a) Slot Opening Variations

There are several sizing calculation from several authors as mentioned before, however these rules are not necessarily always applicable but they help to give an idea [16]. In the same way before carrying out the sand retention test, calculations based on the PSD of the sample sand using two methods were done. The suggested slot opening from Gillespie's method was 134 µm. The second method based on Schwartz's paper suggested a slot opening of 200 µm. Based on this information, it was agreed to conduct the sand retention experiments for 3 slot openings, namely 150 µm, 200 µm and 250 µm.

Although the aim of the thesis is to compare the various sand screen materials. In the course of investigating the differences, it has become evident that the wire-wrapped screens are having a vast discrepancy from the nominal slot opening size. This then brings about the question of accuracy of the standard sand retention tests if the slot size would always differ in such a way. The standard screen sizing selection based on various criteria such as screen's retention capabilities and rate of pressure build [16, p. 6] may be invalid if screens are inconsistent in its slot openings to begin with.

b) Aperture Velocity

At the beginning, the idea was to perform the slurry sand retention test with constant aperture velocity. The aperture velocity is the velocity of the fluid flowing through the slot opening of the sand screen. The flowrate during slurry injection was used to calculate the

aperture velocity. The length of the slot openings on the sand filter available for fluid to flow was measured. Since the slot opening width is known, the area of the aperture can easily be calculated. The aperture velocity can then be determined given the flow rates and area of the aperture for various sand screens as shown in Figure 48. However the flowrate in the main loop controlled by Pump VF-15 on the test rig (Figure 7) has an allowable range between 0.5 L/min and 5.0 L/min. This together with the aperture area of the various slot openings and the constant sand slurry rate of 150 mL/min determines the aperture velocity. This results in a range of possible aperture velocities with a lower limit and upper limit as seen in Figure 48. The lower limit in aperture velocity for every type of screen and slot opening in Figure 48 corresponds to the flowrate of 0.5 L/min in the main loop. Whereas the upper limit in the aperture velocity for every type of screen and slot opening refers to the 5.0 L/min flowrate in the main loop.

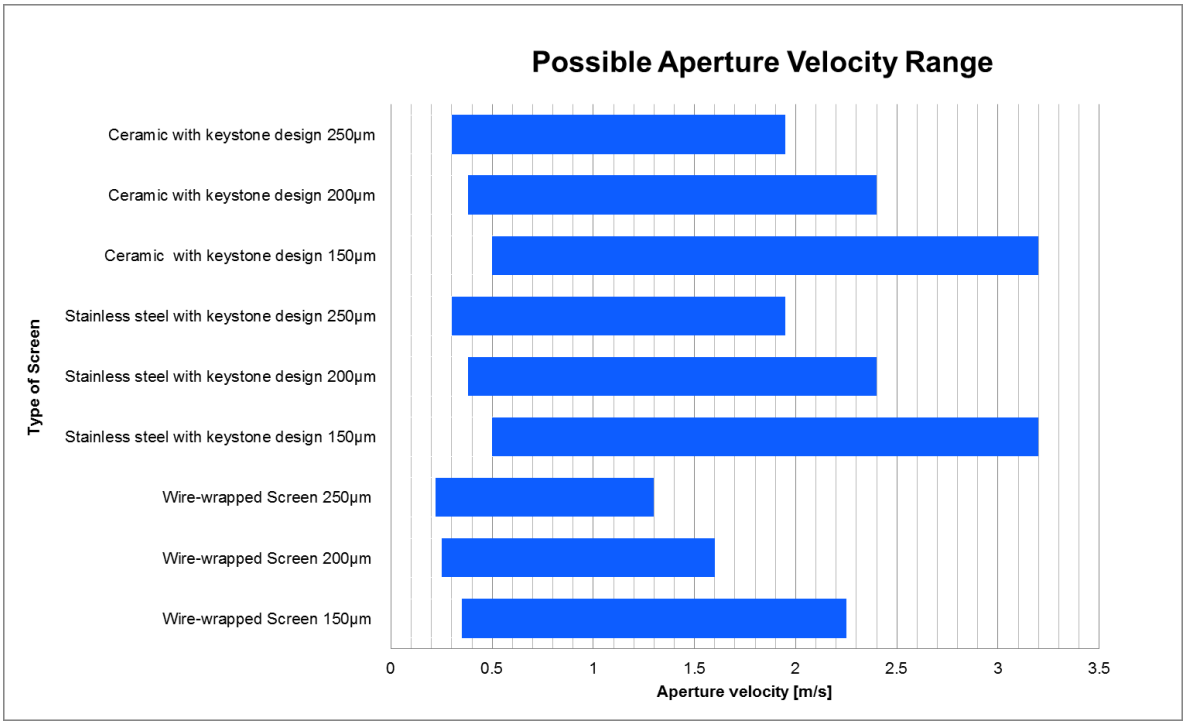

Figure 48: Possible Aperture Velocity Range

In order to find a suitable velocity for all screens, 1 m/s was arbitrarily selected. It must be noted that this velocity is rather high in comparison to velocities mentioned in other papers available in this field, but this is due to the fact that the experimental set up is different. However this should not cause any discrepancy in achieving the aim to investigate the different plugging behavior on the selected sand screens.

Based on the selected aperture velocity of 1 m/s and a constant sand slurry flowrate of 150 mL/min, the flowrate in the main loop is back calculated. The resulting flowrates in main loop for each screen type and slot opening is as shown in Table 7.

Table 7: Aperture Velocity Calculation

Type of filter	Wire wrapped screen			Stainless steel with keystone design			Ceramic with keystone design		
Width of slot openings [µm]	150	200	250	150	200	250	150	200	250
Length of slot openings [mm]	238	238	238	174	174	174	174	174	174
Wire/keystone width [mm]	2.2	2.2	2.2	3.34	3.34	3.34	3.34	3.34	3.34
Aperture area [mm^2]	35.70	47.60	59.50	26.10	34.80	43.50	26.10	34.80	43.50
Aperture velocity (m/s)	1.00								
Flowrate in Main Loop [L/min]	1.99	2.71	3.42	1.42	1.94	2.46	1.42	1.94	2.46
Set Pump Regulator Position to	15.3	20.3	25.06	11.1	15.0	18.6	11.1	15.0	18.6

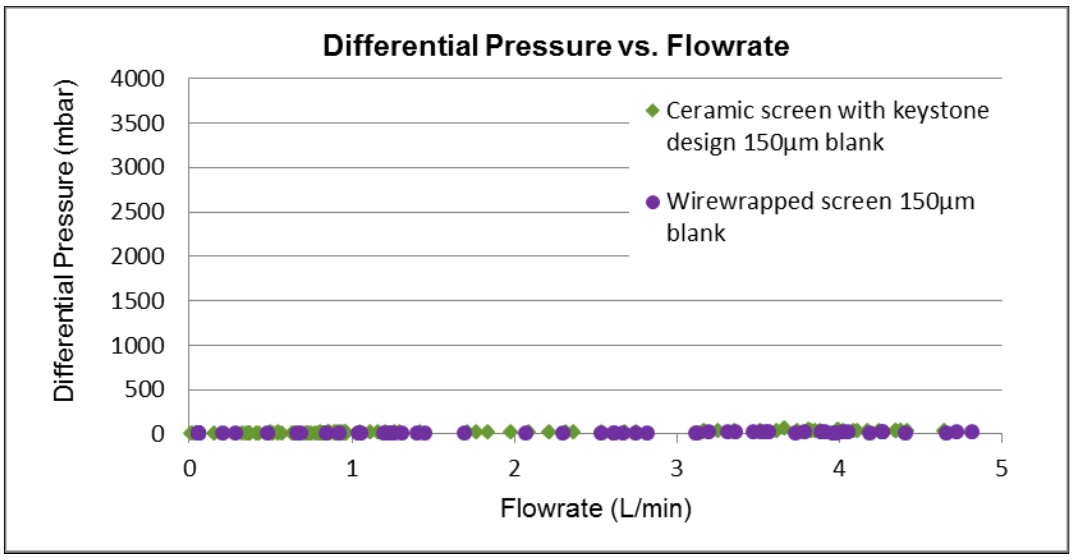

Figure 49: Differential Pressure vs. Flowrate of Sand Screen Alone

On the other hand, differential pressure being the key parameter in a sand retention test caused by the screen itself (Figure 49) is about 40 to 50 mbar for a 150 µm slot opening. The blank reading test was only conducted for the smallest slot opening since this would have the highest differential pressure in comparison to a blank 200 µm or 250 µm slot opening. Therefore it can be concluded that the screen itself can be neglected as compared to the differential pressure caused by the filter cake as seen in Figure 20a), Figure 21a), Figure 22a) and Figure 23a). This is also true for GP completion in which the pressure drop comes from the built gravel rather than the sand screen inside.

To obtain a constant aperture velocity at different slot openings, different flowrate would be required. In other words, changes in differential pressure are mainly caused by different flowrate. Hence the influence of the material or slot opening on sand retention behaviour cannot be seen. It was then decided to have constant flowrate and constant height of filter cake. This allowed for identification of the influence of material and slot opening on the formation of the filter cake and properties of the filter cake.

6.2 Sand Retention Test Results

From Figure 20a), Figure 21a) and Figure 22a) it can be noticed that the pressure build-up, the key parameter of the sand retention test is steep at the beginning of the sand retention test and then levels off slowly. This is because at the beginning, the filter cake is being formed hence the sudden pressure rise. After a certain time the sand particles rearrange themselves in an optimal manner forming a natural sand pack with higher porosity and permeability to allow for further flow [18, p. 22] . This is indicated with the constant differential pressure with time. The formation of filter cake on a sand screen is termed as bridging as illustrated in Figure 50. Sand sizes smaller than the screen opening form a bridge (indicated by the red line in Figure 50) that allows the deposition of sand on the bridge forming a filter cake (representing a GP) with time. The bridges may be stable or unstable [16, p. 4]. When unstable, the bridges can collapse and reform. The collapse and rebuilding of bridges on the screen can be related to a scenario of well that has gone through shut-in operations several times. This is because the differential pressure across a filter cake is changed by the numerous shut-ins altering the filter cake.

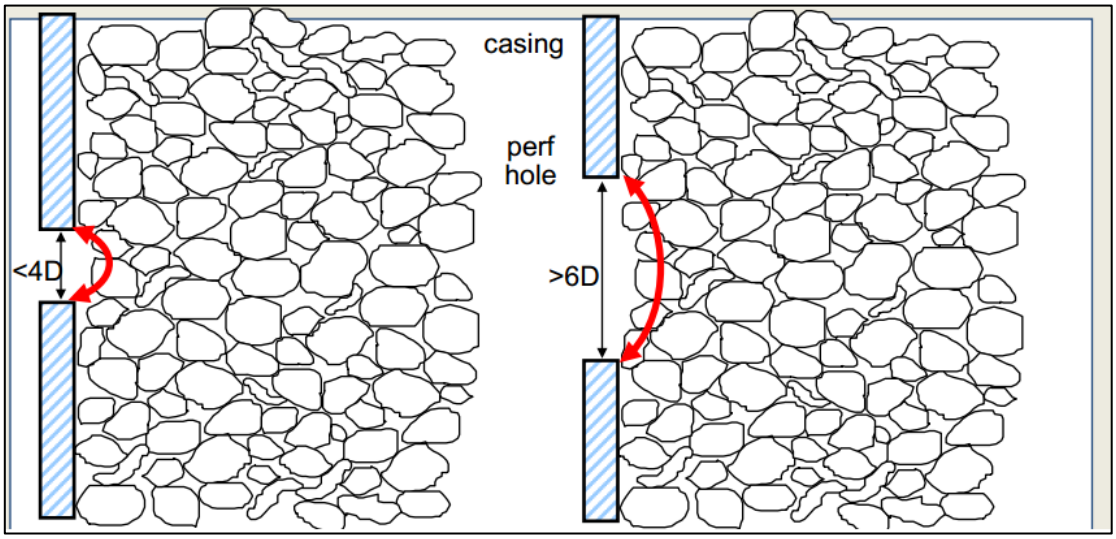

Figure 50: Bridging Lab Experiments [18, p. 18]

The pressure build-up is more gradual with increasing slot opening size regardless of screen types. This is convincing, since a smaller slot opening would be more selective in allowing sand to pass through the screen, hence retaining a great amount immediately at the start of the sand retention test as compared to a screen with a bigger slot opening.

In terms of differential pressure vs. flowrate as depicted in Figure 20b), Figure 21b) and Figure 22b); it is plausible that for all slot openings and types of screens with increasing flowrate the differential pressure across the filter cake increases implying the presence of flow resistance. The stainless steel wire-wrapped screen is distinctly the least resistant to flow across the filter cake for all slot openings. This is strongly believed to be due to the aperture area. As can be seen in Table 7, the aperture area for the stainless steel wire-

wrapped screen is 37% more than that of the screen with keystone design which corresponds to the 37% higher flowrate of wire-wrapped screen for all slot openings as can be seen in Figure 20b), Figure 21b) and Figure 22b).

For a better understanding, from Figure 20b), Figure 21b) and Figure 22b) the differential pressure across filter cake when flowrate is equal to 1 L/min is compared for all screen types and slot openings as portrayed in Table 8. The general trend of decreasing differential pressure with increasing slot opening size is coherent since a bigger slot opening would allow more flow with less resistance across the filter cake. However, the differential pressure across the filter cake formed on a ceramic screen with keystone design does not fall in the general trend. The differential pressure formed across the filter cake on a ceramic screen with keystone design remains constant or reaches saturation; strongly suggesting that the differential pressure is independent of slot opening sizes.

Table 8: Differential Pressure when flowrate across Filter Cake is 1L/min for Various Screen Types and Slot Openings

Screen Type	Ceramic Screen with Keystone Design	Stainless Steel Screen with Keystone Design	Stainless Steel Wire-wrapped Screen
Slot Opening [µm]	Differential Pressure when flowrate across Filter Cake is 1 L/min [mbar]	Differential Pressure when flowrate across Filter Cake is 1 L/min [mbar]	Differential Pressure when flowrate across Filter Cake is 1 L/min [mbar]
150	2500	2750	1800
200	2700	2100	1600
250	2700	2000	1400

When the stainless steel wire-wrapped screen and stainless steel screen with keystone design were roughened to simulate an eroded surface, the differential pressure across the filter cake was significantly higher than non-roughened stainless steel wire-wrapped screen and screen with keystone design as seen in Figure 23b). In some cases, the screen plugged immediately as seen in Figure 24. It is a clear that the tendency of plugging is caused by erosion on the surface and not because of slot opening size.

The results of the special cases shown in Figure 26 indicate that if channeling occurs, the initial flow through the screen is high and hence a high amount of sand is retained in the filtrate as seen in Table 5. If it is prolonged, it could lead to areas with high flow rate of fluids with sand, hence causing the formation of hotspots and soon erosion. Furthermore, a higher differential pressure across the filter cake for the same type of screen and slot opening recorded by W14 as compared to W8 referring to Figure 26b, does not mean that it would

plug soon. This is because almost the same amount of sand is retained in both filtrates, W8 and W14 referring to Table 5 although W8 has a lower differential pressure across filter cake as seen in Figure 26b).

Plugging occurs as a consequence when the screen is eroded due to wear therefore causing uneven rough surfaces, where sand particles get stuck obstructing flow through the slot openings as shown in Figure 24.

6.2.1 Mass Balance

A portion of the mass balance presented earlier in Table 11 in Section 5.1.1, the average sand retained in filtrate is combined with the differential pressure for a flowrate of 1 L/min across filter cake to have a better insight of the behaviour of the various types of sand screen.

Table 9: Differential Pressure when flowrate across Filter Cake is 1 L/min and Average Sand Retained in Filtrate for Various Sand Screen Types and Slot Opening

Screen Type	Ceramic Screen with Keystone Design		Stainless Steel Screen with Keystone Design		Stainless Steel Wire-wrapped Screen	
Slot Opening [µm]	Differential Pressure when flowrate across Filter Cake is 1 L/min [mbar]	Average Sand Retained in Filtrate [%]	Differential Pressure when flowrate across Filter Cake is 1 L/min [mbar]	Average Sand Retained in Filtrate [%]	Differential Pressure when flowrate across Filter Cake is 1 L/min [mbar]	Average Sand Retained in Filtrate [%]
150	2500	0.51	2750	0.97	1800	0.65
200	2700	0.75	2100	1.46	1600	0.73
250	2700	1.53	2000	1.51	1400	0.51

For stainless steel wire-wrapped screen, the significant variations in slot opening is believed to be the prime reason that the amount of sand retained in the filtrate is nearly constant at 0.63% regardless of the slot opening. Hence less can be said about the behaviour of stainless steel wire-wrapped screen towards sand retention testing in terms of slot opening sizes.

For the stainless steel screen with keystone design, with increasing slot opening size, the differential pressure across the filter cake decreases while the amount of sand retained in the filtrate increases. Based on Bernoulli's principle, with decreasing differential pressure, i.e. increasing slot opening size, the velocity after the screen (representing the velocity of fluid in the production tubing of a well) increases. Therefore turbulence may occur. Additionally, with increasing slot opening size, the percentage of fines in the filtrate increases as seen in

Table 9. The increasing amount of fines together with possible turbulent flow could be a vital reason for causing hotspots and sooner or later erosion.

The more or less constant differential pressure across the filter cake for varying slot openings for ceramic screen with keystone design suggests that in a condition of a GP, the possibility of transitioning to a turbulent flow regime is not likely with increasing slot opening size. Therefore, the GP formed behind a ceramic screen with keystone design is more stable than that for a stainless steel sand screen with keystone design. This is believed to be an effect purely due to the material.

As may be expected, in the case of Test W6 where channelling occurred, a substantial amount of sand, 20.4% [Refer to Table 5] flowed through the screen due to the delayed formation of filter cake. This highlights the importance of considering proper formation of the filter cake or GP more than the slot opening sizing calculation conducted during a screen selection. In the case of W14, where the resistance to flow across filter cake was significantly higher than W8 as seen in Figure 26b); less sand is retained in the filtrate W14, 0.59% as compared to W8 with 0.63% as shown in Table 5. The difference is negligible suggesting that the influence of differential pressure across the filter cake formed is almost minimal in terms of amounts of fines produced.

From Figure 27 and Figure 28, it is interpreted that having a low pressure build-up during the filter cake formation does not mean that the screen with filter cake has a lower flow resistance. This is because although in Figure 27, the pressure build-up for 250 µm ceramic screen with keystone design is significantly lower, there were scenarios of which the same screen having the highest resistance to flow in Figure 28. Once again this finding reiterates that the performance of a sand producing well with a sand screen installed is dominantly characterized by the filter cake formation behaviour rather than the screen itself.

From Figure 30 it can be concluded that as soon as production begins from a well with a screen installed, the majority of the sand produced comes in the initial phase of production. This then affirms the fact that the first phase of production of a well after installation of a screen is the most crucial. Whether the well produces more or less fines is purely dependent of the filter cake formation behaviour very much less to do with the slot opening sizing. This is clearly proved in the sand retention test conducted for this thesis.

6.2.2 Particle Size Distribution (PSD) Analyses

The cumulative particle size distribution of the residue (marked as dotted line) for all slot openings for all types of screens as depicted in Figure 31, Figure 32 and Figure 33 is close to the original sand used for slurry preparation (marked in yellow). This indicates that the residue retained by the screen, i.e. sand successfully prevented from entering the production tubing is almost identical to the reservoir sand. An apparent disparity between the cumulative PSD of all residue sand and reservoir sand is in the region of particle size 1 µm and 80 µm. This means that the sand in the size range of 1 µm to 80 µm is least present in the residue sand since it has flown through the screen. Once again, regardless of which slot opening or

screen type, for particle size more than 80 µm, the residue sand is very much similar to the reservoir sand indicating that to restrain the reservoir sand centred around 100 µm in the series of sand retention tests carried out, the screen type or slot opening plays hardly a role. Therefore the most significant problem in hand is not how to hold back the sand but to avoid hotspots and hence erosion, that would be the onset of sand production.

In terms of filtrate analyses comparing the solid lines in Figure 31, Figure 32 and Figure 33, it can be concluded that the ceramic screen with keystone design manages to consistently retain finer sand in the filtrate, than the stainless steel screen with keystone design for all slot openings. This is persistent considering that the standard deviation for the slot openings for the stainless steel screen with the keystone design is at 11.9 µm as mentioned in Section 3.1.4.2b). The standard deviation in the slot opening variations for the ceramic screen with keystone design is 6.05 µm as shown in Table 3 being less than that of the stainless steel screen with keystone design. Therefore it can be summarized that the negligible difference in slot opening precision seems to play an important role in the fines distribution in the filtrate.

The cumulative PSD results for all slot openings considering the effect of the slot opening variations is expected to look like Figure 31 where stainless steel wire-wrapped screen having the highest standard deviation in slot opening variation as much as 27.45 µm [Table 3] has the coarsest sand in the filtrate. However as the slot opening for the stainless steel wire-wrapped screen increases, the trend of the stainless steel wire-wrapped screens changes. The sand retained in the filtrate for a stainless steel wire-wrapped screen becomes finer as the slot opening size increases. As in Figure 32, stainless steel wire-wrapped screen although having a higher standard deviation in slot opening has finer fines in the filtrate as compared to the stainless steel screen with keystone design which has a stand deviation of only 11.9 µm. The reason behind this anomaly could be due to the fact that the stainless steel wire-wrapped screens previously used screens. Perhaps the use of new stainless steel wire-wrapped screens would have provided different results. The behaviour of sand retained in the filtrate for the stainless steel wire-wrapped screen due to its considerable slot opening variation is believed to cause the notable wave form noticed to be more pronounced with increasing slot opening in Figure 31, Figure 32 and Figure 33.

6.2.3 Scanning Electron Microscope (SEM)

The reason for only showing the results for one magnification and one slot opening in Section 5.1.3 is due to the fact that no difference was noticed before and after the sand retention experiment. If there was erosion due to the sand particles from the sand slurry, a scouring would have been expected in the direction of the flow, i.e. in the vertical direction. However no of such behaviour is noticed. This is acceptable due to the very short time of the experiment although high aperture velocity used. However it is interesting to see the difference in material property of the ceramic and stainless steel material. It is also interesting to note that the stainless steel wire-wrapped screen shown in Figure 38, although not roughened are seemed to have more wear. The roughened stainless steel screens shown in Figure 39 and Figure 40, shows the extremely uneven and angular surface caused

by the act of blasting it with B_4C. This is clearly a reason that causes sand particles to get stuck in this angular uneven surface causing a high differential pressure across filter cake resulting in plugging.

6.3 Optimization of Scaling Behaviour Evaluation

There is little literature available at present relating to scaling behaviour testing within existing laboratory environment. Therefore numerous optimizations are conducted for the scale formation (first part of the scaling behaviour evaluation test) as described in Section 6.3.1 and scale removal (second part of the scaling behaviour evaluation test) as described in Section 6.3.2. Additionally some variables had to be adjusted to obtain fair experimental results. This is described in Section 6.3.3.

6.3.1 Scale Formation

There were a few optimizations on how to form the scale. It is understood that pressure changes and high temperature fosters scale formation. A vacuum condition would be ideal however not very suitable to conduct the experiment. Furthermore atmospheric pressure is sufficiently low as compared to downhole pressures. The maximum temperature achievable is 100°C because the medium used to obtain scale is water. Initially the probes were boiled to 100°C. However it was found that boiling the water, causes steam bubbles to constantly move upwards which reduced the tendency for scale to adhere tightly to the probe surface. Therefore it was then decided to heat up to a maximum temperature of 90°C± 2°C to avoid having steam bubbles in the water.

The probes were immediately removed from the water to cool down to room temperature after boiling without holding the probes at 100°C for 10 minutes. Thereafter it was decided to hold the probes constantly at 90± 2°C for 10 minutes before allowing them to cool down. This procedure assisted in the formation of a tightly adhered scale layer on the probes.

In general, the scale formation procedure of heating to 90°C ± 2°C and holding at this temperature for 10 minutes for 10 times seemed to form a better adhered scale layer than the previous boiling to 100°C and allowing it to cool down to room temperature immediately.

6.3.2 Scale Removal

Again there were several optimizations on how to remove the scale from the probes. The probes were initially treated in US bath at 1 minute time intervals. However, it was realized that the initial phase of the US bath treatment is crucial as significant amount of scale is removed. However with increasing time, the percentage of scale removal per minute becomes less. Therefore to capture the scale removal behaviour in an efficient manner, the probes are placed in the US bath with increasing time steps from 0.5 minutes, 1 minute, 2 minutes, 3 minutes, 4 minutes until a total cumulative time of 45 minutes.

US waves were thought to be used to remove scale in laboratory environment, since it has been successfully used to remove wax, asphaltenes and scales [45]. Moreover it is a way towards being 'green' and avoiding the usage of chemical downhole.

6.3.3 Scaling Behaviour Evaluation Variable

This section explains the consideration given to one variable in the experiment conducted i.e.:

a) Volume of distilled water in the 1 liter 89 mm OD glass beaker placed in the US bath

Initially, all probes were placed simultaneously in a 2 liter 131 mm OD glass beaker looking similar to Figure 19, however it was noticed that due to the vibrations caused by US emissions, the probes overlapped one another causing interference not allowing for an effective scale removal. Hence it was then decided to place only 2 probes per glass beaker as shown in Figure 16.

6.4 Scaling Behaviour Evaluation Test Results

The results gathered for the scaling behaviour evaluation test, namely the scale formation and scale removal are discussed in detail in Section 6.4.1 and Section 6.4.2; respectively.

6.4.1 Scale Formation

When comparing a stainless steel material and a ceramic material of the same design, i.e. stainless steel coupon with ceramic coupon, stainless steel screen with keystone design with stainless steel screen with keystone design etc. the stainless steel had more scale deposited than a ceramic material as clearly seen in Figure 42. This was believed in the beginning to be an effect due to the surface roughness where more scale is deposited with increasing surface roughness. However this was not true for all cases as seen in Table 6. To understand this behaviour a paper by Cheong et. al. [46] was evaluated.

This matches the results of a scaling tendency ($CaCO_3$ adhesion tendency) experiment carried out by Cheong et.al [46], where scaling tendency is evaluated on various coatings using untreated stainless steel as a base material for comparison. One of the coatings used by Cheong et.al was Tech 23 which is a composite ceramic material made up of individual chromium oxide (Cr_2O_3) ceramic particles. Tech 23 is a dense ceramic coating almost without porous sections which is similar to the Sintered Silicon Carbide (SSiC) ceramic material used in this thesis. In Cheong et. al's findings, Tech 23 has exhibited the least scaling tendency as compared to other polymer surfaces, while bare stainless steel has the highest scaling tendency. The process in which scale is formed is called nucleation through which $CaCO_3$ crystallizes. Nucleation is an extremely localized budding of a new phase (such as crystals) due to changes in thermodynamics and reaction kinetics [47] . Nucleation is dependent on three parameters namely interfacial tension, temperature and super saturation coefficient as expressed in **eq.3**, **eq.4 and eq. 5** [46, pp. 7-8] below:

$$Log\ T_{n,theoretical} = A + (B/log^2 S) \quad (3)$$

$$\sigma_{cl} \cos\theta = \sigma_{sl} - \sigma_{sc} \quad (4)$$

$$B \propto \frac{\sigma_{cl}}{T} \quad (5)$$

T_n Nucleation time [s]
S Super Saturation Ratio
A constant
B constant
σ_{cl} interfacial tension
θ intrinsic contact angle
σ_{sl} substrate liquid interface
σ_{sc} substrate crystal interface
T Temperature [°C]

Since interfacial tension as seen in **eq. 4** and **eq. 5** plays an important role in nucleation, it is also important to discuss wettability which is a closely related property. Wettability is a property governed by the surface's chemical composition and its roughness [46, p. 8]. This property is usually measured in terms of contact angle or wetting angle. Wettability also gives indication to the surface energy. A large contact angle is associated with a low surface energy therefore causing less feasible adhesion. The relationship between wetting/ contact angle (θ^*) and intrinsic angle (θ) based on Wenzel model is as shown in **eq. 6** [46, p. 8] below.

$$\cos\theta^* = \frac{r(\sigma_{cl} - \sigma_{cs})}{\sigma_{sl}} = r\cos\theta \quad (6)$$

θ^* wetting/contact angle
r roughness factor which is the ratio of factual surface area, S_r to smooth surface area, S_o of the substrate

For a smooth surface area of a probe, S_o the wetting angle of solution on the surface is described by the intrinsic contact angle, θ because r is equal 1. However with increasing surface unevenness called asperities, r increases. For any substrate (probe) with a contact angle of less than 180°, the nucleation on the substrate interface (heterogeneous nucleation) is energetically more favourable than the nucleation on liquid interface (homogeneous nucleation). For the scaling behaviour evaluation test, water is used as the solution therefore the water contact angle represents the wetting angle of the solution.

From **eq. 4** and **eq. 6** [46, pp. 7-8], it is clear that as wetting angle (θ^*) increases, intrinsic contact angle (θ) increases, hence the interfacial tension σ_{cl} decreases. A low σ_{cl} is associated with low surface energy, hence resulting in lower adhesion forces, i.e. lower propensity for scale formation [46].

Additionally, based on Wenzel's model, roughness plays a role in wettability as shown in **eq. 6**. When θ is less than 90°, θ^* will decrease with the increase of r; when θ is greater than 90°, θ^* will increase with r. r has no effect on wettability when $\theta = 90°$.

Additionally, ion implantation of elements such as C, H and Si etc. on metal surfaces causes the number of free electrons to decrease [46]. This is another reason causing reduction in wettability and hence a reduction in surface energy.

Table 10: Water Contact Angle[5], Surface Roughness and $CaCO_3$ Deposited per Hour for Substrates [46, p. 11&14]

Substrate	Water Contact Angle , θ* [°]	Surface Roughness, Ra[µm]	Average $CaCO_3$ deposited per hour [mg/hr]
Bare Stainless Steel	84.00	0.13	11.50
Tech 23	103.00	0.61	1.00

Based on Table 10, it can be seen that Tech 23 (sintered ceramic coating material) has a higher contact angle than bare stainless steel in the experiments conducted by Cheong et.al, therefore strongly suggesting that in the scale formation experiment conducted in this thesis, the scale formed on stainless steel is evidently more than the ceramic due to effect of surface energy.

The general belief of surface roughness being directly proportional to scaling formation as reported in Keysar et.al (0.1-22.5 µm) [48] , Herz et. Al (0.54-1.55 µm) [49] and Kukulka and Devgun (0.254-5.84 µm) [50] is not coherent with Cheong et.al as shown in Table 10 and scale formation test conducted for this thesis as shown in Table 6. This difference is believed to be a contribution of more factors than surface roughness. For instance, presence of interfacial defects due to surface geometry can affect wetting and adhesion.

[5] Water contact angle was not determined in this thesis.

Therefore it can be concluded that scale adhesion tendency is an effect contributed by the differing surface energy of the different materials. Stainless steel appears to have a higher surface energy, hence scales adheres strongly on a stainless steel material as compared to ceramic material. The effect of surface roughness on scaling tendency is still unclear. The results obtained in the experiment conducted are supported by observations from Cheong et. al in terms of surface energy and roughness.

6.4.2 Scale Removal

A qualitative analysis to understand the adherence of scale on the various types of probes, the probes was swiped with the tip of the finger. Although the scale was not removed completely, it was observed that the scale deposited on a ceramic coupon came off easier than from a stainless steel coupon. This can be explained by looking at the nature of nucleation. There are two ways nucleation can occur; either in a heterogeneous manner or homogeneous manner [46, p. 17]. A heterogeneous manner is a situation where strong interaction between the nucleating phase (in this case the scale) and the substrate (the probes) is expected. In such a case, the adherence of scale to the probe will be strong, and the structure of the scale formed will be compact and strongly adhered as shown in Figure 51. Conversely in a homogeneous nucleation, the probe does not have an effect on nucleation and nucleation occurs randomly in the bulk solution. This reduces the adherence characteristic at the scale crystal and probe interface significantly as shown in Figure 52.

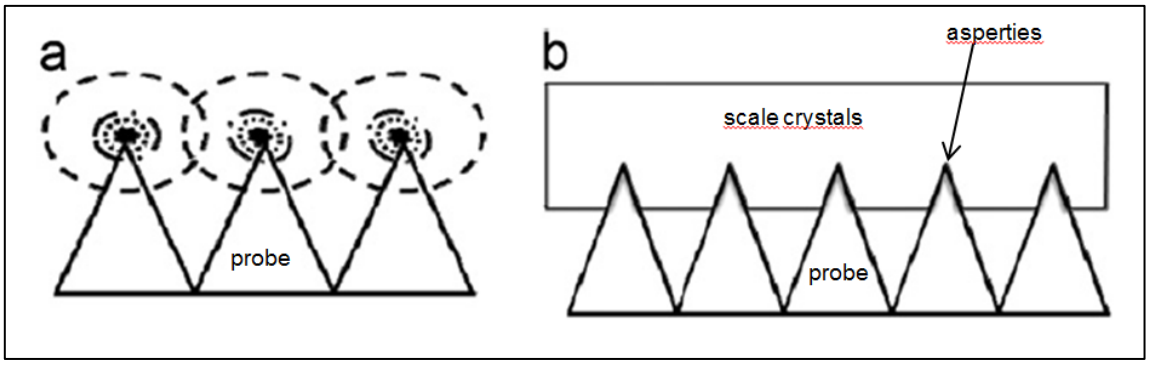

Figure 51: Heterogeneous Nucleation. a) Crystals nucleating from the asperities[6] tips; b) crystals lying on top of the nano-/micro-structures with larger surface area in contact between crystal and substrate(probe) relative to a homogeneous nucleation [46, p. 18]

[6] Asperities: surface unevenness

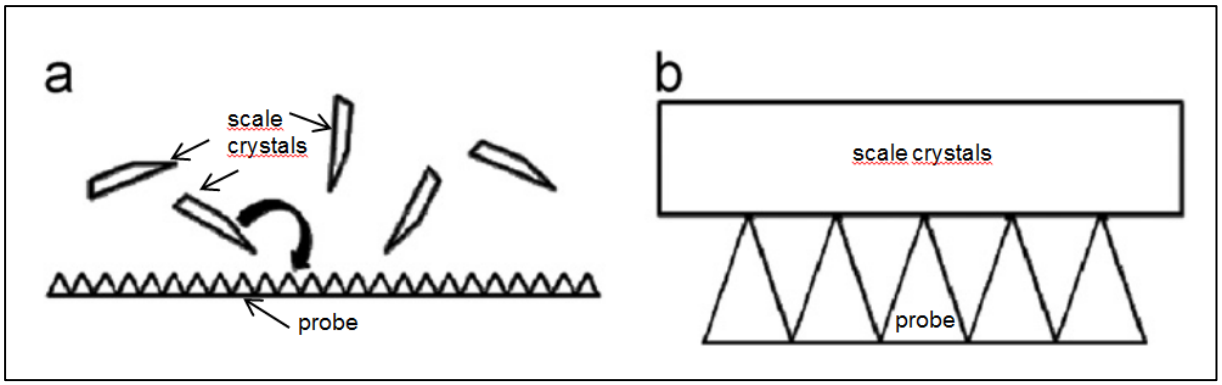

Figure 52: Homogeneous Nucleation. a) Crystals migrating from the bulk solution and depositing on top of asperities; b) crystals lying on the tip of the asperities just after being deposited [46, p. 18]

Therefore it can be deduced that the scale that was removed by using a finger tip from a ceramic and stainless steel probe was the scale crystals that had been deposited from the bulk solution i.e. those crystals formed through homogeneous nucleation.

Additionally, a quantitative analysis was done to verify this observation in the scale removal process. Scale was more easily removed from a ceramic material than a stainless steel material regardless of the design as shown in Figure 45. This is again accepted to be due to the higher water contact angle and lower surface energy for ceramic material.

After 45 minutes exposure in US bath, the scale was almost completely removed for all screens except, stainless steel screen with keystone design [Figure 45b)] and stainless steel wire-wrapped screen #1 and #2 [Figure 44]. The percentage of scale that remained after 45 minutes in US bath were 10%, 20% and 30% for stainless steel screen with keystone design, stainless steel wire-wrapped screen #1, and #2; respectively. These remainders left on the sand screens are the cause of new scale precipitation when the well is set on production again after cleaning. This is concluded to be a combined effect of the material being stainless steel and the slot design. This is because all the 3 types of probes where a significant amount of scale was noticed after 45 minutes of US bath had a slit.

In other words, the patterned surface plays a significant role more than the surface roughness as can be seen in Figure 45b). Cheong et. al also believed that scale deposits were easier to be removed in rougher surfaces contrary to other papers by Keysar et.al (0.1-22.5 μm) [48] , Herz et. al (0.54-1.55 μm) [49] and Kukulka and Devgun (0.254-5.84 μm) [50] since surface patterns that were not considered in other papers. Cheong et. al and the scale removal evaluation in this thesis considers the effect of material and design (slit pattern).

6.5 Comparison of Materials

In the sand retention test, various sand screen materials were compared namely the ceramic screen with keystone design, stainless steel with keystone design and stainless steel wire-wrapped screen. It was clear that the stainless steel wire-wrapped screen was not a valid comparison in terms of sand retention behaviour since it had a different aperture area as shown in Table 7. However it was good to have an idea of where the stainless steel wire-wrapped screen that is available on the market stands in relation to the ceramic screen with keystone design.

In general the ceramic screen appears to have numerous advantages. In terms of sand retention test, it appears to be that ceramic works equally well or in fact better in a simulated reservoir condition than a stainless steel material. This is of course not taking into consideration the effect of erosion and the resistance to chemicals and sour gas (H_2S and CO_2) of the material with the lifetime of a well. Furthermore, it has been proven by RAG in its operation in a well in Zistersdorf, that a wire wrapped screen without GP failed after only one day of production [51, p. 71]. Whereas no screen out was observed with a ceramic screen without GP. This reiterates the robustness of ceramic screen being able to be installed as a stand-alone screen unlike a wire-wrapped screen.

The scaling tendency of ceramic material is evidently lower than that of stainless steel material. Additionally turbulent flow conditions which are very likely to occur in a stainless steel screen but not in ceramic screen as mentioned earlier accelerate corrosion and scaling [46, p. 12].

Despite these advantages of ceramic screens, there are certain adverse characteristics of ceramics that makes them always a troublesome candidate to be selected especially for downhole completions. Ceramics are brittle and have no ductility. Therefore during placement of ceramic screens down hole, extreme care has to be taken as to avoid it from failing in which a catastrophic failure occurs. Additionally it is more expensive as compared to a stainless steel screen without GP. Thus in an event of a catastrophic failure due to the ceramic screen breaking during a completion workover, the cost incurred in such a failure is high.

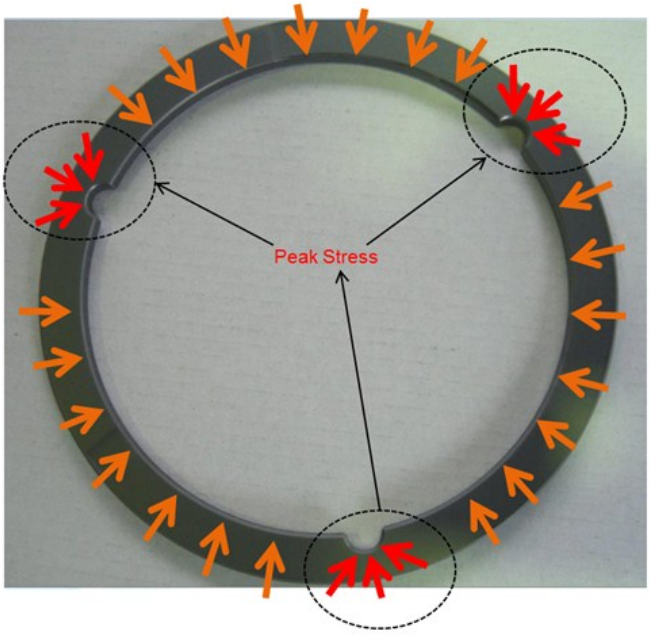

Figure 53: Peak Stress occurring in a Ceramic Ring

Moreover, the ceramic screen built from a stack of ceramic rings encounters peak stress in regions marked in red in Figure 53. The arrows in orange show the presence of stress which is not critical. However the peak stress marked in red are critical which could cause failure of the screen. This is an area that is under improvement carried out by the Research and Development (R&D) team in ESK.

Furthermore ceramic screen has a low resistance to thermal shock, however in a well; the geothermal gradient is about 2.5 °C/100m [52]. Keeping this is mind, while lowering a ceramic screen during completion operation, the ceramic screen will not undergo any sort of thermal shock. However when hot or cold well treatments are conducted, ceramic screen could be affected by thermal shocks. Hot or cold treatment also can have an adverse effect on other subsurface equipment of steel. These sort of treatments can cause expansion or contraction of the steel; which may result in tubular collapse.

6.6 Areas of Improvement

Based on the tests conducted and results obtained Section 6.6.1 and Section 6.6.2 below consider possible improvements that could be undertaken for the sand retention test and scaling behaviour evaluation test, respectively.

6.6.1 Sand Retention Test

Conducting a reproducible sand retention test has been the main obstacle. A few measures were taken to improve the results. Many of the measures taken, concern the sand retention test flow loop [Figure 7] from lessons learnt from the experiments carried out in the initial phase of the thesis. These measures are such as placing the flowrate sensor further downstream away from Peristaltic Pump VF 15. This was done to ensure that the pulsation of the flowrate seen by the flowrate sensor was minimal. Additionally Control Valve, CV-3 were not present initially in the Sand Retention Test Rig, however CV-3 was installed to allow for a better control of sand slurry flow to injection point A. Other improvements were also thought of to achieve a reproducible result however were not able to be carried out due to the time constraints. Such measures are to change the Peristaltic Pump VF-10 in the sand slurry loop to a piston pump. This measure will affirm that no dilution occurs in the sand slurry loop before Injection Point A. In this way, a constant sand slurry dosing rate into the main loop can be achieved. Additionally, it was extremely hard to regulate the flow in the main loop using Flow Control Valve, FCV-15 which is a manual FCV to achieve a constant flow in the main loop. This becomes especially harder when the slurry injection begins. Therefore installing an electronic FCV to maintain the flowrate in the main loop would solve the issue. Moreover, the sand that enters the measuring cell does not fall evenly on to the screen. To overcome this problem, the installation of a diffuser upstream of the measuring cell in the flow loop will allow the sand to be forming a leveled off filter cake instead of heaped filter cake.

Additionally, stainless steel wire-wrapped screens with more accurate slot opening sizes would allow for an optimized comparison contradictory to the used wire-wrapped screens obtained from Baker Hughes Inc. which had significant variations in slot openings. Without the significant slot opening variations, the v-shaped wire design could be compared with the keystone design of the same material type as shown in Figure 13. This could give knowledge about the optimal screen design to be adopted in future.

6.6.2 Scaling Behaviour Evaluation Test

The wetting/ contact angle of the ceramic and stainless steel materials are not measured in for the scaling behaviour test conducted for this thesis. The measurement of contact angle may clarify the wetting behaviour and hence the scaling behaviour of the ceramic and stainless steel material.

7 Conclusion

Through the comparison tests, namely sand retention tests and scaling behaviour evaluation tests; carried out in this thesis to investigate the sand production, scaling and plugging behaviour of selected sand screen materials, a better understanding has been achieved not only in terms of the differences in sand screen materials but also the enlightenment in the state of the art procedures carried out in the oil and gas industry. Section 7.1 summarizes the key points from the sand retention test and Section 7.2 concludes the scaling behaviour evaluation test

7.1 Summary of Sand Retention Test

When the sand slurry dosing rate which is extremely sensitive is well controlled, the effect of the slot opening can be seen. In general, the effect is: the smaller the slot opening, the higher the differential pressure across the filter cake. However for ceramic screen, the differential pressure across the filter cake, is somewhat constant, indicating that regardless of which slot opening used, the differential pressure remains approximately same therefore the risk of entering in the turbulent phase where erosion and corrosion can occur is avoided. More importantly it must be understood, that in a laboratory environment the sand dosing rate can be well controlled; however in a real case scenario in a field, the sand rate can hardly be manipulated. In such a case, the filter cake built acting as a GP is unpredictable, which causes flowrate across filter cake to be independent of the slot opening size as shown in Figure 28. In other words, for the sand sample used for the series of experiments conducted in this thesis, slot opening is not a key determining criteria for sand screen application.

For a fair comparison, the ceramic screen keystone design is to be compared with the stainless steel screen with keystone design. This is because the stainless steel wire-wrapped screen had a different aperture area as compared to the other two screens.

The mass balance reiterates the small impact that slot opening variation has on amount of sand retained in the filtrate. In terms of PSD Analyses, the residue sand is very much similar to the sample sand used. Whereas the fines retrieved in the filtrate are comparable, showing that ceramic screen with keystone design had smaller fines as compared to the stainless steel screen with keystone design. This is due the less precision slot opening that the stainless steel screen had. Therefore this difference is not an effect caused by the material but by the precision in manufacturing.

As expected no differences were found through SEM examination since the flowrates were low. According to erosion experiments conducted by J. Feyerl [53] on various types of stainless steel materials in the gas phase as seen in Figure 54, a sand velocity of 40 m/s is required to instigate erosion [53, p. 148]. In the liquid phase, as a rule of thumb this would mean that about 4 m/s of sand velocity would be required to prompt erosion [54]. In the

series of sand retention experiments carried out in this thesis, a maximum of about 2 m/s fluid velocity is reached due to the apparatus set up.

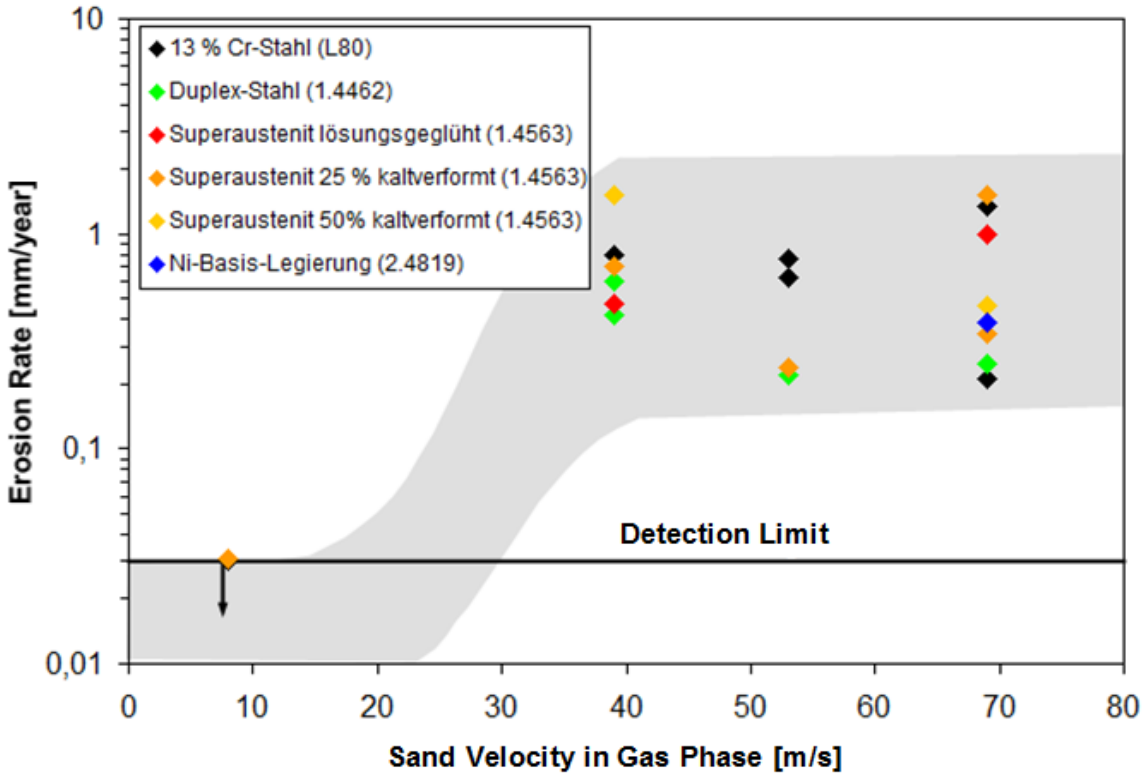

Figure 54: Influence of sand particle (of diameter 100 µm) velocity at CO_2 partial pressure of 15 bar in the main loop with sand slurry consisting of 27 g/L of brine and sand concentration of 0.9 g/L [53, p. 148]

7.2 Summary of Scaling Behaviour Evaluation Test

Scale deposits less on ceramic material than a stainless steel material due to the lower surface energy that ceramic possesses. Additionally, through the scale removal test it has become clear, that the slot design gives rise to a heterogeneous nucleation, causing scale to adhere more strongly than to a solid coupon. The effect of surface roughness on scale formation and removal is yet to be firmly established. But at present it is found to be less significant factor than material and screen design (pattern) in scaling tendency.

7.3 Recommendation

Based on the various advantages of ceramic screen such as erosion resistance, corrosion resistance, less prone to scaling, ability to work as a sand-alone screen and good ability to prevent sand from entering the production tubing; it is recommended that ceramic screens be considered to tackle sand production problems.

The cost involved in installing a ceramic screen in comparison to the state of the art wire-wrapped screen is debateable. This is because when installing a wire-wrapped screen, cost incurred for GP (wire-wrapped screen is rarely used as stand-alone), workover for cleaning due to scaling etc. and production loss during workover period needs to be considered. When these factors are given due consideration, the perception of ceramic screen being expensive is outweighed in comparison to stainless steel wire-wrapped screens complete with GP. This is especially true for offshore applications. Moreover ceramic screens provide a competitive advantage in horizontal well applications (onshore and offshore) where deploying a wire-wrapped screen with a properly formed GP is a considerable challenge.

Of course, ceramic sand screen application is still new in the oil and gas industry therefore hesitation to use it may persist. However ceramic sand screens have been successfully installed in the Danish Offshore Sector by MAERSK, in Gaiselberg field Austria by RAG and in Bolivia by British Gas (BG) and have proved to be both technically and economically feasible.

8 Outlook

Ceramic sand screens clearly provide a competitive advantage in sand screen application. The further advancement in design and construction of ceramic screens will enhance their application e.g. with respect to reducing peak stresses.

8.1 Scaling Behaviour Evaluation Test

To better understand the difference in scaling behaviour between ceramic sand screens and stainless steel sand screens, the determination of surface energy (water contact angle) will be helpful. Additionally the effect of roughness should be subject to further investigation.

8.2 Sand Retention Test

Sand retention tests should be conducted with other sand samples having different PSD with varying slot opening sizes. These would be expected to show that the slot opening size is not a key determining factor in sand screen applications.

Additionally, from Figure 55 it can be seen that after 60 minutes of sand blasting experiment conducted by PetroCeram®, erosional hot spot is created on a stainless steel but not on a ceramic. This verifies the erosion resistance of ceramic as compared to stainless steel [55].

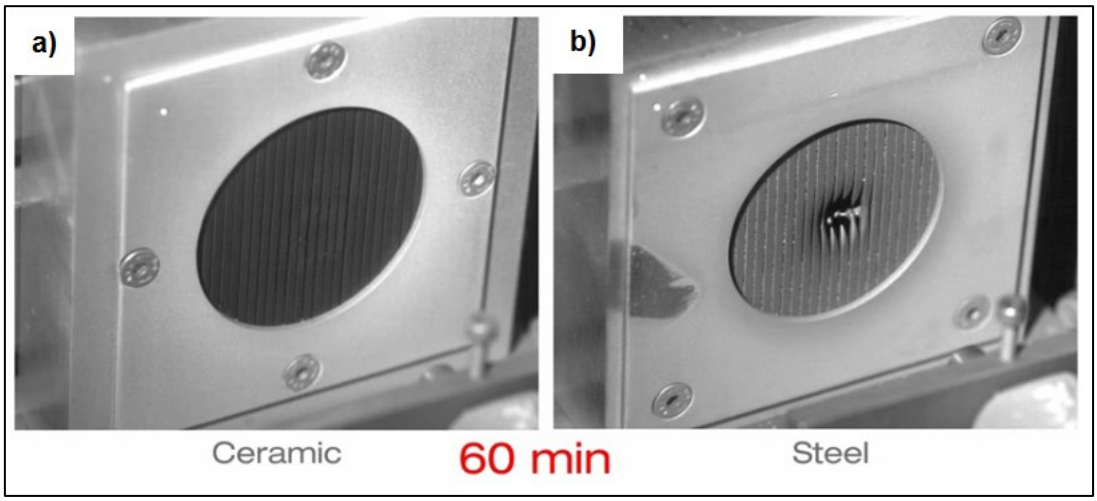

Figure 55: Sand erosion test on a) ceramic and b) stainless steel [55]

Based on the observation seen in Figure 56, it can be concluded that the volumetric erosion is far less than stainless steel. The blue line in Figure 57 is a first guess extrapolated based on the different hardness of the materials. To confirm the position of this blue line in Figure 57 further investigations are necessary.

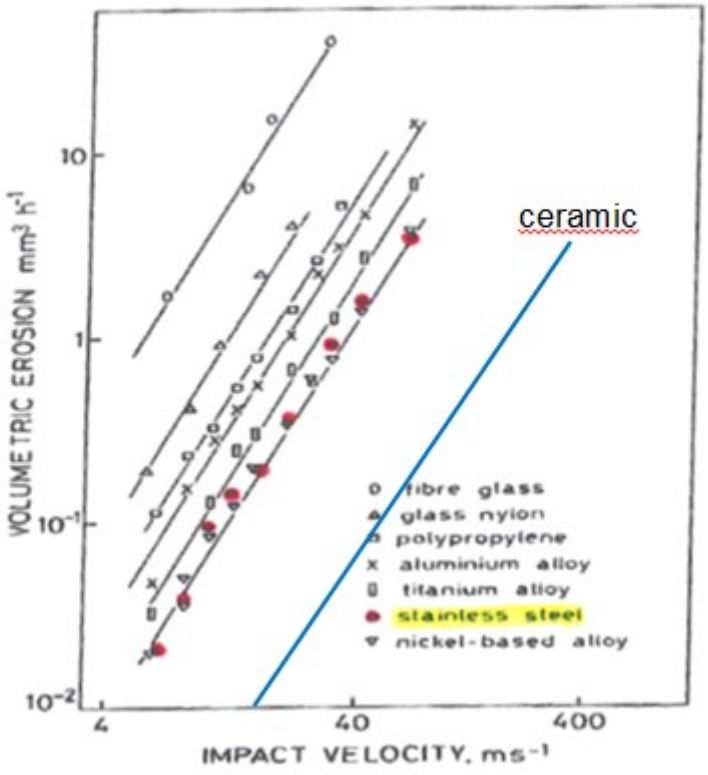

Figure 57: Influence of Solid Particle Velocity on Erosion Rate of Different Materials [37, p. 150]

9 References

[1] K. Shaikh, R. Adesegha and N. Talib, "Sucessful Through-Tubing Gravel Pack Unlocks Production in Mature Fields Offshore Brunei," in *CPS/SPE International Oil & Gas Conference and Exhibition*, Beijing, China, 2010.

[2] Schlumberger Limited, "Oilfield Glossary," 2013. [Online]. Available: http://www.glossary.oilfield.slb.com/en/Terms/i/induced_particle_plugging.aspx. [Accessed 8 September 2013].

[3] M. Dusseault, "Comparing Venenzuelan and Canadian Heavy Oil and Tar Sands," in *Canadian International Petroleum Conference*, Calgary, Alberta, 2001.

[4] J. A. Kupecz, J. Gluyas and S. Bloch, Reservoir Quality Prediction in Sandstones and Carbonates, Amer Assn of Petroleum Geologists Memoir 69, 1997.

[5] J. K. Daemen and R. A. Schultz, Rock Mechanics: Proceedings of the 35th U.S. Symposium, University of Nevada, A.A. Balkema, 1995.

[6] Pang, Zhanxi, Liu and Huiqing, "The Study on Permeability Reducton during Steam Injection in Unconsolidated Porous Media," *Journal of Petroleum Science and Engineering,* pp. 77-84, 11 May 2013.

[7] G. Stosur, Writer, *Global Warming and the Petroleum Industry – Conflict of Science and Politics. Past, Present and What the Future May Bring.* [Performance]. Society of Petroleum Engineers Swiss Section, 2011.

[8] Schlumberger Limited, "Oilfield Glossary," 2013. [Online]. Available: http://www.glossary.oilfield.slb.com/en/Terms.aspx?LookIn=term%20name&filter=API%20gravity. [Accessed 8 September 2013].

[9] H. Ye, M. Patarroyo and N. Lopey, "Innovative Well-Completion Strategy for Challeging Heavy-Oil Wells within Mature Fields Requiring Sand Control in Colombia," *Society of Petroleum Engineers,* 12-14 December 2011.

[10] Society of Petroleum Engineers, "SPE," 2013. [Online]. Available: http://www.spe.org/events/12ado4/pages/about/index.php. [Accessed 8 August 2013].

[11] H. Hofstätter, Writer, *Advanced Well Completions- Sand Control.* [Performance]. Chair for Petroleum and Geothermal Energy Recovery, MontanUniversität Leoben, Austria, 2012.

[12] R. Hodge, R. Burton, V. Constien and V. Skidmore, "An Evaluation Method for Screen-Only and Gravel-Pack Completions," in *SPE International Symposium and Exhibition*, Louisiana, 2002.

[13] A. Damgaard, D. Bangert, D. Murray, Rubbo, R.P. and G. Stout, "A Unique Method for Perforating, Fracturing and Completing Horizontal Wells.," *SPE Production Engineering 7,* pp. 61-69, 1992.

[14] J. a. Hansen, "Controlled Acid Jet (CAJ) Technique for Effective Single Operation Stimulation of 14,000+ ft Long Reservoir Sections.," in *European Petroleum Conference*, Aberdeen, 2002.

[15] S. Müssig, Writer, *Mature Fields.* [Performance]. RAG Rohöl-Aufsuchungs Aktiengesellschaft, 2010.

[16] G. Gillespie, C. Deem and C. Malbrel, "Screen Selection for Sand Control Based on Laboratory Tests," in *SPE Asia Pacific Oil and Gas Conference and Exhibition*, Brisbane, 2000.

[17] U. Romanova and T. Ma, "An Investigation fo the Plugging Mechanisms in a Slotted Liner from the Steam Assisted Gravity Operations," in *SPE European Formation Damage and Exhibition*, Noordwijk, 2013.

[18] *Sand Control Overview.* [Performance]. George E. King Engineering, 2009.

[19] S. Isehunwa and A. Farotade, "Sand Failure Mechanism and Sanding," *International Journal of Engineering Science and Technology Vol. 2(5),* pp. 777-782, 2010.

[20] J. Friedrich, J. Arguello, G. Deitrick and E. Rouggignac, "Geomechanical Modelling of Reservoir Compaction, Surface Subsidence, and Casing Damage at the Belridge Diatomite Field," *SPE Reservoir Eval. & Eng. 3,* pp. 348-359, August 200.

[21] Schlumberger Limited, "Schlumberger Oilfield Glossary," 2013. [Online]. Available: http://www.glossary.oilfield.slb.com/en/Terms/p/particle-size_distribution.aspx. [Accessed 11 September 2013].

[22] M. Crabtree, D. Eslinger, P. Fletcher, M. Miller, A. Johnson and G. King, "Fighting Scale-Removal and Prevention," *Oilfield Review,* pp. 30-45, Autumn 1999.

[23] Geoscience Resources, "Precipitation and Solution of Calcium Carbonate".

[24] L. Clancy, Aerodynamics, Great Britain: Sir Isaac Pitman & Sons Ltd, 1975.

[25] Finco,Inc., "Horizontal Directional Drilling Information Guide," Finco, Inc., Kansas, 2006.

[26] L. Leising, A. Ali, J. Young and O. Arciniegas, "Re-enterable Through-Tubing Gravel-Pack System," in *SPE/ ICoTA Coiled Tubing Conference and Exhibition*, Houston, 2004.

[27] S. N. Gulrajani, D. Pittman and X. Herve, "Imaging Gravel-Pack Quality: Application to Deviated and Horizontal Wells," in *European Petroleum Conference*, Aberdeen, 2002.

[28] Weatherford, "Gravel Pack and Frac Pack Systems," 2011. [Online]. Available: www.weatherford.com/dn/WFT174871 . [Accessed 5 September 2013].

[29] J. van Vliet, H. Lau, O. Skilbrei, S. H. Rahman, L. Bernardi, E. Shumilak and A. Halal, "Horizontal Openhole Gravel Packs Boost Oil Production in Brunei," in *APE Asia Pacific Improved Oil Recovery Conference*, Kuala Lumpur, 2001.

[30] M. Oberndorfer, Interviewee, *SchadenKatalogue.* [Interview].

[31] S. Wildhack, S. Müssig, F. Strahammer and M. Leitner, "Sand Control with Ceramic Screens in Unconsolidated Reservoirs demonstrated in the mature Gaiselberg Oilfield," in *Oil Gas European Magazine* , Celle, 2012.

[32] S. W. C. Lesniak, Writer, *PetroCeram Ceramic Sand Screen Key Features.* [Performance]. Ceradyne,inc., 2009.

[33] T. Ballards and S. Beare, "Media Sizing for Premium Sand Screens: Dutch Twill Weaves," in *SPE European Formation Damage Conference*, The Hague, 2003.

[34] T. Ballard and S. Beare, "An Investigation of Sand Retention Testing With a View To Developing Better Guidelines for Screen Selection," in *SPE Internation Symposium and Exhibition on Formation Damage Control*, Louisiana, 2012.

[35] A. Mathisen, G. Aastveit and E. Alteras, "Successful Installation of Stand Alone Sand Screen in More Than 200 Wells- The Importance of Screen Selection Process and Fluid Qualification," in *European Formation Samage Conference*, Scheveningen, 2007.

[36] US Environmental Protection Agency, "Underground Storage Tanks," 20 December 2012. [Online]. Available: http://www.epa.gov/OUST/cat/lttd.htm. [Accessed 15 July 2013].

[37] M. Oberndorfer, Metallurgie und Korrosion für Erdölingenieure, 2006.

[38] Korea Internation Trade Association, "Johnson Screen, Stainless Steel Wire Screen," 2000-2013. [Online]. Available: http://www.tradekorea.com/product-detail/P00239738/Johnson_screen__Stainless_steel_Water_well_screen__wedge_wire

_screen___wire_wrap_water_well_screen_.html#. [Accessed 10 September 2013].

[39] A. Belz, "3M pays $860M for Calif. firm," *Startribune business,* 2012.

[40] Environmental Expert S.L., "Johnsonscreens-Weatherford International Inc.," 1999-2003.

[41] M. Dumler, "KKU- Kemptener Kommunalunternehmen Wasser, Abwasser, Bäder," [Online]. Available: http://www.kku-kempten.de/m_wasser_haerte.php. [Accessed 8 July 2013].

[42] Weatherford International Ltd., "weatherford.com," 2010. [Online]. Available: http://www.weatherford.com/weatherford/groups/web/documents/weatherfordcorp/WFT027565.pdf. [Accessed 18 September 2013].

[43] T. Ballard and S. Beare, "Sand Retention Testing : The More You Do, the Worse It Gets," in *SPE International Symposium and Exhibition on Formation Damage Control*, Lafayette, 2006.

[44] A. Andiappan, *Sand Retention Test Rig Manual,* Kempten, 2013.

[45] H.Hofstätter, Writer, *GSU und Ultraschallwellen, Neue Wege in der Erdöl- und Erdgasproducktionstechnik.* [Performance]. Petroleum Production and Processing, Montanuniversität Leoben, Austria, 2012.

[46] W. Cheong, P. Gaskell and A. Neville, "Substrate effect on surface adhesion/crystallisation of calcium carbonate," *Journal of Crystal Growth 363,* pp. 7-21, 2013.

[47] R. Sear, "The non-classical nucleation of crystals: microscopic mechanisms and applications to molecular crystals, ice and calcium carbonate," *Internation Materials Reviews Vol 57 No.6,* pp. 328-356, 2012.

[48] Keysar.S, Semiat.R, Hasson.D and Yahalom.J, "Effect of surface roughness on morphology of calcite crystalliyation on mildsteel," *Journal of Colloid and Interface Scien 162,* pp. 311-319, 1994.

[49] A. Herz, M. Malayeri and H. Müller-Steinhagen, "Fouling of roughened stainless steel surfaces during convective heat transder to aqueous solutions," *Energy Conversion and Management 49,* pp. 3381-3386, 2008.

[50] D. Kukulka and M. Devgun, "Fouling surface finish evaluation," *Applied Thermal Engineering 27,* pp. 1165-1172, 2006.

[51] K. Soliman, *The Economic Value of TEchnology for Lifting Hydrocarbon Fluids in Mature Field Operation,* Leoben, 2013.

[52] C. Bromley, M. Mongillo, G. Hiriart, B. Goldstein, R. Bertani, E. Huenges, A. Ragnarsson, J. Tester, H. Muraoka and V. Zui, "Contribution of Geothermal Energy to Climate Change Mitigation: the IPCC Renewable Energy Report," in *Proceedings WOrld Goethermal Congress 2010*, New Zealand, 2010.

[53] J. Feyerl, *Erosionkorrosion in Öl- und Gasfördersystemen,* Leoben, 2006.

[54] M. Oberndorfer, Interviewee, *Erosionkorrosion Beständigkeit.* [Interview]. 30 September 2013.

[55] *PetroCeram Sandsiebrohr.* [Film]. Ceradyne,inc. PetroCeram, 2010.

[56] T. O. Allen and A. P. Roberts, Production Operations, Well Completion, Workover, and Stimulation Volume 2, Tulsa, Oklahoma: OGCI,Inc.,PetroSkills,LLC., 2008.

[57] T. J. Mason and J. P. Lorimer, Applied Sonochemistry, Weinheim: Wiley-VCH, 2002.

[58] S. Polczer, “Petroleum Economist,” 15 02 2012. [Online]. Available: http://www.petroleum-economist.com/Article/2979412/News-Analysis-Unconventional/Mind-the-oil-sands-price-gap.html. [Accessed 20 02 2012].

Appendices

Appendix A: Photo of the Sand Retention Test Rig

Appendix B: Measuring Cell Assembly

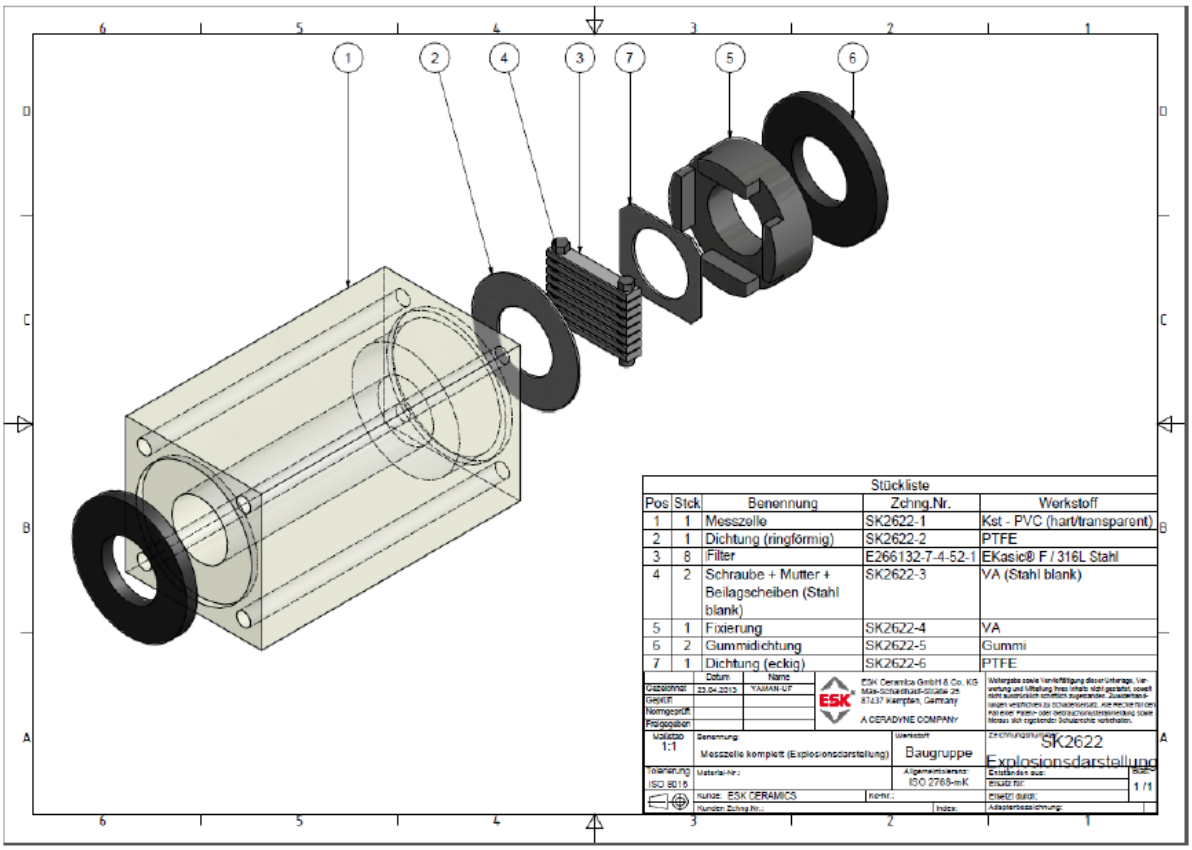

Stückliste

Pos	Stck	Benennung	Zchng.Nr.	Werkstoff
1	1	Messzelle	SK2622-1	Kst - PVC (hart/transparent)
2	1	Dichtung (ringförmig)	SK2622-2	PTFE
3	8	Filter	E266132-7-4-52-1	EKasic® F / 316L Stahl
4	2	Schraube + Mutter + Beilagscheiben (Stahl blank)	SK2622-3	VA (Stahl blank)
5	1	Fixierung	SK2622-4	VA
6	2	Gummidichtung	SK2622-5	Gummi
7	1	Dichtung (eckig)	SK2622-6	PTFE

	Datum	Name
Gezeichnet	23.04.2015	YAMAN-UF
Geprüft		
Normgeprüft		
Freigegeben		

ESK Ceramics GmbH & Co. KG
Max-Schaidhauf-Straße 25
87437 Kempten, Germany
A CERADYNE COMPANY

Maßstab 1:1 | Benennung: Messzelle komplett (Explosionsdarstellung) | Werkstoff: Baugruppe | Zeichnungsnr.: SK2622 Explosionsdarstellung

Toleranzen ISO 8015 | Material-Nr.: | Allgemeintoleranz: ISO 2768-mK | Ersetzt für: | Ersetzt durch: | Blatt 1 / 1

Kunde: ESK CERAMICS | Kom.Nr.: | Index: | Adapterbezeichnung:

Kunden Zchng.Nr.:

Appendix C: Mass Balance of Various Slot Openings Compared for the Same Type of Sand Screen Material

Table 11: Mass Balance for Ceramic Screen with Keystone Design for Various Slot Openings

Slot Opening [µm]	Tests	Mass of:		Percentage of:	
		Residue [g]	Sand Retained in Filtrate [g]	Residue [%]	Sand Retained in Filtrate [%]
150	C11: Ceramic Screen with Keystone Design 050813	16.0583	0.0915	99.43	0.57
	C12: Ceramic Screen with Keystone Design 050813	20.4114	0.0915	99.55	0.45
	C13: Ceramic Screen with Keystone Design 050813	20.3597	0.0915	99.55	0.45
	C24: Ceramic Screen with Keystone Design 190813	19.9618	0.0925	99.54	0.46
200	C14: Ceramic Screen with Keystone Design 060813	20.8234	0.0924	99.56	0.44
	C15: Ceramic Screen with Keystone Design 060813	25.1987	0.0919	99.64	0.36
	C22 : Ceramic Screen with Keystone Design 140813	20.0973	0.0933	99.54	0.46
250	C6: Ceramic Screen with Keystone Design 260713	20.5946	0.0945	99.54	0.46
	C8: Ceramic Screen with Keystone Design 050813	21.5149	0.0919	99.57	0.43
	C9: Ceramic Screen with Keystone Design 050813	21.8159	0.0921	99.58	0.42
	C10: Ceramic Screen with Keystone Design 050813	20.7647	0.0923	99.56	0.44
	C17: Ceramic Screen with Keystone Design 05081	20.0280	0.0928	99.54	0.46
	C18: Ceramic Screen with Keystone Design 050815	20.2218	0.0927	99.54	0.46

Table 12: Mass Balance for Stainless Steel Screen with Keystone Design for Various Slot Openings

Slot Opening [µm]	Tests	Mass of:		Percentage of:	
		Residue [g]	Sand Retained in Filtrate [g]	Residue [%]	Sand Retained in Filtrate [%]
150	S1: Stainless Steel Screen with Keystone Design 070813	20.2409	0.1477	99.28	0.72
	S2: Stainless Steel Screen with Keystone Design 070813	20.2757	0.2173	98.94	1.06
	S3: Stainless Steel Screen with Keystone Design 080813	20.0419	0.2293	98.87	1.13
200	S6: Stainless Steel Screen with Keystone Design 120813	20.2318	0.1817	99.11	0.89
	S7: Stainless Steel Screen with Keystone Design 120813	19.5258	0.5067	97.47	2.53
	S11: Stainless Steel Screen with Keystone Design 190813	20.1889	0.2495	98.78	1.22
	S12: Stainless Steel Screen with Keystone Design 190813	20.1962	0.2428	98.81	1.19
250	S8: Stainless Steel Screen with Keystone Design 130813	20.6653	0.3986	98.11	1.89
	S9: Stainless Steel Screen with Keystone Design 130813	20.5365	0.3707	98.23	1.77
	S10: Stainless Steel Screen with Keystone Design 130813	20.1870	0.1771	99.13	0.87

Table 13: Mass Balance for Stainless Steel Wire Wrapped Screen with Various Slot Openings

Slot Opening [µm]	Tests	Mass of:		Percentage of:	
		Residue [g]	Sand Retained in Filtrate [g]	Residue [%]	Sand Retained in Filtrate [%]
150	W1: Stainless Steel Wire-wrapped Screen 080813	22.1895	0.1653	99.26	0.74
	W3: Stainless Steel Wire-wrapped Screen 080813	21.8652	0.1172	99.47	0.53
	W4: Stainless Steel Wire-wrapped Screen 080813	20.4024	0.1746	99.15	0.85
	W7: Stainless Steel Wire-wrapped Screen 080813	22.0999	0.1090	99.51	0.49
200	W5: Stainless Steel Wire-wrapped Screen 120813	21.1443	0.2150	98.99	1.01
	W8: Stainless Steel Wire-wrapped Screen120813	22.1792	0.1409	99.37	0.63
	W13: Stainless Steel Wire-wrapped Screen 190813	23.5545	0.1319	99.44	0.56
250	W9: Stainless Steel Wire-wrapped Screen 120813	21.2300	0.0982	99.54	0.46
	W10: Stainless Steel Wire-wrapped Screen 130813	22.2190	0.1207	99.46	0.54
	W11: Stainless Steel Wire-wrapped Screen 130813	22.0330	0.1141	99.48	0.52

Appendix D: PSD Analyses Results

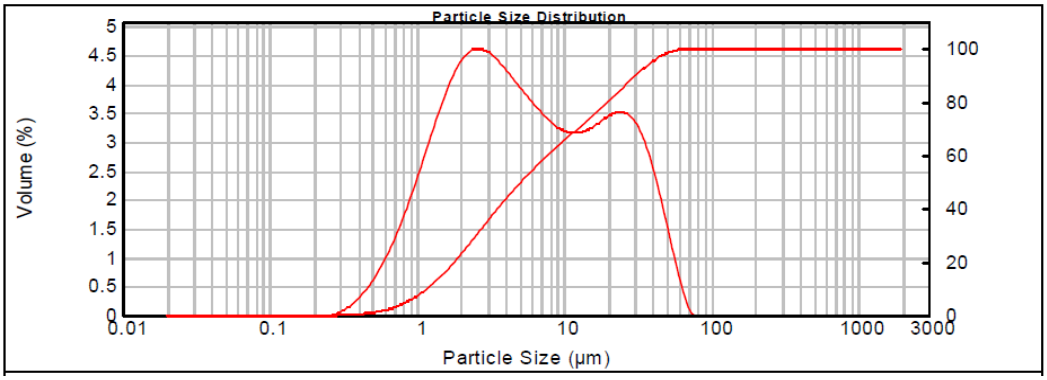

Figure 58: PSD for filtrate of C11-Ceramic Screen with Keystone Design with 150 µm Slot Opening

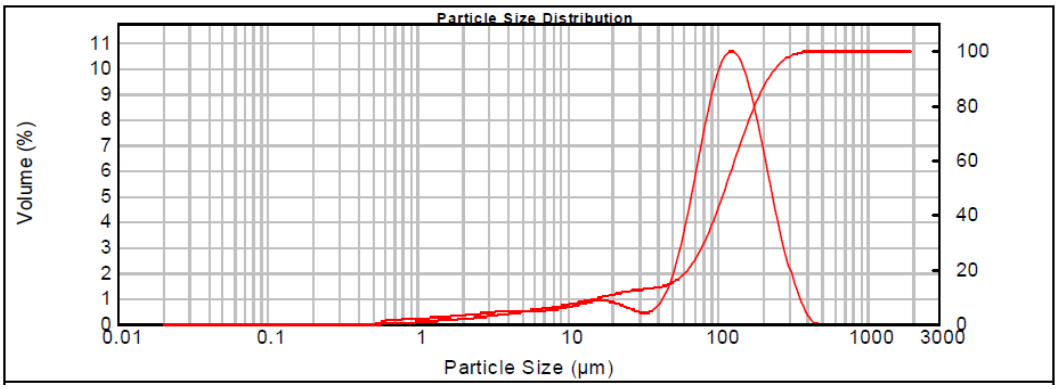

Figure 59: PSD for residue of C11-Ceramic Screen with Keystone Design with 150 µm Slot Opening

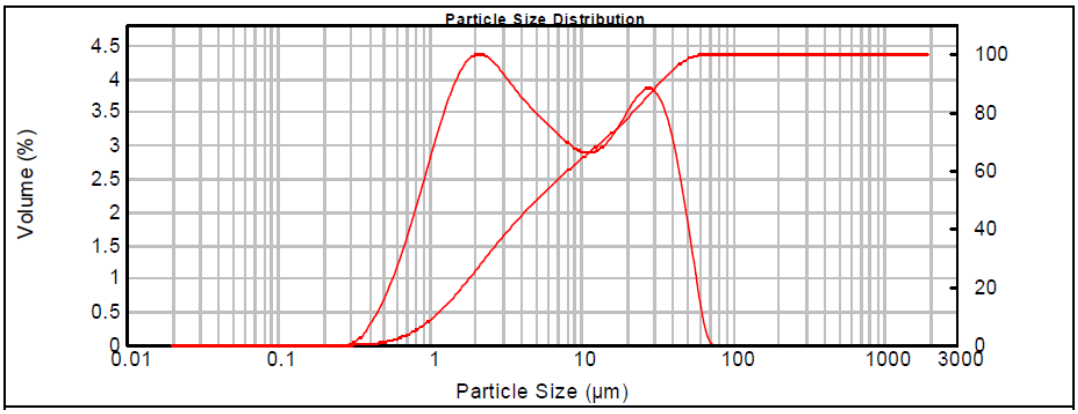

Figure 60: PSD for filtrate of C13-Ceramic Screen with Keystone Design with 150 µm Slot Opening

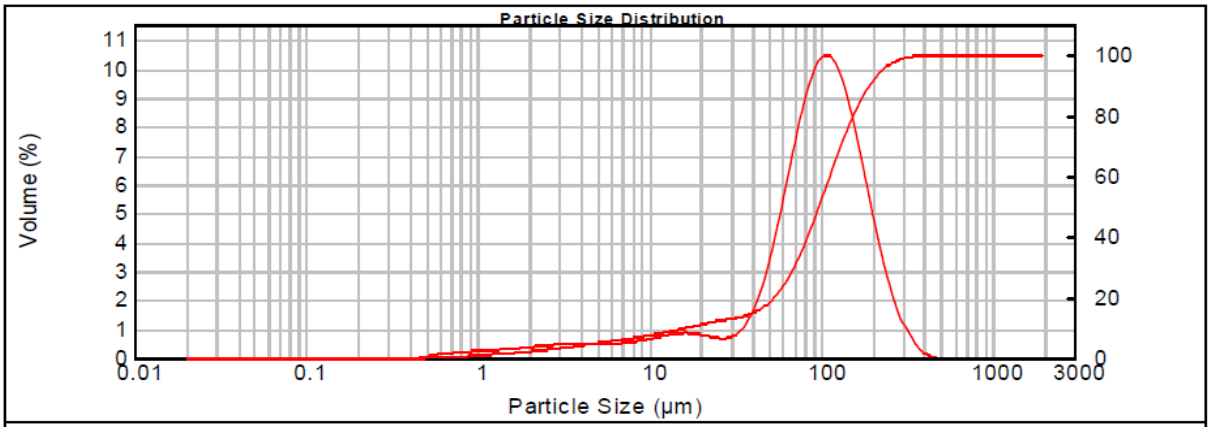

Figure 61: PSD for residue of C13-Ceramic Screen with Keystone Design with 150 µm Slot Opening

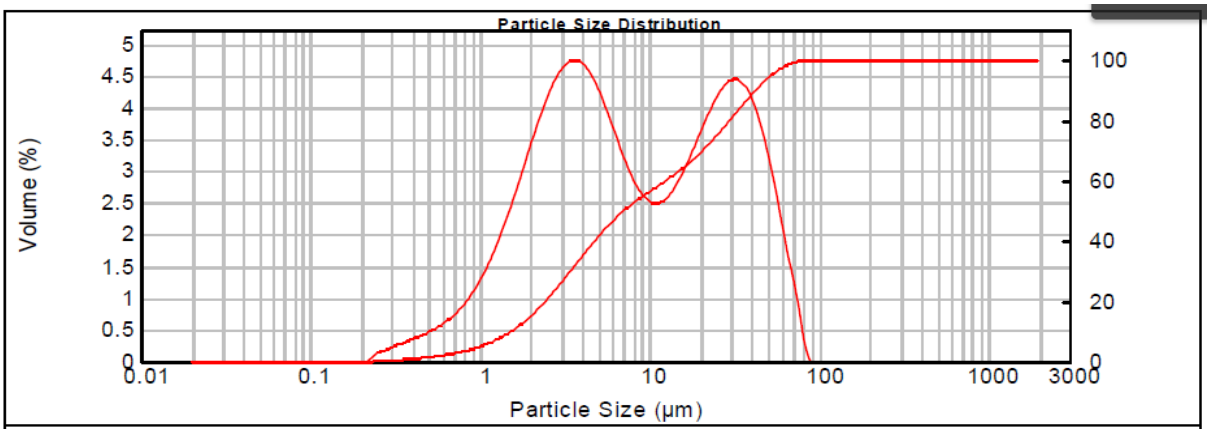

Figure 62: PSD for filtrate of S2-Stainless Steel Screen with Keystone Design with 150 µm Slot Opening

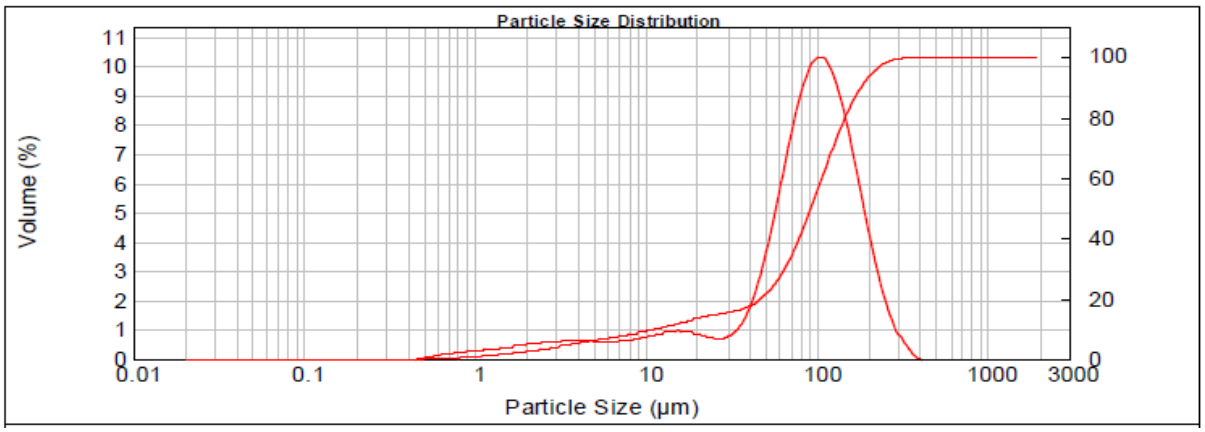

Figure 63: PSD for residue of S2-Stainless Steel Screen with Keystone Design with 150 µm Slot Opening

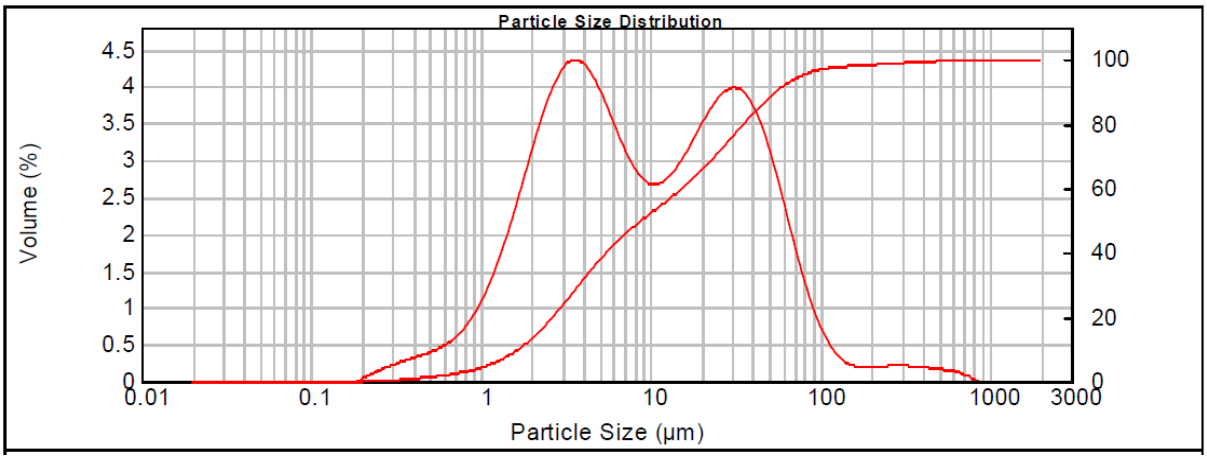

Figure 64: PSD for filtrate of S3-Stainless Steel Screen with Keystone Design with 150 µm Slot Opening

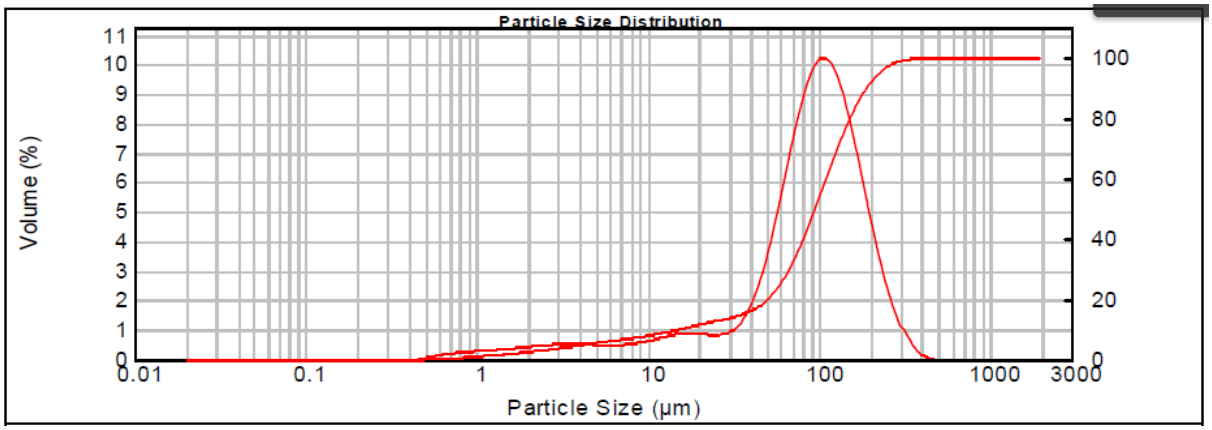

Figure 65: PSD for residue of S3-Stainless Steel Screen with Keystone Design with 150 µm Slot Opening

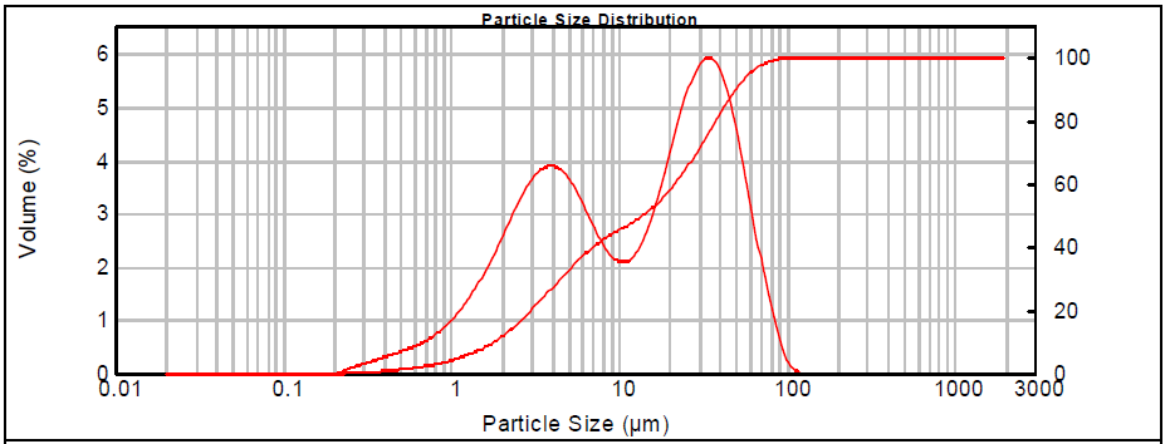

Figure 66: PSD for filtrate of W3-Stainless Steel Wire-wrapped Screen with 150 µm Slot Opening

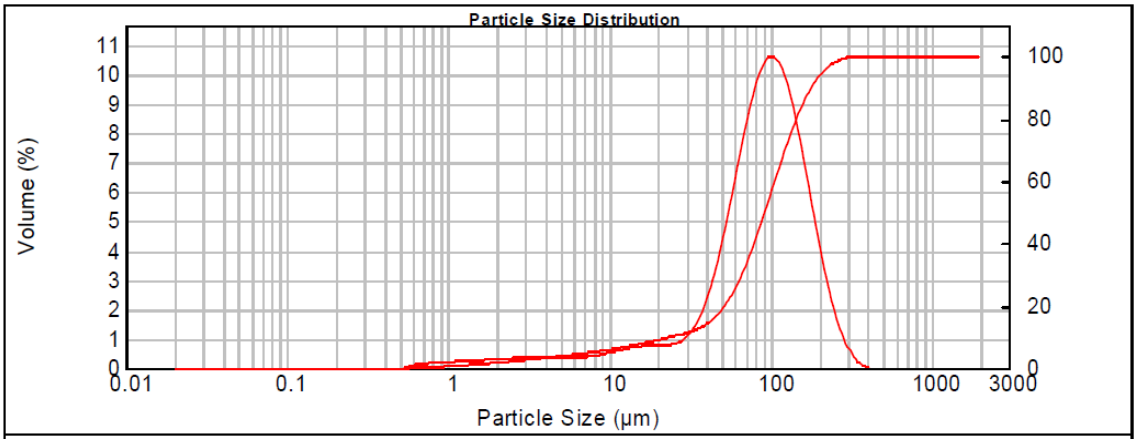

Figure 67: PSD for residue of W3-Stainless Steel Wire-wrapped Screen with 150 µm Slot Opening

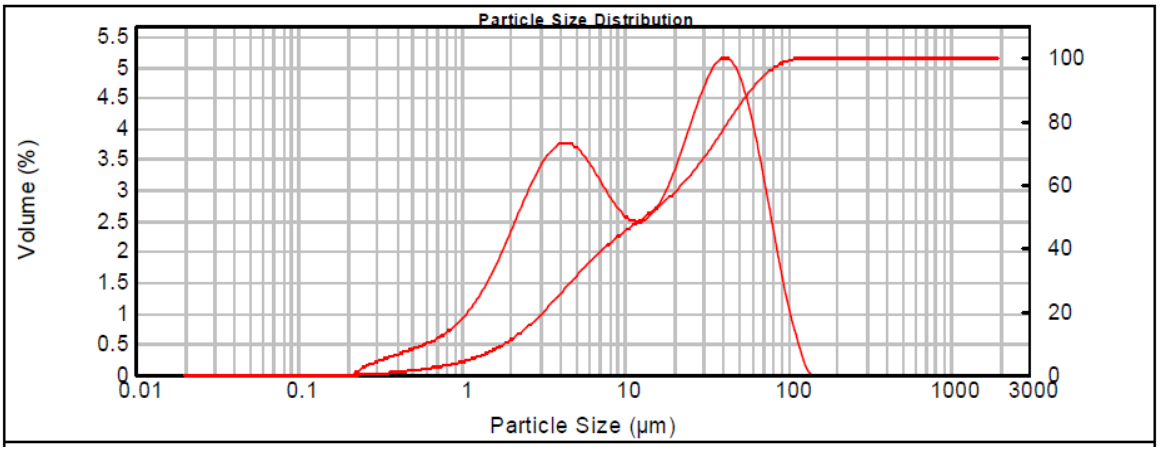

Figure 68: PSD for filtrate of W4-Stainless Steel Wire-wrapped Screen with 150 µm Slot Opening

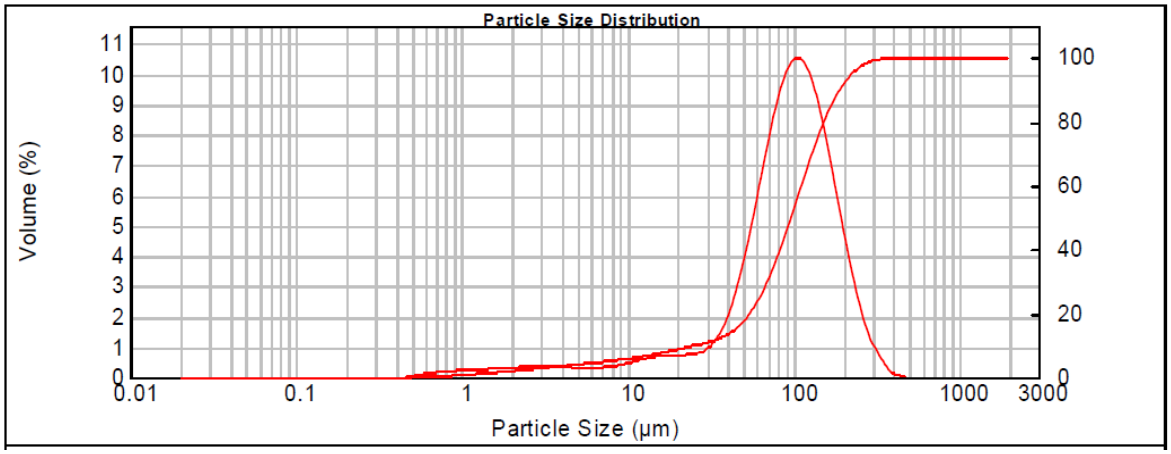

Figure 69: PSD for residue of W4-Stainless Steel Wire-wrapped Screen with 150 µm Slot Opening

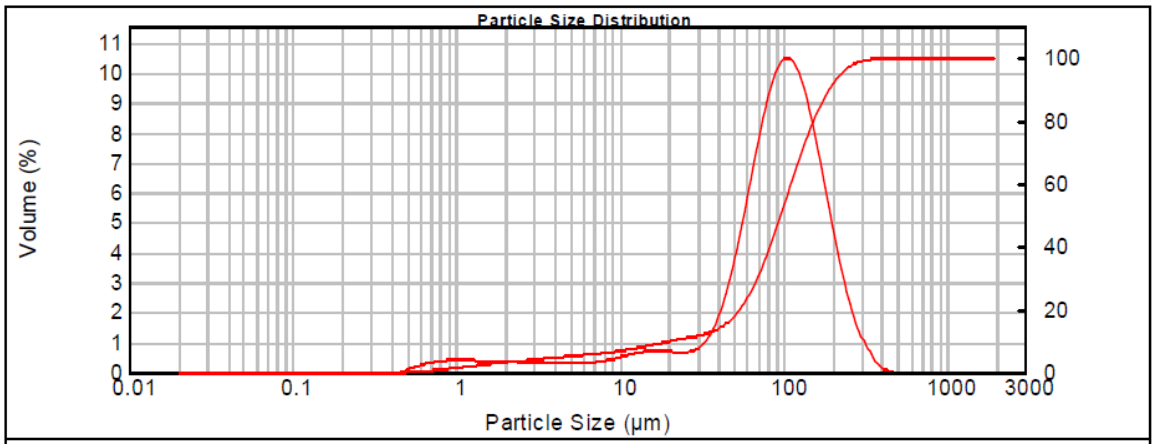

Figure 70: PSD for filtrate of C14-Ceramic Screen with Keystone Design with 200 µm Slot Opening

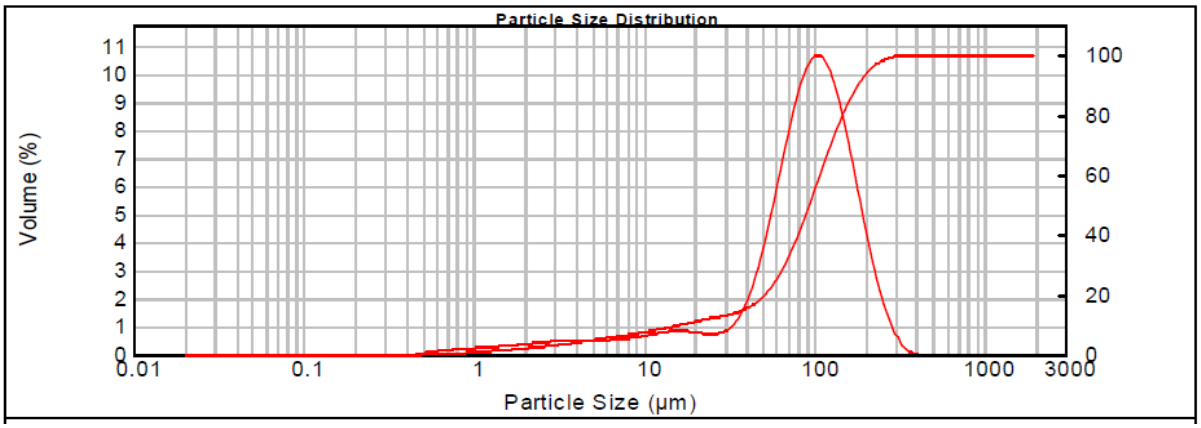

Figure 71: PSD for residue of C14-Ceramic Screen with Keystone Design with 200 µm Slot Opening

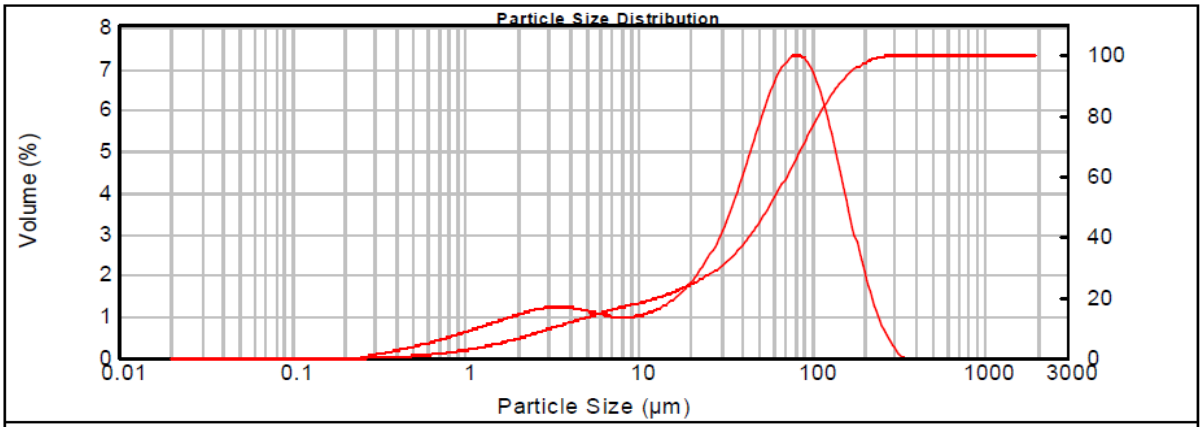

Figure 72: PSD for filtrate of S7- Stainless Steel Screen with Keystone Design with 200 µm Slot Opening

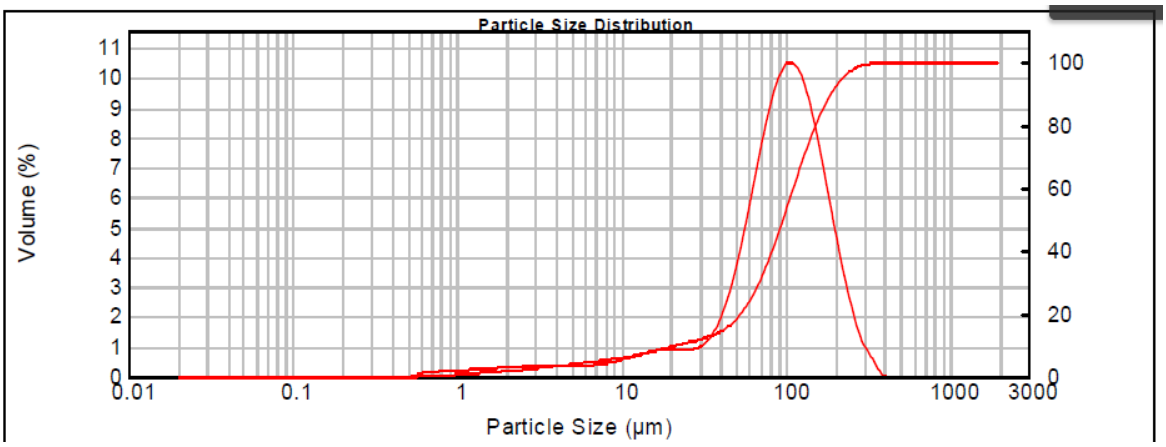

Figure 73: PSD for residue of S7- Stainless Steel Screen with Keystone Design with 200 µm Slot Opening

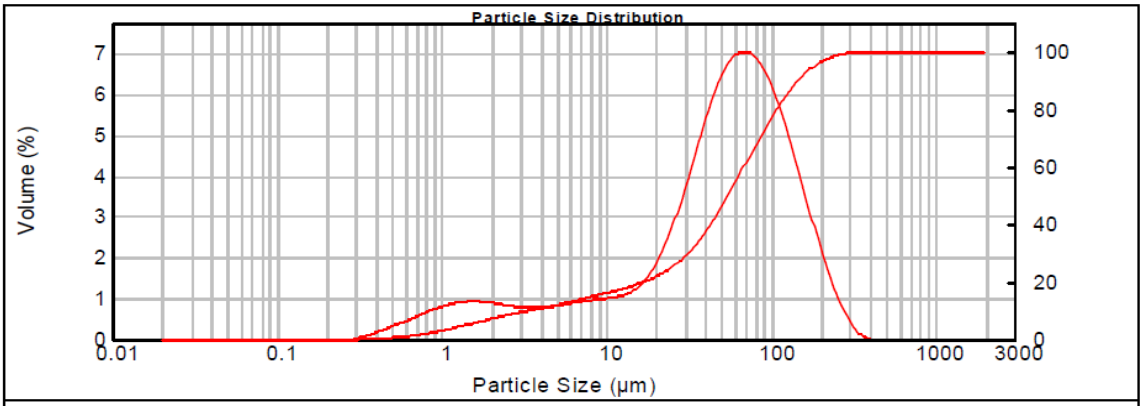

Figure 74: PSD for filtrate of S12- Stainless Steel Screen with Keystone Design with 200 µm Slot Opening

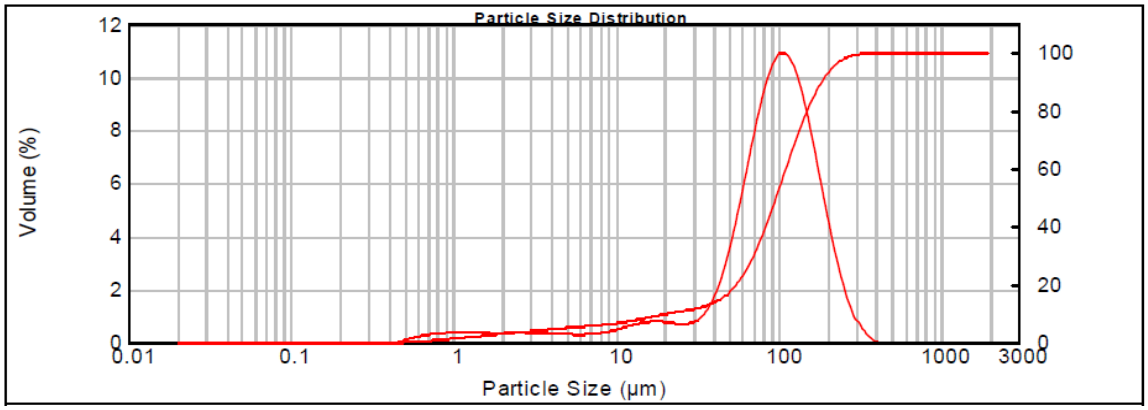

Figure 75: PSD for residue of S12- Stainless Steel Screen with Keystone Design with 200 µm Slot Opening

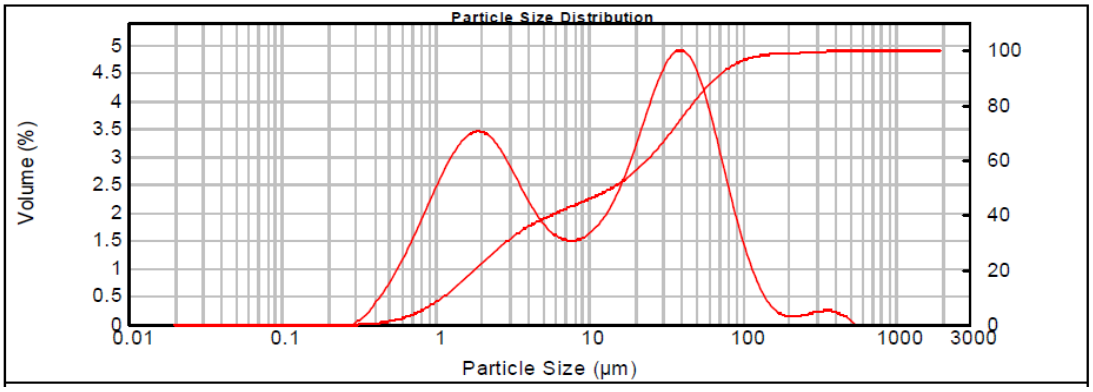

Figure 76: PSD for filtrate of W8-Stainless Steel Wire-wrapped Screen with 200 µm Slot Opening

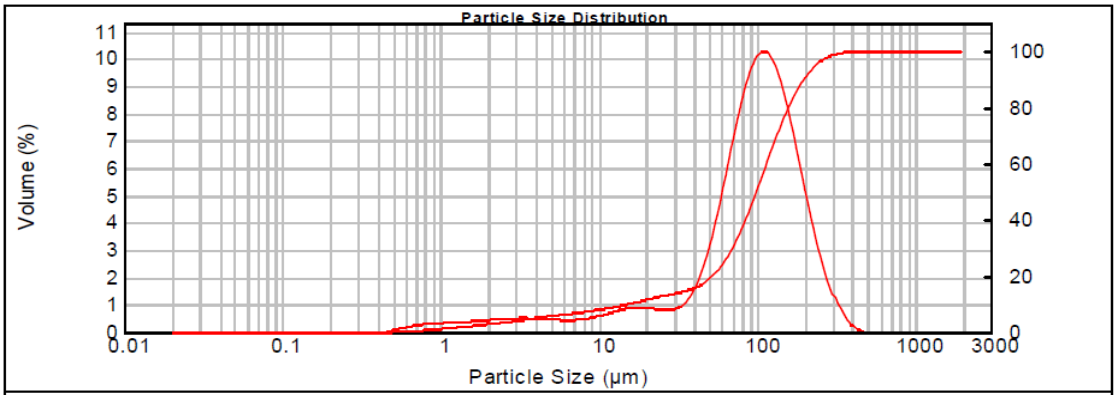

Figure 77: PSD for residue of W8-Stainless Steel Wire-wrapped Screen with 200 µm Slot Opening

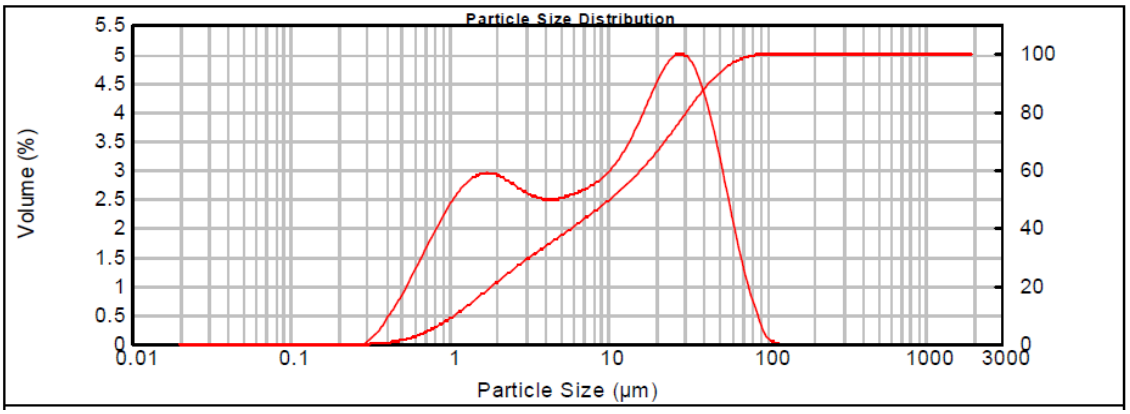

Figure 78: PSD for filtrate of W13-Stainless Steel Wire-wrapped Screen with 200 µm Slot Opening

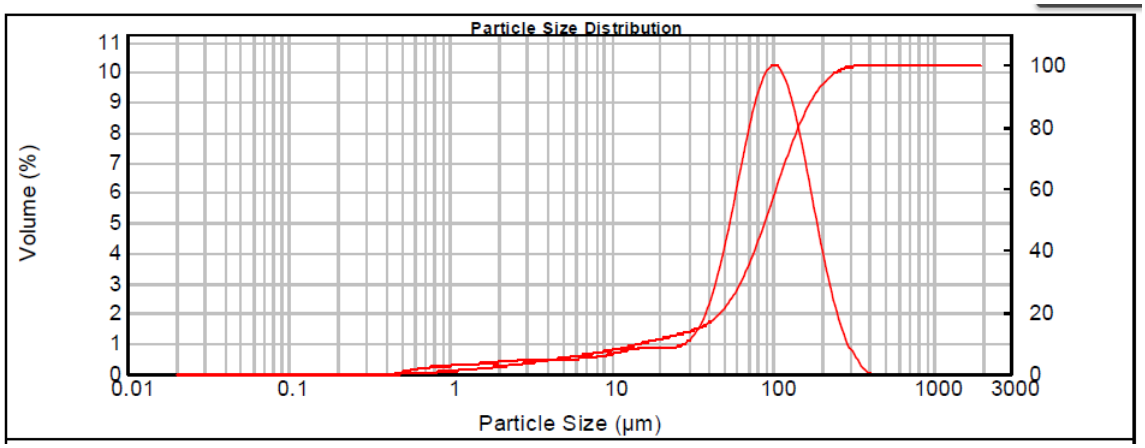

Figure 79: PSD for residue of W13-Stainless Steel Wire-wrapped Screen with 200 µm Slot Opening

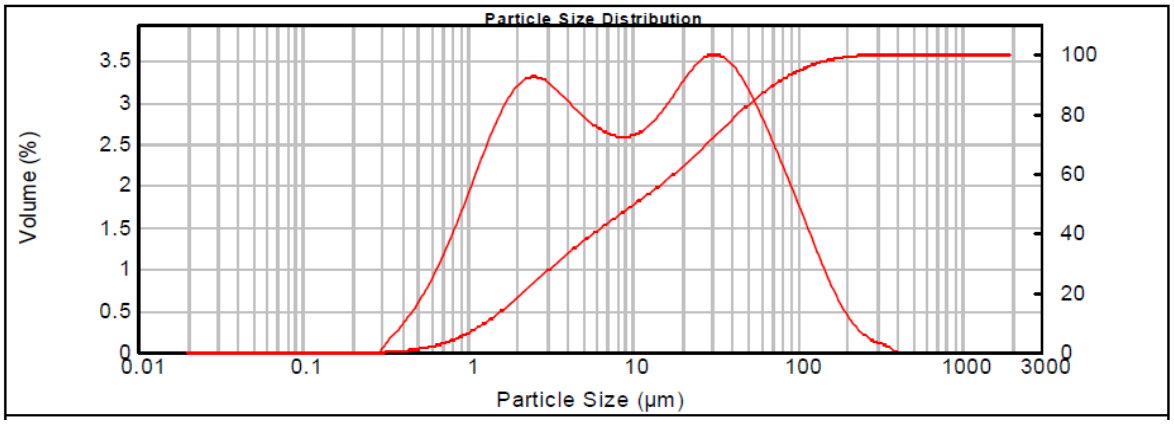

Figure 80: PSD for filtrate of C8-Ceramic Screen with Keystone Design with 250 µm Slot Opening

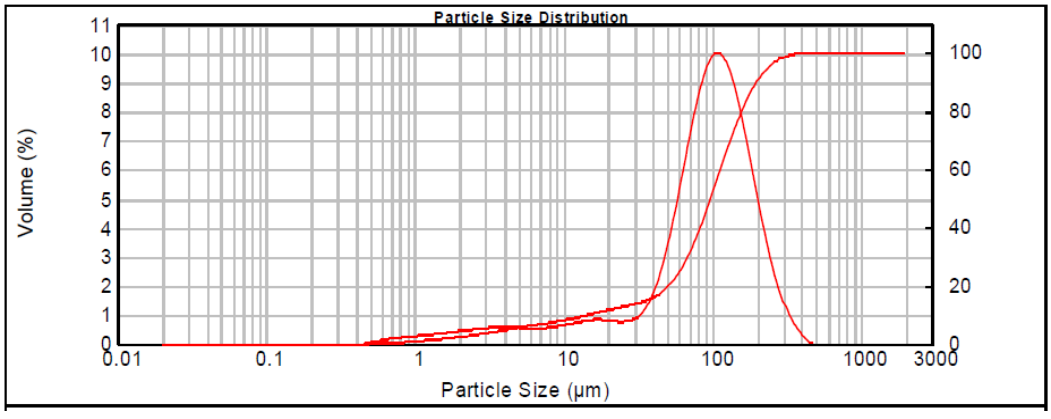

Figure 81: PSD for residue of C8-Ceramic Screen with Keystone Design with 250 µm Slot Opening

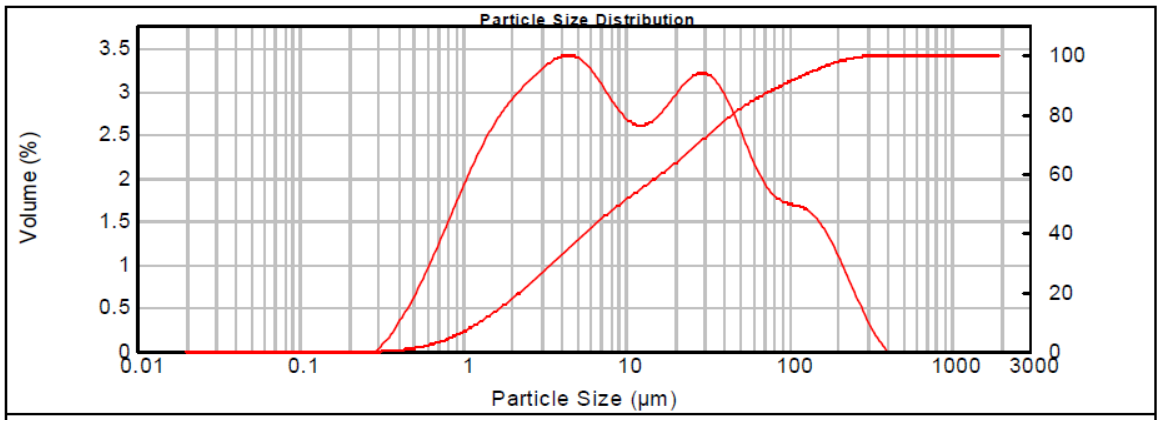

Figure 82: PSD for filtrate of C17-Ceramic Screen with Keystone Design with 250 µm Slot Opening

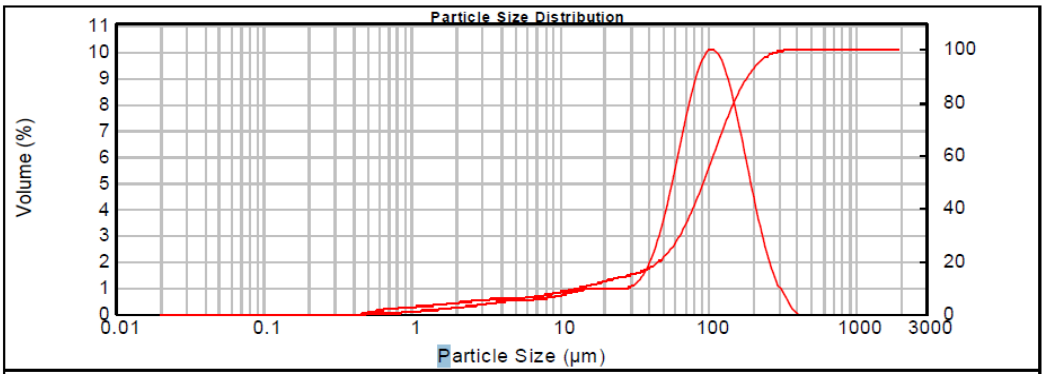

Figure 83: PSD for residue of C17-Ceramic Screen with Keystone Design with 250 µm Slot Opening

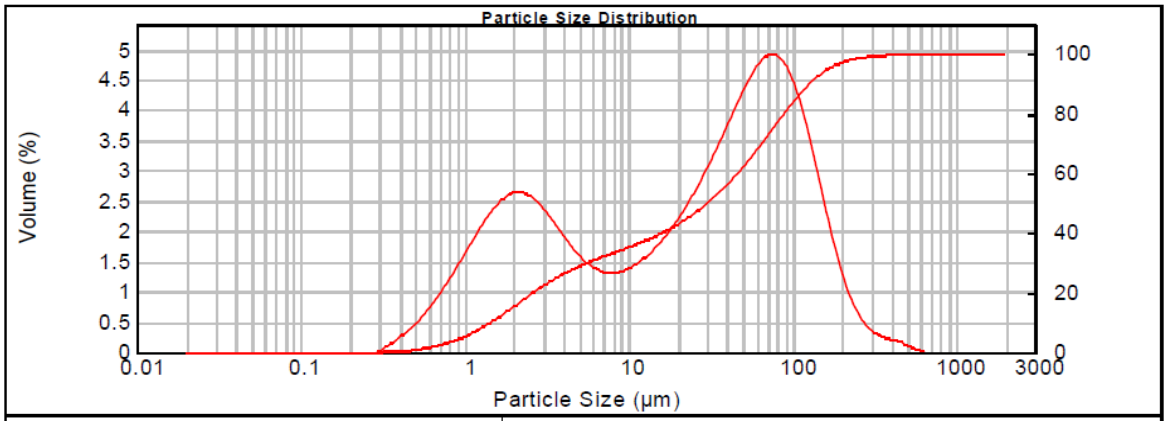

Figure 84: PSD for filtrate of S9-Stainless Steel Screen with Keystone Design with 250 µm Slot Opening

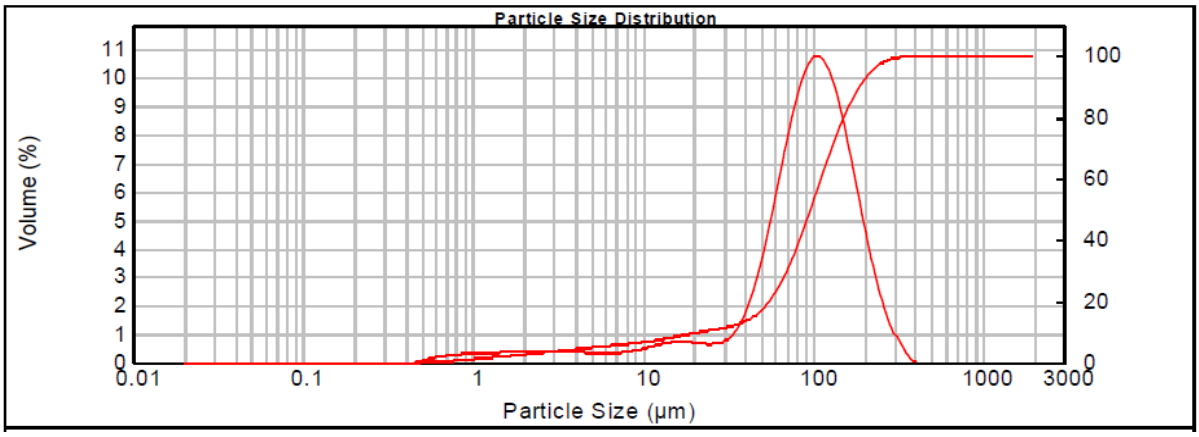

Figure 85: PSD for residue of S9-Stainless Steel Screen with Keystone Design with 250 µm Slot Opening

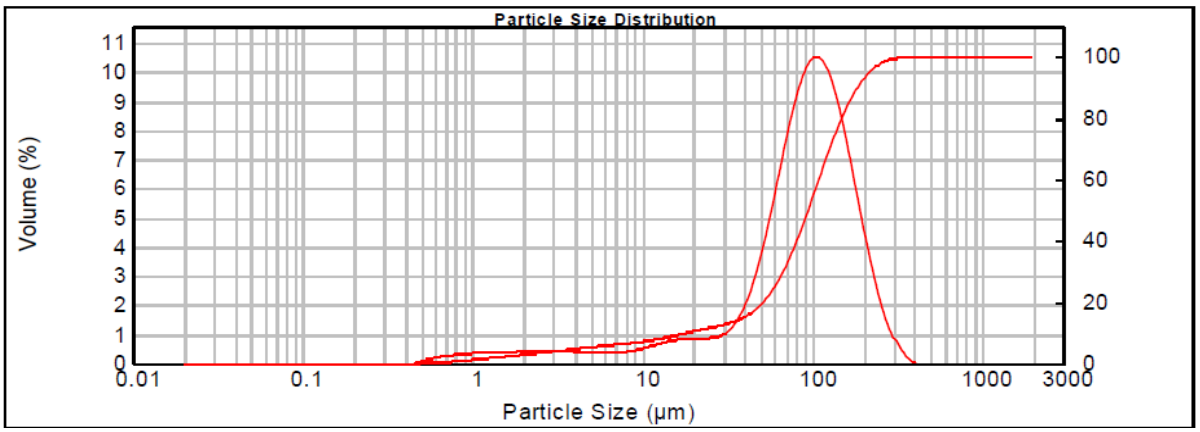

Figure 86: PSD for filtrate of S10-Stainless Steel Screen with Keystone Design with 250 µm Slot Opening

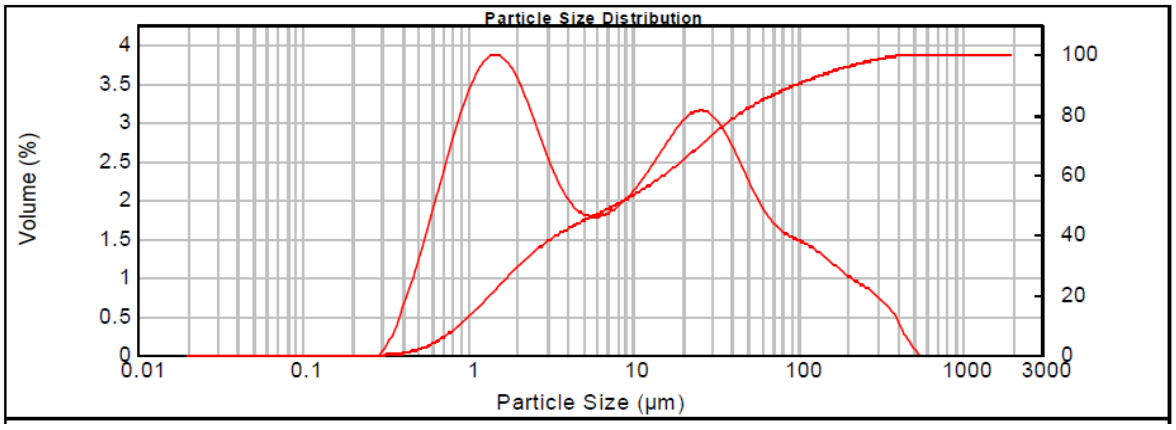

Figure 87: PSD for residue of S10-Stainless Steel Screen with Keystone Design with 250 µm Slot Opening

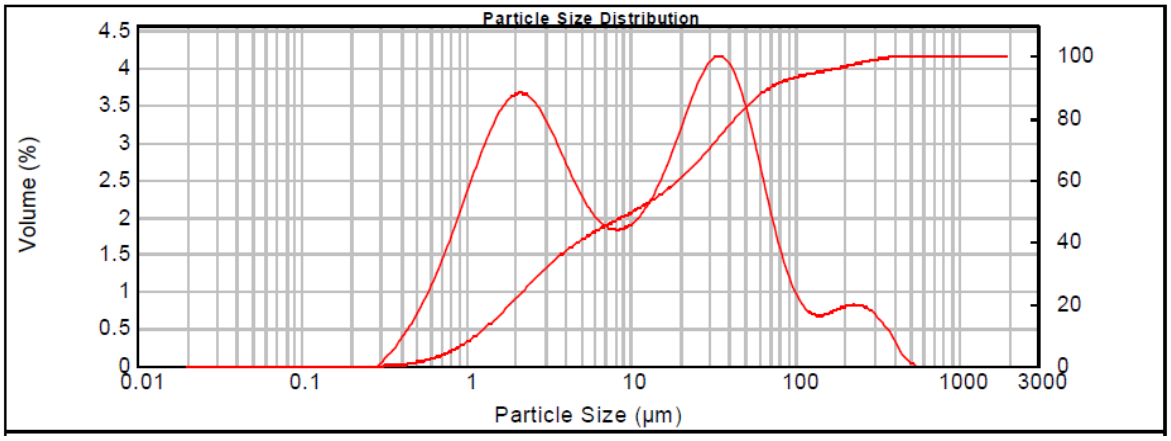

Figure 88: PSD for filtrate of W9-Stainless Steel Wire-wrapped Screen with 250 µm Slot Opening

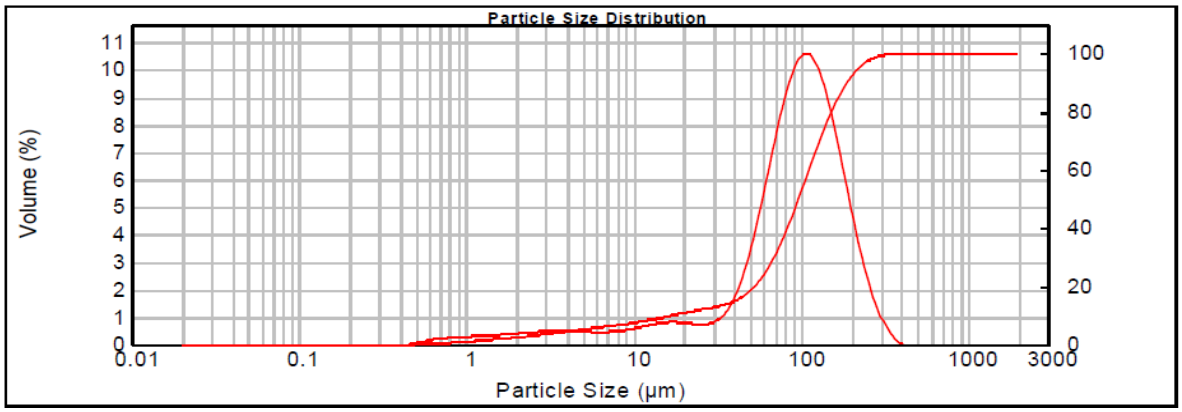

Figure 89: PSD for residue of W9-Stainless Steel Wire-wrapped Screen with 250 µm Slot Opening